Ct 4180

Plate analysis, theory and application

Volume 2, Numerical Methods

November 2006

Prof.dr.ir. J. Blaauwendraad

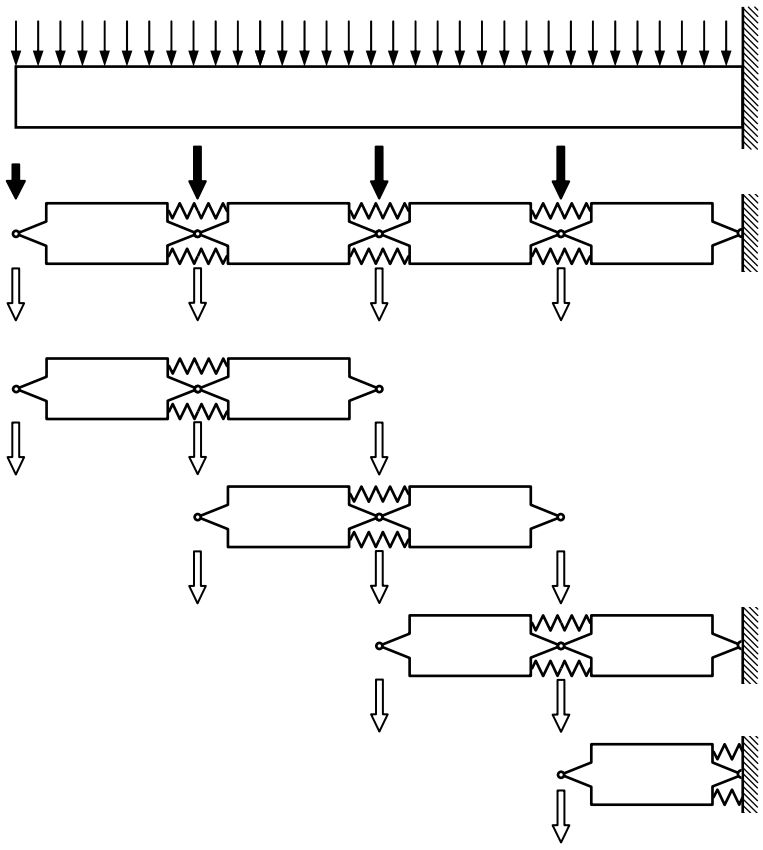

Faculty of Civil Engineering and Geosciences
Department of Mechanics, Materials and Structures
Section of Structural Mechanics

Delft University of Technology
Faculty of Civil Engineering and Geosciences

Plate analysis, theory and application CT4180

Volume 2, Numerical Methods

Prof.dr.ir. J. Blaauwendraad

November 2006

Table of contents

Preface 5

1 Bar loaded axially. Approximations 7
1.1 Stiffness method. Approximation 1 9
1.2 Stiffness method. Approximation 2 10
1.3 Convergence criteria 11

2 Plates. Discrete Element Approximations 13
2.1 Assembly for Spring Elements and Shear Panels. Approximation 1 13
2.2 Assembly of Bar Elements and Shear Panels. Approximation 2 19
2.3 Refined Approximation 2 23

3 Plates. Finite Element Method (FEM) 27
3.1 Truss Element (introduction) 27
3.2 Rectangular Element 31
3.3 Constant Shear Element 39
3.4 Comparison of elements 43
3.5 Convergence criteria 44
3.6 Implicit interpolation method 45
3.7 Consistent load vector 49
3.8 Some other elements 51
3.9 Examples of plate structures loaded in-plane 52

4 Plates. FEM for discrete elements 57
4.1 Derivation of the Spring Element 57
4.2 Derivation of the Shear Panel 59
4.3 Derivation of the Constant Shear Element 61

5 Case history of cable-stayed wide-box bridge 67
5.1 Introduction 67
5.2 Calculation of a construction phase 69
5.2.1 Problem definition and finite element mesh 69
5.2.2 Results of the finite element calculation 72
5.2.3 Comparison of the results with a model test 74
5.3 Interpretation of the results 77
5.3.1 Stress σ_{xx} 77
5.3.2 Stress σ_{yy} 79
5.3.3 Stress σ_{xy} 80
5.3.4 Deflection curve 81
5.4 Lessons from this case history 83

6 Beam loaded laterally (bending). Approximation 85
6.1 Stiffness Matrix of Discrete Bending Element 85
6.2 Global Stiffness Matrix of cantilever Beam 88

7 Slabs. Discrete Element Approximation 93
7.1 Assembly of Spring Elements and Torsion Panels. Approximation 1 94
7.2 Application of discrete slab model for office building at Amsterdam Airport (Schiphol) 100
7.3 Comparison with result for double-sine load on Square Plate 101
7.3.1 Exact solution 101
7.3.2 Analysis with a discrete model of Bending Spring Elements and Torsion Panels 103
7.3.3 Comparison 105
7.4 Assembly of Beam Elements and Torsion Panels. Approximation 2 106
7.5 Grid Model. Approximation 3 107

8 Slabs. Finite Element Method 109
8.1 Rectangular Element 109
8.2 Some other element types 113

9 Slabs. FEM for Discrete Elements 115
9.1 Derivation of Bending Spring Element 115
9.2 Derivation of Torsion Panel 116

10 Case study of L-shaped slab with various support conditions 119
10.1 Problem definition 119
10.2 Bending moments and equilibrium 125
10.3 Shear forces and support reactions 126

11 Non-linear applications of plates, slabs and shells 131
11.1 Masonry mechanics 131
11.2 Slab of Mc Neice 131
11.3 Shell A2 tested by Bouma 132

Books on the Finite Element Method 135

Preface

The course “Plate analysis, theory and application” (Ct 4180) is part of the Master Curriculum of the Faculty Civil Engineering and Geosciences. In general plates are two-dimensional structures, which can be loaded in two different ways. In this course the word “plate” is reserved for plate structures, which are loaded in their plane. The state of plane stress in such structures consists of membrane forces. Shear-walls belong to this class of problems, but also deep beams, beam webs with holes and other structures of this kind.
The word “slab” will be used for the other type of plates, which is loaded perpendicular to its plane. The stress state in slabs consists of bending moments and shear forces.

The lecture notes consist of two volumes with titles “Theory” and “Numerical Methods”. The volume titled “Theory” covers the theory of plates and slabs, presents differential equations and includes a number of exact solutions. The volume “Numerical Methods” deals with approximating techniques on basis of the direct stiffness method for both plates and slabs. This volume fits in with commercial software for the analysis of plates and slabs.

It is a principal idea of the lecture notes that first the classical theory should be presented and must be understood before the numerical methods can be judged for its value. The theoretical part creates understanding and insight and provides a basis for the discussion of the numerical methods. Two different theories for slabs are discussed: the theory for thick plates and the theory for thin plates. This is done because commercial software packages offer both options.

In conventional books, a different theory is applied for plates if compared to slabs. For plates loaded in plane, a differential equation is derived in the flexibility approach (leading to a differential equation for a stress function) and for slabs loaded perpendicular to plane a stiffness approach is applied (leading to a differential equation for the displacement). In the volume “Theory” we quit with this approach. The decision has been made to apply the stiffness approach for both plates and slabs. This has been done by purpose in order to fit in with modern computational methods. Then no difference exists for plates and slabs, because both structure types are computed in the framework of the direct stiffness method.

I am thankful to Kelly Greene, student of the Faculty of Architecture, for her rewarded contribution to a correct English text and I am much indebted to dr.ir. C. Sitters, who was in control of the translation of existing parts of lecture notes, correctly processed new parts, produced clear pictures and accurately handled the composition of all parts. His cooperation and care guarantees wonderful lecture notes.

J. Blaauwendraad
March 2004

1 Bar loaded axially. Approximations

To achieve a good approximation of the behaviour of plates it is worth wile to examine the approximation of a bar first. Here we restrict ourselves to a bar that is loaded axially, so that only normal forces (N) occur (a truss element).

When one wants to introduce the finite element method for a truss element one can consider a structure as is shown in Fig. 1.1. In this structure, the cross-sectional area A is constant and both the load and the elasticity are continuously distributed.

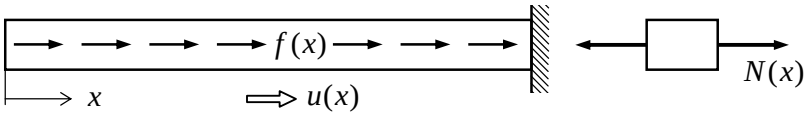

Fig. 1.1: Bar loaded in axial direction by a distributed load.

How can we approximate such a continuous system? One approach is that we can select nodes and keep the load distributed, but we lump the elastic deformation in discrete springs. This means that we consider the structure as an assemblage of rigid parts and lumped springs. We call this *approximation 1*. The load still is homogeneously distributed, but the structure is discretized.
We can also do the reverse. We select nodes and lump the distributed load into discrete nodal forces. The structure itself is left unchanged. The elasticity is homogeneously distributed, but the load is discretized. We will call this *approximation 2* (see Fig. 1.2).

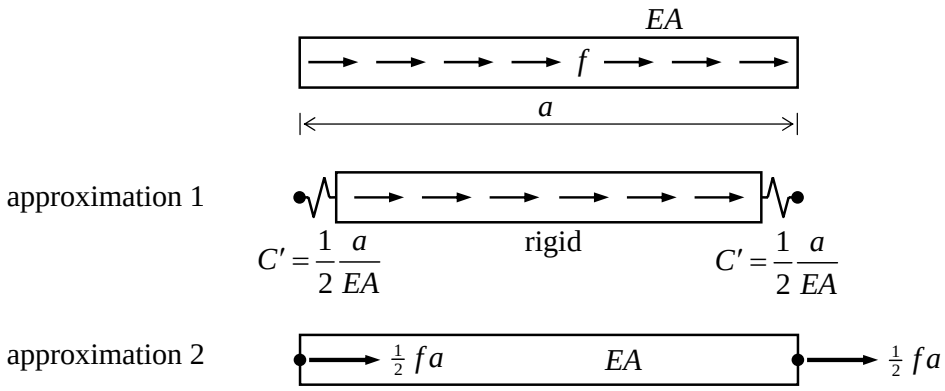

Fig. 1.2: The two types of discretization.

To explain the difference in the two approximations we distinct four equal parts of length a in the total structure of Fig. 1.1 and we discuss the case of a homogeneously distributed load f and axial stiffness EA (see Fig. 1.3). For an element of length a we have to lump the load in case of approximation 2 and the elastic deformation in case of approximation 1.

The compliance (flexibility) of the two lumped springs in approximation 1 is $a/(2EA)$. The stiffnesses are therefore $2EA/a$. Fig. 1.3 shows the results that are found for the two different

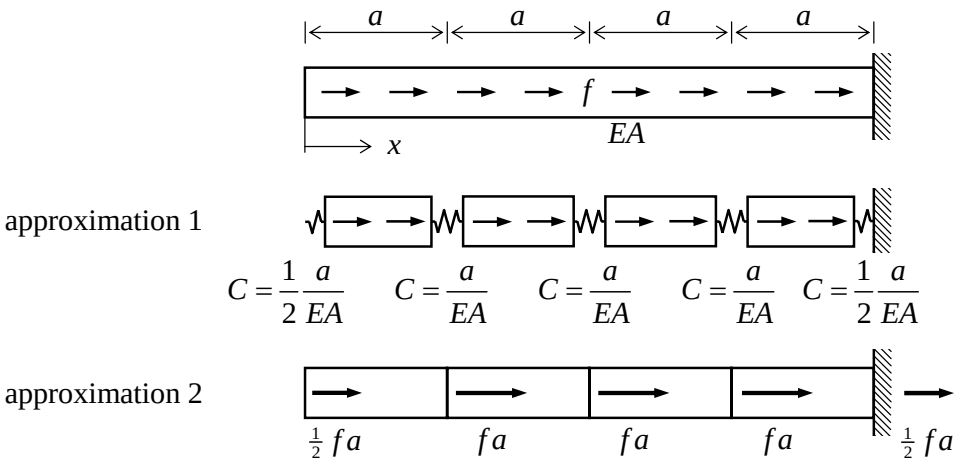

Fig. 1.3: Structure divided into four discrete elements.

approximations. In approximation 1 the lumped springs of two adjacent elements must be linked serially. This means that we sum up the compliances ($C = C' + C' = a/EA$).

In approximation 2 the displacements $u(x)$ are continuous and the nodal displacements are even exact. However, the normal force $N(x)$ is discontinuous. In approximation 1 the normal force $N(x)$ is continuous and the displacements $u(x)$ show discontinuities (see Fig. 1.4).

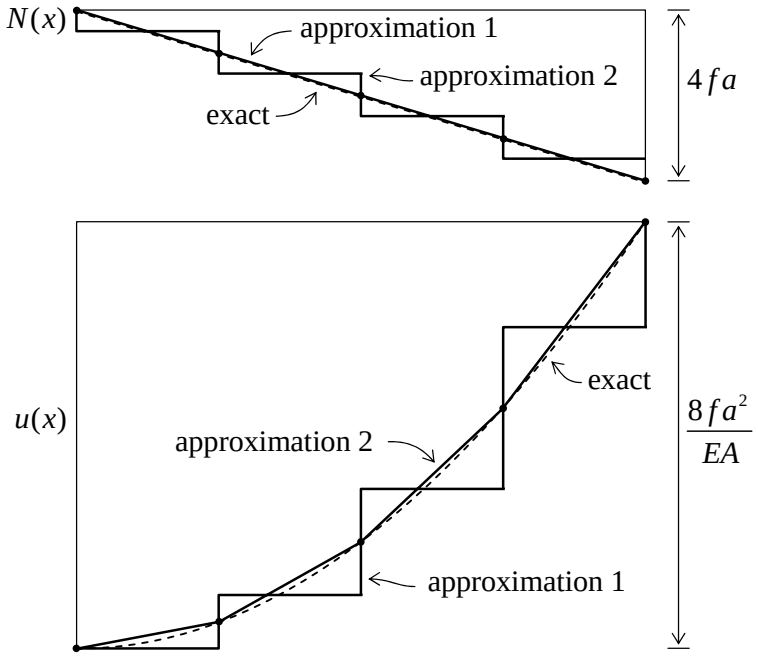

Fig. 1.4: Displacement and normal force distributions for the exact solution (dashed line) and the two approximations.

1.1 Stiffness method. Approximation 1

The presented example is a very simple one because the structure is a statically determinate one. So, we can calculate $N(x)$ immediately from equilibrium and from this $u(x)$ can be obtained using the compliances. In more general statically indeterminate cases we better apply the stiffness method (the finite element method).
In case of approximation 1 we can look upon the structure as an assembly of four degrees of freedom and four elements as shown in Fig. 1.5.

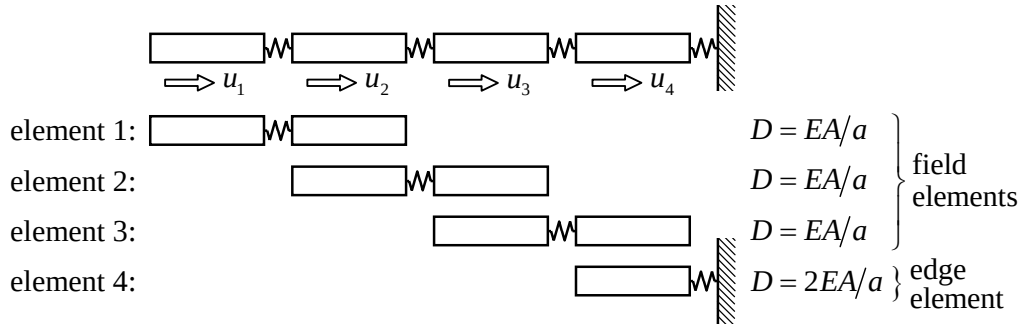

Fig. 1.5: Application of the stiffness method in approximation 1.

The discrete field elements 1, 2 and 3 have a stiffness matrix of two rows and two columns. For edge element 4 the stiffness matrix consists of one number:

$$\underbrace{\frac{EA}{a}\begin{bmatrix} 1 & -1 \\ -1 & 1 \end{bmatrix}}_{\text{element 1}} \; ; \; \underbrace{\frac{EA}{a}\begin{bmatrix} 1 & -1 \\ -1 & 1 \end{bmatrix}}_{\text{element 2}} \; ; \; \underbrace{\frac{EA}{a}\begin{bmatrix} 1 & -1 \\ -1 & 1 \end{bmatrix}}_{\text{element 3}} \; ; \; \underbrace{\frac{EA}{a}[\,2\,]}_{\text{element 4}}$$

The assemblage of the stiffness matrix of the global system yields:

$$\frac{EA}{a}\begin{bmatrix} 1 & -1 & 0 & 0 \\ -1 & 2 & -1 & 0 \\ 0 & -1 & 2 & -1 \\ 0 & 0 & -1 & 3 \end{bmatrix} \begin{Bmatrix} u_1 \\ u_2 \\ u_3 \\ u_4 \end{Bmatrix} = \begin{Bmatrix} fa \\ fa \\ fa \\ fa \end{Bmatrix}$$

The contribution of all four elements is shown by the four squares of dashed lines from the top left-hand corner to the bottom right-hand corner of the global stiffness matrix. The terms in the right-hand load vector consist of the (total) load on each rigid part in the structure.

The solution $\boldsymbol{u}$ of this set of equations reads:

$$\boldsymbol{u}^T = \{u_1 \quad u_2 \quad u_3 \quad u_4\} = \frac{fa^2}{EA}\{8 \quad 7 \quad 5 \quad 2\}$$

From these displacements, one can easily calculate the stress resultants (normal forces) in the springs of the four elements. To distinguish the element number from the number of a degree of freedom, we apply the first one as a superscript and the last mentioned as a subscript.

$$\boldsymbol{\sigma}^T = \begin{Bmatrix} N^1 & N^2 & N^3 & N^4 \end{Bmatrix} = f a \begin{Bmatrix} 1 & 2 & 3 & 4 \end{Bmatrix}$$

In this example all elements have the same length a and axial stiffness EA.

Remark
In the rows of the stiffness matrix which correspond to u_2 and u_3 we notice the pattern as shown in Fig. 1.6.

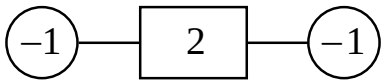

Fig. 1.6: Discretization scheme (molecule).

The same scheme (molecule) is found when a discretization of the governing differential equation $-EA\, d^2u/dx^2 = f$ is made on the basis of finite differences (in Dutch: differentierekening). For the second derivative the scheme 1, –2, 1 applies.

Exercise
Consider two parts of a structure as shown in Fig. 1.7 with lengths a_i and a_j and with axial stiffnesses EA_i and EA_j. The element for this part has a spring stiffness D_{ij} and a stiffness matrix $\boldsymbol{K}$. Determine D_{ij} and $\boldsymbol{K}$.

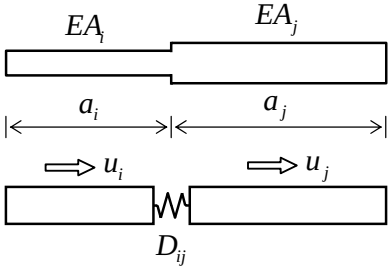

Fig. 1.7: Structure with a discontinuity in axial direction.

1.2 Stiffness method. Approximation 2

In approximation 2 we have, as shown in Fig. 1.8, four equal elements and five degrees of freedom (dof's) of which one is set to zero (the support). The element stiffness matrices and the assembled global system are:

$$\underbrace{\frac{EA}{a}\begin{bmatrix} 1 & -1 \\ -1 & 1 \end{bmatrix}}_{\text{element 1}} ; \underbrace{\frac{EA}{a}\begin{bmatrix} 1 & -1 \\ -1 & 1 \end{bmatrix}}_{\text{element 2}} ; \underbrace{\frac{EA}{a}\begin{bmatrix} 1 & -1 \\ -1 & 1 \end{bmatrix}}_{\text{element 3}} ; \underbrace{\frac{EA}{a}\begin{bmatrix} 1 & -1 \\ -1 & 1 \end{bmatrix}}_{\text{element 4}}$$

$$\frac{EA}{a}\begin{bmatrix} 1 & -1 & 0 & 0 & 0 \\ -1 & 2 & -1 & 0 & 0 \\ 0 & -1 & 2 & -1 & 0 \\ 0 & 0 & -1 & 2 & -1 \\ 0 & 0 & 0 & -1 & 1 \end{bmatrix}\begin{Bmatrix} u_1 \\ u_2 \\ u_3 \\ u_4 \\ u_5 \end{Bmatrix} = \begin{Bmatrix} \frac{1}{2}fa \\ fa \\ fa \\ fa \\ \frac{1}{2}fa + r \end{Bmatrix}$$

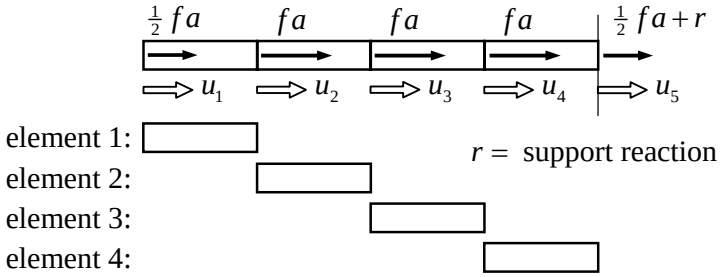

Fig. 1.8: Application of the stiffness method in approximation 2.

Now the load exists of lumped nodal forces. The solution for this case is:

$$\boldsymbol{u}^T = \{u_1 \quad u_2 \quad u_3 \quad u_4 \quad u_5\} = \frac{fa^2}{EA}\{8 \quad 7\tfrac{1}{2} \quad 6 \quad 3\tfrac{1}{2} \quad 0\}$$

and from this we find:

$$\boldsymbol{\sigma}^T = \{N^1 \quad N^2 \quad N^3 \quad N^4\} = fa\{\tfrac{1}{2} \quad 1\tfrac{1}{2} \quad 2\tfrac{1}{2} \quad 3\tfrac{1}{2}\}$$

These values differ from the ones found in approximation 1, but note that they hold for different positions in the bar.

1.3 Convergence criteria

The method has been shown for a simple structure and a simple type of loading. In general, the load $f(x)$ can be distributed arbitrarily and therefore also $N(x)$ can have any distribution. We accept a discretization error, but require that the error will vanish when the number of elements approaches infinity. In the limit case, the elements are so small that the normal force $N(x)$ does not vary along one element anymore. That means that the used elements to approximate some solution at least have to show exact results for the case in which a constant normal force occurs in the structure. The used elements in approximation 1 and approximation 2 meet this requirement. So, these elements can be used for any loading and convergence to the exact solution will occur when the number of elements is increased.

A second criterion is that the element remains stress-free when a rigid body displacement is considered. This requirement is met for both types of approximation.

2 Plates. Discrete Element Approximations

In this chapter we consider plates that are loaded in-plane. The thickness of the plate is t, the modulus of elasticity (Young's modulus) is E and Poisson's ratio is υ. We restrict ourselves to rectangular shaped plates. The loads per unit area of the pate are p_x and p_y. Edge loads f can also occur. The loads produce stresses σ_{xx}, σ_{yy} and σ_{xy} and stress resultants across the plate thickness n_{xx}, n_{yy} and n_{xy}. We call these stress resultants *membrane forces* or *extension forces*. The corresponding strains are ε_{xx}, ε_{yy} and γ_{xy}. The relation between the stress resultants and the strains is, in the case of plane stress problems:

$$\begin{Bmatrix} n_{xx} \\ n_{yy} \\ n_{xy} \end{Bmatrix} = \frac{E\,t}{1-\upsilon^2} \begin{bmatrix} 1 & \upsilon & 0 \\ \upsilon & 1 & 0 \\ 0 & 0 & \frac{1-\upsilon}{2} \end{bmatrix} \begin{Bmatrix} \varepsilon_{xx} \\ \varepsilon_{yy} \\ \gamma_{xy} \end{Bmatrix} \tag{2.1}$$

or in short:

$$\boldsymbol{\sigma} = \boldsymbol{D}\,\boldsymbol{\varepsilon} \tag{2.2}$$

The convention for positive signs is shown in Fig. 2.1.

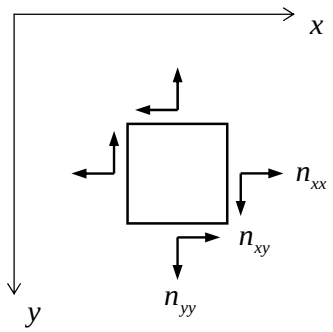

Fig. 2.1: Convention for positive signs.

A proper approximation must account for each of the three types of stress transfer and must accurately model the possibility of the membrane forces n_{xx}, n_{yy} and n_{xy}. In section 2.1 we start from the results of chapter 1 for truss elements and will make the extension for plates. This section matters for insight and understanding. In order to keep it simple, lateral contractions are excluded from this chapter (so $\upsilon = 0$).
In chapter 3 a formal and general derivation is made for a rectangular plate element. Then, we apply the variational principle of virtual work. This case will also be applicable for $\upsilon \neq 0$.

2.1 Assembly for Spring Elements and Shear Panels. Approximation 1

We take into consideration a rectangular plate part of finite sizes a and b, and try to approximate its behaviour with a spring system. First, the shear transfer caused by the membrane forces n_{xy} is neglected and we focus on the normal forces n_{xx} and n_{yy}. As shown

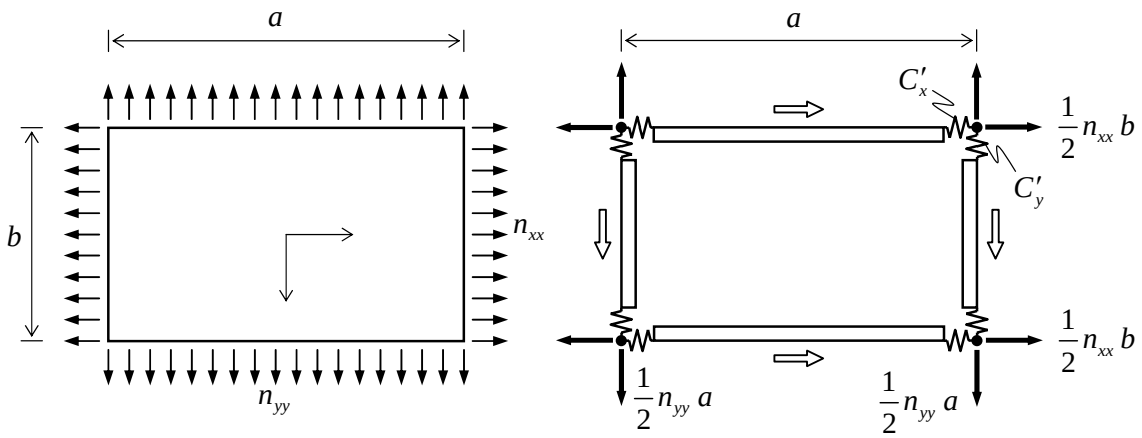

Fig. 2.2: Discretization of rectangular plate part by four truss elements (approximation 1).

in Fig. 2.2, the rectangular plate part is replaced by four truss elements of the type used in approximation 1, in which a rigid bar and lumped springs occur. The spring characteristics are chosen such that the strains ε_{xx} and ε_{yy} for a homogeneous field of n_{xx} and n_{yy}, are equal in the actual plate part and in the spring model. This yields the following compliances:

$$C'_x = \frac{\alpha}{Et} \quad ; \quad \alpha = \frac{a}{b}$$

$$C'_y = \frac{\beta}{Et} \quad ; \quad \beta = \frac{b}{a}$$

The four corners of the plate part are called nodes. In an assemblage of many plate parts four plate parts surround an arbitrary node within the plate (see Fig. 2.3). The four springs of these plate parts are composed to one global spring C_x in the *x*-direction, and one global spring C_y in the *y*-direction.

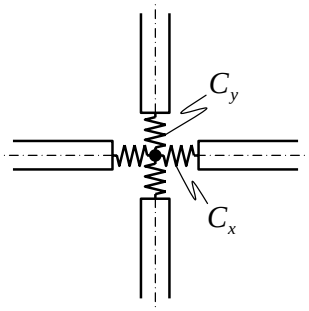

Exercise
Show that:

$$C_x = \frac{\alpha}{E\,t}$$

$$C_y = \frac{\beta}{E\,t}$$

Fig. 2.3: Four meeting rectangular plate parts.

Now, the neglected n_{xy}-action of the plate part still has to be modelled. For this a shear panel in which a constant shear stress is present is used. In the case of a constant shear stress being present, also a constant shear strain γ_{xy} will be present, and therefore the deformed panel still has straight edges. Moreover, the edges do not elongate. So, the state of stress and strain can be expressed using the four degrees of freedom as shown in Fig. 2.4.

The shear panel is a discrete element that fits perfectly in an orthogonal assemblage of axial discrete spring elements. The stiffness matrix of the panel is derived as follows. The

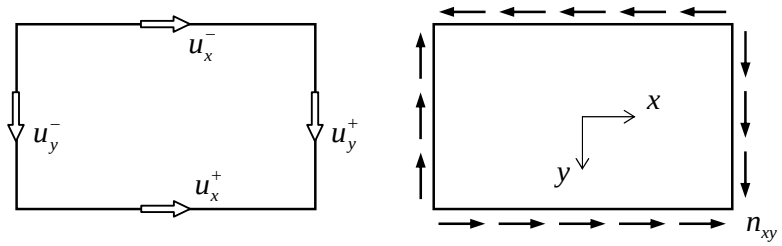

Fig. 2.4: Shear panel.

generalised forces which correspond to the degrees of freedom u_x^-, u_x^+, u_y^- and u_y^+ for a deep beam are respectively F_x^-, F_x^+, F_y^- and F_y^+. Taking into account the sizes a and b of the panel and knowing that γ_{xy} is constant over the panel, we find:

$$\gamma_{xy} = \frac{\Delta u_x}{b} + \frac{\Delta u_y}{a} = \frac{u_x^+ - u_x^-}{b} + \frac{u_y^+ - u_y^-}{a}$$

Further we know:

$$n_{xy} = G\,t\,\gamma_{xy} = \tfrac{1}{2} E\,t\,\gamma_{xy}$$
$$F_x^- = -a\,n_{xy} \quad ; \quad F_x^+ = a\,n_{xy}$$
$$F_y^- = -b\,n_{xy} \quad ; \quad F_y^+ = b\,n_{xy}$$

From this kinematic relation, constitutive equation and equilibrium relations it follows that:

$$\begin{Bmatrix} F_x^- \\ F_x^+ \\ F_y^- \\ F_y^+ \end{Bmatrix} = \frac{1}{2} E\,t \begin{bmatrix} \alpha & -\alpha & 1 & -1 \\ -\alpha & \alpha & -1 & 1 \\ 1 & -1 & \beta & -\beta \\ -1 & 1 & -\beta & \beta \end{bmatrix} \begin{Bmatrix} u_x^- \\ u_x^+ \\ u_y^- \\ u_y^+ \end{Bmatrix} \quad \text{where} \quad \alpha = \frac{a}{b} = \beta^{-1}$$

Now, we know all the components to model rectangular shaped plates. Axial spring elements and shear panels are necessary. In Fig. 2.5 it is shown how the global stiffness matrix is filled in for a specific example of a deep beam (line of symmetry is used). For row 9 the stiffnesses are calculated for the case in which a and b are equal.
Row 9 of the stiffness matrix receives contributions from four elements as displayed in Fig. 2.6. Two elements are spring elements for axial forces and two elements are shear panels. The four stiffness matrices are (apart from a factor $E\,t$):

$$\begin{array}{c} \\ 4 \\ 9 \end{array} \begin{array}{c} \begin{array}{cc} 4 & 9 \end{array} \\ \left[\begin{array}{c|c} 1 & -1 \\ \hline -1 & 1 \end{array}\right] \end{array}$$
element 4-9

$$\begin{array}{c} \\ 9 \\ 14 \end{array} \begin{array}{c} \begin{array}{cc} 9 & 14 \end{array} \\ \left[\begin{array}{c|c} 1 & -1 \\ \hline -1 & 1 \end{array}\right] \end{array}$$
element 9-14

$$\begin{array}{c} \\ 6 \\ 11 \\ 8 \\ 9 \end{array} \begin{array}{c} \begin{array}{cccc} 6 & 11 & 8 & 9 \end{array} \\ \left[\begin{array}{c|c|c|c} \frac{1}{2} & -\frac{1}{2} & \frac{1}{2} & -\frac{1}{2} \\ \hline -\frac{1}{2} & \frac{1}{2} & -\frac{1}{2} & \frac{1}{2} \\ \hline \frac{1}{2} & -\frac{1}{2} & \frac{1}{2} & -\frac{1}{2} \\ \hline -\frac{1}{2} & \frac{1}{2} & -\frac{1}{2} & \frac{1}{2} \end{array}\right] \end{array}$$
element 6-11-8-9

$$\begin{array}{c} \\ 7 \\ 12 \\ 9 \\ 10 \end{array} \begin{array}{c} \begin{array}{cccc} 7 & 12 & 9 & 10 \end{array} \\ \left[\begin{array}{c|c|c|c} \frac{1}{2} & -\frac{1}{2} & \frac{1}{2} & -\frac{1}{2} \\ \hline -\frac{1}{2} & \frac{1}{2} & -\frac{1}{2} & \frac{1}{2} \\ \hline \frac{1}{2} & -\frac{1}{2} & \frac{1}{2} & -\frac{1}{2} \\ \hline -\frac{1}{2} & \frac{1}{2} & -\frac{1}{2} & \frac{1}{2} \end{array}\right] \end{array}$$
element 7-12-9-10

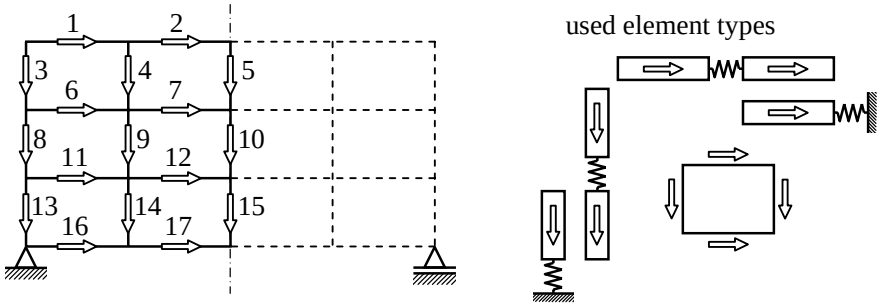

	1	2	3	4	5	6	7	8	9	10	11	12	13	14	15	16	17
1	*	*	*	*		*											
2	*	*		*	*		*										
3	*		*	*		*		*									
4	*	*	*	*	*	*	*		*								
5		*		*	*		*			*							
6	*		*	*		*	*	*	*		*						
7		*		*	*	*	*		*	*		*					
8			*			*		*	*		*		*				
9				*		*	*	*	*	*	*	*		*			
10					*		*		*	*		*			*		
11						*		*	*		*	*	*	*		*	
12							*		*	*	*	*		*	*		*
13								*			*		*	*		*	
14									*		*	*	*	*	*	*	*
15										*		*		*	*		*
16											*		*	*		*	*
17												*		*	*	*	*

row 9 ($a = b$)	0	0	0	–1	0	$-\frac{1}{2}$	$\frac{1}{2}$	$-\frac{1}{2}$	3	$-\frac{1}{2}$	$\frac{1}{2}$	$-\frac{1}{2}$	0	–1	0	0	0

Fig. 2.5: Construction of the global stiffness matrix for a deep beam (approximation 1).

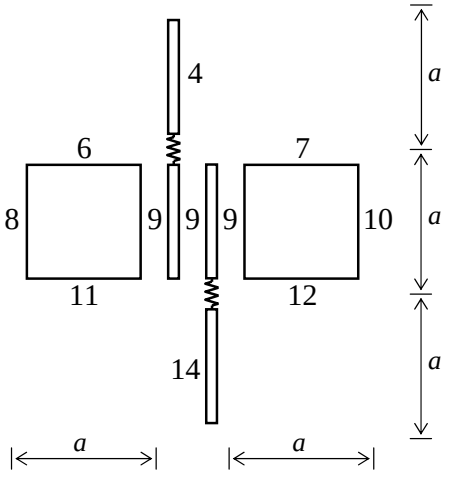

Fig. 2.6: Construction of row 9 of the stiffness matrix in Fig. 2.5.

To find row 9 of the global stiffness matrix of all four element matrices the rows corresponding with row 9 are added up. The result is:

	4	6	7	8	9	10	11	12	14
row 9	-1	$-\frac{1}{2}$	$\frac{1}{2}$	$-\frac{1}{2}$	$1+1+\frac{1}{2}+\frac{1}{2}$	$-\frac{1}{2}$	$\frac{1}{2}$	$-\frac{1}{2}$	-1

Indeed this is the row shown in Fig. 2.5.

Example:
In the example with 17 degrees of freedom the numerical results shown in Fig. 2.7 are found. These results are for a dead load $p_y = 1$ and $E = t = 1$, $a = 2$ and $b = 1$.

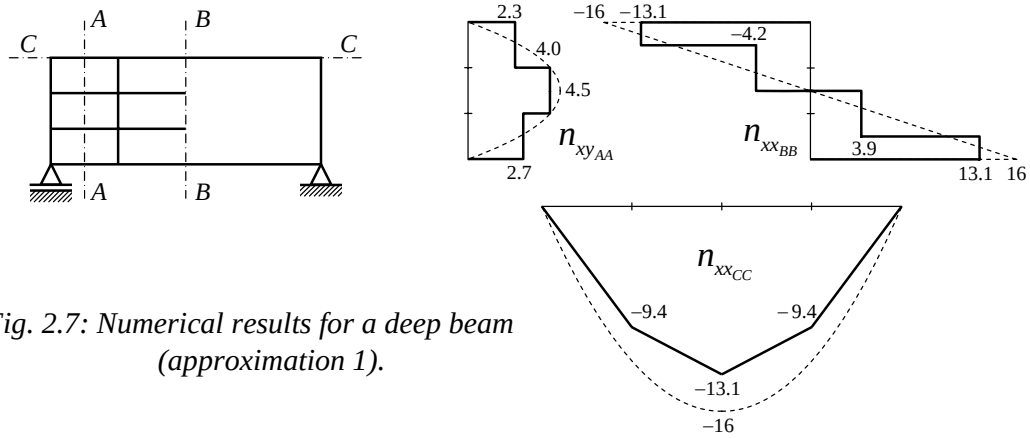

Fig. 2.7: Numerical results for a deep beam (approximation 1).

In cross-section *AA* the distribution of n_{xy} can be seen and it shows that n_{xy} is constant per panel. The distribution of n_{xx} over cross-section *BB* is achieved from the normal force in the lumped horizontal springs. The lumped normal force is converted to a distributed force n_{xx} taking into account the relevant plate parts. In edge *CC* we see the distribution of n_{xx} along the horizontal top edge of the deep beam.
For comparison in all the diagrams the solution that holds for slender beams according to the bending theory is given (dashed).

Remark
Usually, when the Finite Difference Method (Dutch: differentierekening) is applied, *molecules* are used, as was mentioned in chapter 1, which express the contribution of the surrounding degrees of freedom to the equilibrium equation of a given degree of freedom. When no interaction occurs with boundary conditions, the molecules for an equal a and b in the *x*-direction and *y*-direction are given in Fig. 2.8 (except for a factor $E\,t$).
Row 9 of the stiffness matrix corresponds with the molecule for the *y*-direction.
The molecule for the *x*-direction will be proved, leaving the proof for the *y*-direction to the reader. The partial differential equation is:

$$-E\,t\left(\frac{\partial^2 u_x}{\partial y^2}+\frac{1}{2}\frac{\partial^2 u_x}{\partial y^2}+\frac{1}{2}\frac{\partial^2 u_y}{\partial x \partial y}\right)=p_x$$

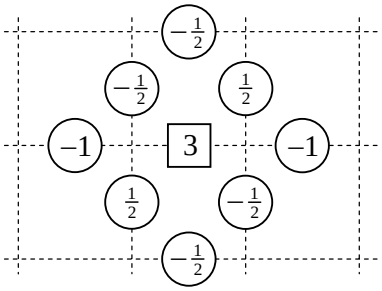

Molecule for *x*-direction

$$-E\,t\left(\frac{\partial^2 u_x}{\partial x^2}+\frac{1}{2}\frac{\partial^2 u_x}{\partial y^2}+\frac{1}{2}\frac{\partial^2 u_y}{\partial x\partial y}\right)=p_x$$

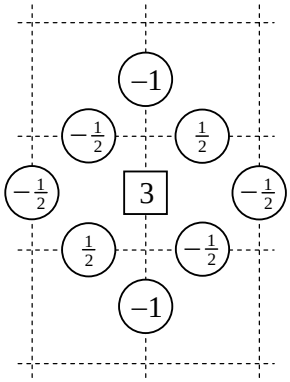

Molecule for *y*-direction

$$-E\,t\left(\frac{\partial^2 u_y}{\partial y^2}+\frac{1}{2}\frac{\partial^2 u_y}{\partial x^2}+\frac{1}{2}\frac{\partial^2 u_x}{\partial x\partial y}\right)=p_y$$

Fig. 2.8: Molecules for the differential equations for the x- and y-directions.

A grid of unknown displacements is used according to Fig. 2.9. In the centre of the grid (position e) $\partial^2 u_x/\partial x^2$ can be replaced by:

$$\frac{\partial^2 u_x}{\partial x^2}=\frac{u_d-2u_e+u_f}{a^2} \tag{2.3}$$

Similarly $\partial^2 u_x/\partial y^2$ is replaced by:

$$\frac{\partial^2 u_x}{\partial y^2}=\frac{u_a-2u_e+u_i}{a^2} \tag{2.4}$$

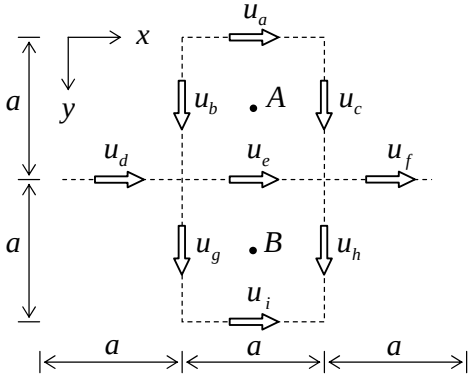

Fig. 2.9: Grid with displacements.

The term $\partial^2 u_y/\partial x\partial y$ can be replaced by $\partial H/\partial y$ in which $H=\partial u_y/\partial x$.
We calculate H in the positions A and B:

$$H_A=\frac{u_c-u_b}{a}\quad;\quad H_B=\frac{u_h-u_g}{a}$$

The value of $\partial H/\partial y$ in position e is:

$$\frac{\partial H}{\partial y} = \frac{H_B - H_A}{a} = \frac{u_h - u_g - u_c + u_b}{a^2}$$

So:

$$\frac{\partial^2 u_y}{\partial x \partial y} = \frac{u_b - u_c + u_h - u_g}{a^2} \tag{2.5}$$

Using (2.3), (2.4) and (2.5) the differential equation now becomes:

$$-E\,t\left\{\left(\frac{u_d - 2u_e + u_f}{a^2}\right) + \frac{1}{2}\left(\frac{u_a - 2u_e + u_i}{a^2}\right) + \frac{1}{2}\left(\frac{u_b - u_c + u_h - u_g}{a^2}\right)\right\} = p_x$$

Reassembly, and multiplication by a^2 yields:

$$E\,t\left(-\frac{1}{2}u_a - \frac{1}{2}u_b + \frac{1}{2}u_c - u_d + 3u_e - u_f + \frac{1}{2}u_g - \frac{1}{2}u_h - \frac{1}{2}u_i\right) = p_x\,a^2$$

The right-hand member is the loading term. The coefficients in the left-hand member produce the required scheme as given in Fig. 2.10.

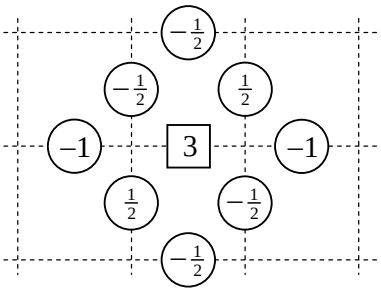

Fig. 2.10: Differential molecule in u_x direction.

The conventional Finite Difference Method is difficult to apply to nodes close to or on the boundary. Also, abrupt changes in thickness are difficult to deal with. The concept of springs and shear panels explained here provides an elegant way to overcome such difficulties.

2.2 Assembly of Bar Elements and Shear Panels. Approximation 2

In chapter 1 “approximation 2” was introduced for beam elements under axial loading. The same approximation can be used for plate elements. As before, first we consider the plate action for n_{xx} and n_{yy}.

Now the approximation of a rectangular plate part consists of four elastic truss elements (Fig. 2.11). The corners of the plate part are nodes, and each node has two degrees of freedom, one in the *x*-direction, and one in the *y*-direction. The axial stiffnesses of the four truss elements are chosen such that ε_{xx} equals ε_{yy} for the same homogeneous field of stresses n_{xx} and n_{yy}.

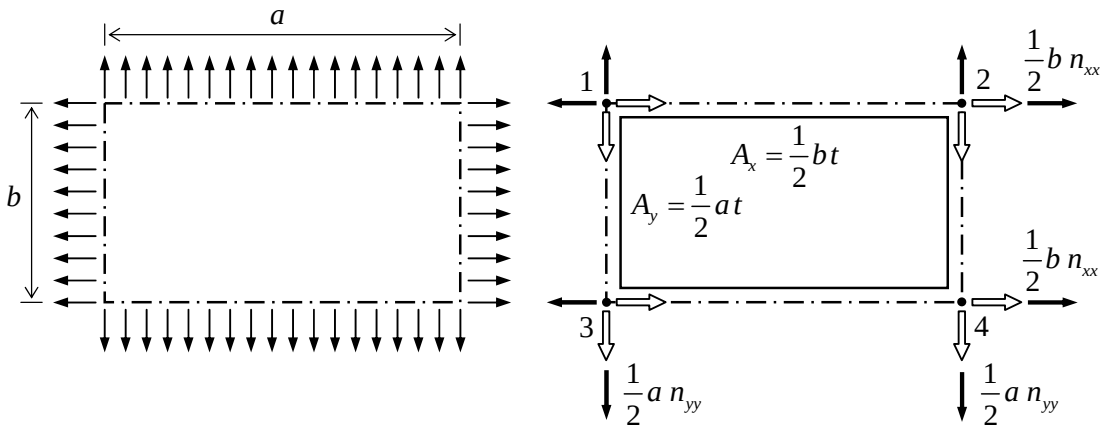

Fig. 2.11: Discretization of rectangular plate by four truss elements (approximation 2).

This approximation has the advantage that a replacing element is used, of which the stiffness can be determined from that plate part. Other surrounding plate parts need not be considered as is the case for "approximation 1". This makes "approximation 2" more suitable for application in general purpose computer programs. Once again, using the quantities $\alpha = \beta^{-1} = a/b$ the stiffness matrix of the element now is:

$$\begin{Bmatrix} F_{x1} \\ F_{y1} \\ F_{x2} \\ F_{y2} \\ F_{x3} \\ F_{y3} \\ F_{x4} \\ F_{y4} \end{Bmatrix} = \frac{1}{2}Et \begin{bmatrix} \beta & 0 & -\beta & 0 & 0 & 0 & 0 & 0 \\ 0 & \alpha & 0 & 0 & 0 & -\alpha & 0 & 0 \\ -\beta & 0 & \beta & 0 & 0 & 0 & 0 & 0 \\ 0 & 0 & 0 & \alpha & 0 & 0 & 0 & -\alpha \\ 0 & 0 & 0 & 0 & \beta & 0 & -\beta & 0 \\ 0 & -\alpha & 0 & 0 & 0 & \alpha & 0 & 0 \\ 0 & 0 & 0 & 0 & -\beta & 0 & \beta & 0 \\ 0 & 0 & 0 & -\alpha & 0 & 0 & 0 & \alpha \end{bmatrix} \begin{Bmatrix} u_{x1} \\ u_{y1} \\ u_{x2} \\ u_{y2} \\ u_{x3} \\ u_{y3} \\ u_{x4} \\ u_{y4} \end{Bmatrix}$$

Next, the contribution of the stresses n_{xy} is added. As was done in "approximation 1" a shear panel with a constant shear stress is used. Now, the problem is that this panel does not use the same degrees of freedom as the element representing the contribution of the stresses n_{xx} and n_{yy}, see Fig. 2.12.
This inconsistency is solved by assuming that the shear displacements are the average of the corresponding displacements in the element for n_{xx} and n_{yy}. The generalised forces in the

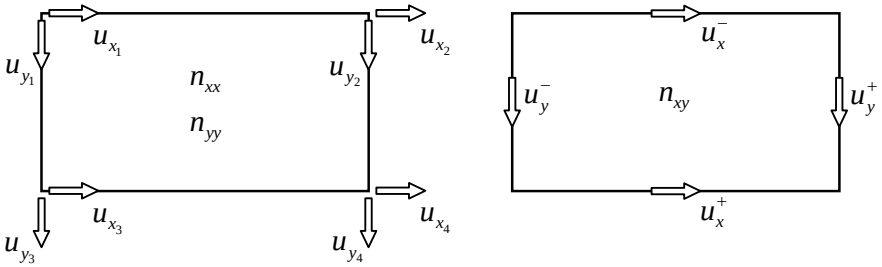

Fig. 2.12: Different displacements for trusses and panel in approximation 1 and approximation 2.

shear panel are distributed equally over the corresponding generalised forces in the element corners. So, we reach:

$$u_x^- = \frac{1}{2}(u_{x1} + u_{x2}) \quad ; \quad F_{x1} = F_{x2} = \frac{1}{2}F_x^-$$
$$u_x^+ = \frac{1}{2}(u_{x3} + u_{x4}) \quad ; \quad F_{x3} = F_{x4} = \frac{1}{2}F_x^+$$
$$u_y^- = \frac{1}{2}(u_{y1} + u_{y3}) \quad ; \quad F_{y1} = F_{y3} = \frac{1}{2}F_y^-$$
$$u_y^+ = \frac{1}{2}(u_{y2} + u_{y4}) \quad ; \quad F_{y2} = F_{y4} = \frac{1}{2}F_y^+$$

Applying these relations and the relation which already was found between the displacements u_x^-, u_x^+, u_y^-, u_y^+ and the generalised forces F_x^-, F_x^+, F_y^-, F_y^+ we can derive the stiffness matrix for the new shear panel:

$$\begin{Bmatrix} F_{x1} \\ F_{y1} \\ F_{x2} \\ F_{y2} \\ F_{x3} \\ F_{y3} \\ F_{x4} \\ F_{y4} \end{Bmatrix} = \frac{1}{8}Et \begin{bmatrix} \alpha & 1 & \alpha & -1 & -\alpha & 1 & -\alpha & -1 \\ 1 & \beta & 1 & -\beta & -1 & \beta & -1 & -\beta \\ \alpha & 1 & \alpha & -1 & -\alpha & 1 & -\alpha & -1 \\ -1 & -\beta & -1 & \beta & 1 & -\beta & 1 & \beta \\ -\alpha & -1 & -\alpha & 1 & \alpha & -1 & \alpha & 1 \\ 1 & \beta & 1 & -\beta & -1 & \beta & -1 & -\beta \\ -\alpha & -1 & -\alpha & 1 & \alpha & -1 & \alpha & 1 \\ -1 & -\beta & -1 & \beta & 1 & -\beta & 1 & \beta \end{bmatrix} \begin{Bmatrix} u_{x1} \\ u_{y1} \\ u_{x2} \\ u_{y2} \\ u_{x3} \\ u_{y3} \\ u_{x4} \\ u_{y4} \end{Bmatrix}$$

Exercise:
Show that this matrix can also be found by a formal transformation of the stiffness matrix which holds for “approximation 1”. Use matrix algebra.

Summation of the stiffness matrix for the contribution of n_{xx} and n_{yy} and the stiffness matrix for the contribution of n_{xy} yields the global stiffness matrix of the new element:

$$\begin{Bmatrix} F_{x1} \\ F_{y1} \\ F_{x2} \\ F_{y2} \\ F_{x3} \\ F_{y3} \\ F_{x4} \\ F_{y4} \end{Bmatrix} = Et \begin{bmatrix} \frac{\alpha}{8}+\frac{\beta}{2} & \frac{1}{8} & \frac{\alpha}{8}-\frac{\beta}{2} & -\frac{1}{8} & -\frac{\alpha}{8} & \frac{1}{8} & -\frac{\alpha}{8} & -\frac{1}{8} \\ \frac{1}{8} & \frac{\beta}{2}+\frac{\alpha}{2} & \frac{1}{8} & -\frac{\beta}{8} & -\frac{1}{8} & \frac{\beta}{8}-\frac{\alpha}{2} & -\frac{1}{8} & -\frac{\beta}{8} \\ \frac{\alpha}{8}-\frac{\beta}{2} & \frac{1}{8} & \frac{\alpha}{8}+\frac{\beta}{2} & -\frac{1}{8} & -\frac{\alpha}{8} & \frac{1}{8} & -\frac{\alpha}{8} & -\frac{1}{8} \\ -\frac{1}{8} & -\frac{\beta}{8} & -\frac{1}{8} & \frac{\alpha}{2}+\frac{\beta}{8} & \frac{1}{8} & -\frac{\beta}{8} & \frac{1}{8} & \frac{\beta}{8}-\frac{\alpha}{2} \\ -\frac{\alpha}{8} & -\frac{1}{8} & -\frac{\alpha}{8} & \frac{1}{8} & \frac{\alpha}{8}+\frac{\beta}{2} & -\frac{1}{8} & \frac{\alpha}{8}-\frac{\beta}{2} & \frac{1}{8} \\ \frac{1}{8} & \frac{\beta}{8}-\frac{\alpha}{2} & \frac{1}{8} & -\frac{\beta}{8} & -\frac{1}{8} & \frac{\beta}{8}+\frac{\alpha}{2} & -\frac{1}{8} & -\frac{\beta}{8} \\ -\frac{\alpha}{8} & -\frac{1}{8} & -\frac{\alpha}{8} & \frac{1}{8} & \frac{\alpha}{8}-\frac{\beta}{2} & -\frac{1}{8} & \frac{\alpha}{8}+\frac{\beta}{2} & \frac{1}{8} \\ -\frac{1}{8} & -\frac{\beta}{8} & -\frac{1}{8} & \frac{\beta}{8}-\frac{\alpha}{2} & \frac{1}{8} & -\frac{\beta}{8} & \frac{1}{8} & \frac{\beta}{8}+\frac{\alpha}{2} \end{bmatrix} \begin{Bmatrix} u_{x1} \\ u_{y1} \\ u_{x2} \\ u_{y2} \\ u_{x3} \\ u_{y3} \\ u_{x4} \\ u_{y4} \end{Bmatrix}$$

The correctness of stiffness matrices can be checked in a number of ways. The matrices at least need to satisfy the following requirements:

- symmetry
- positive diagonal terms
- rigid body translations and rotations produce zero generalised forces

The found general stiffness matrix meets all these requirements.

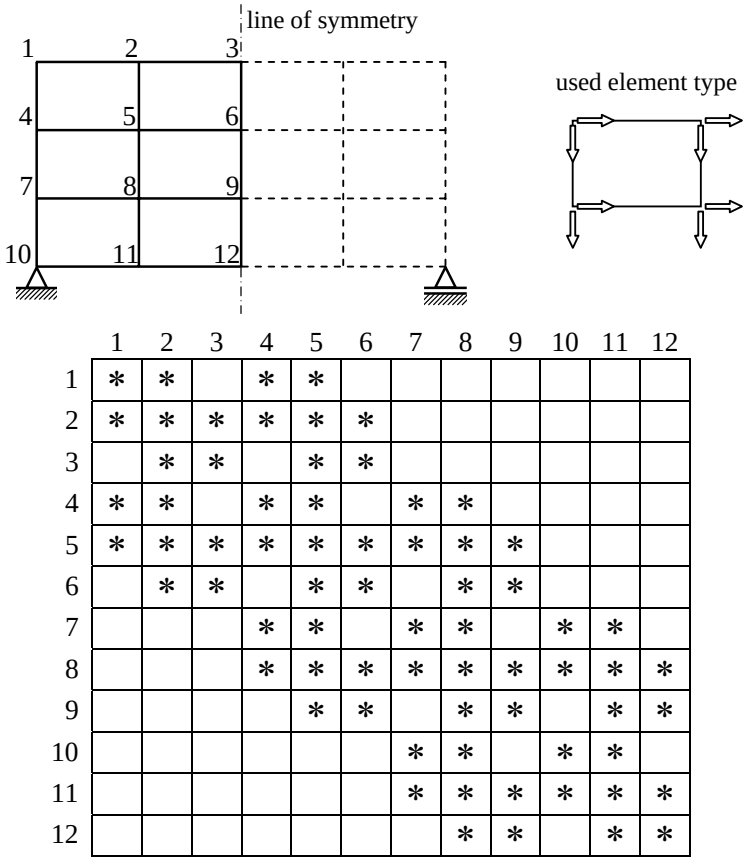

Fig. 2.13: Construction of the global stiffness matrix for a deep beam (approximation 2).

In Fig. 2.13 it is shown what the global stiffness matrix of a total structure will look like. Each partition of this matrix is a two by two matrix in itself. The row corresponding to u_{x8} has been calculated. The result is given, without the multiplication coefficient $E\,t$. Here the dimensions a and b are equal:

	4		5		6		7		8		9		10		11		12	
row 8	$-\frac{1}{8}$	$-\frac{1}{8}$	$-\frac{1}{4}$	0	$-\frac{1}{8}$	$\frac{1}{8}$	$-\frac{3}{4}$	0	$\frac{5}{2}$	0	$-\frac{3}{4}$	0	$-\frac{1}{8}$	$\frac{1}{8}$	$-\frac{1}{4}$	0	$-\frac{1}{8}$	$-\frac{1}{8}$

Numerical results are shown in Fig. 2.14, for only applying dead load again. The other used data is: $p_y = 1,\ E = t = 1,\ a = 2$ and $b = 1$.

Notice that the distribution of n_{xx} along the top of the edge of the beam in cross-section *CC* differs from the one found in “approximation 1”. Therefore, cross-section *BB* was chosen at a different position this time.

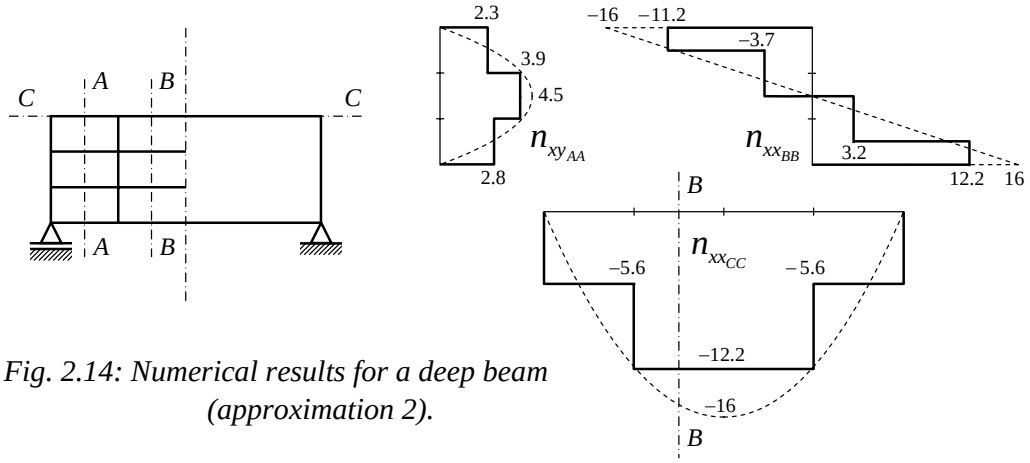

Fig. 2.14: Numerical results for a deep beam (approximation 2).

2.3 Refined Approximation 2

We can improve the element in "Approximation 2" in the following way. For the transfer of the forces n_{xx} a lattice of strings in the *x*-direction is used instead of just two truss elements along the edges (Fig. 2.15). Of course, the strings can transfer both tensile and compressive

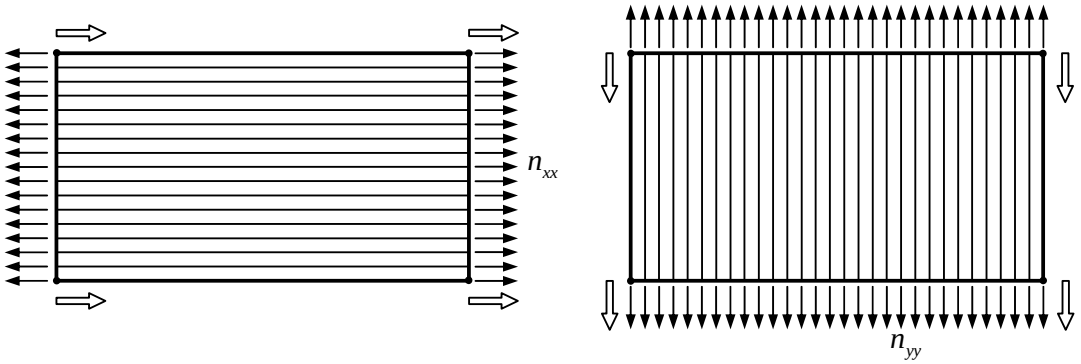

Fig. 2.15: Improved element (refined approximation 2).

forces. Similarly, a lattice of vertical strings is applied for n_{yy}. For the lattice of n_{xx} we assume that the vertical edges remain straight during deformation of the plate. This ensures a linear distribution of horizontal displacements $u_x(y)$ along the vertical edges. In the same fashion, the vertical displacements $u_y(x)$ are distributed linearly along the horizontal edges for the n_{yy} lattice. Summation of the two lattices, produces the stiffness matrix for the combined actions of n_{xx} and n_{yy}.

This 8 by 8 stiffness matrix can be derived column by column. Here, the column that corresponds to the horizontal displacement of the top right-hand corner will be calculated through an example. The terms in this column may be interpreted as the support reactions (generalised element forces) that occur when the considered displacement is given the value 1, and all other degrees of freedom are zero.

In Fig. 2.16, the displacement field that occurs for $u_{x2} \neq 0$ is given. Only linearly distributed strains ε_{xx} and membrane forces n_{xx} occur. These distributed forces are lumped in the nodes, delivering F_{x2} and F_{x4}. These forces have the same resultant (position and value) as the distributed membrane forces n_{xx}. In nodes 1 and 3, $F_{x1} = -F_{x2}$ and $F_{x3} = -F_{x4}$ are found. All

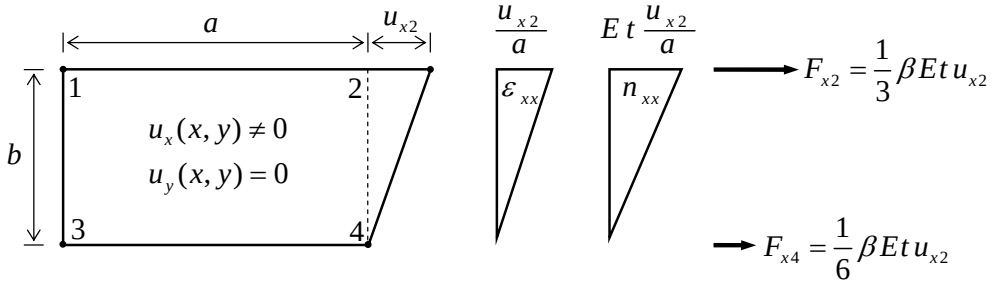

Fig. 2.16: Element with displacement of one node in one direction ($\upsilon = 0$).

generalised forces F_{yi} are zero. Forces found in this way form the values for the column u_{x2} (values for $u_{x2} = 1$). In this way all columns can be calculated:

$$\begin{Bmatrix} F_{x1} \\ F_{y1} \\ F_{x2} \\ F_{y2} \\ F_{x3} \\ F_{y3} \\ F_{x4} \\ F_{y4} \end{Bmatrix} = E\,t \begin{bmatrix} \frac{1}{3}\beta & 0 & -\frac{1}{3}\beta & 0 & \frac{1}{6}\beta & 0 & -\frac{1}{6}\beta & 0 \\ 0 & \frac{1}{3}\alpha & 0 & \frac{1}{6}\alpha & 0 & -\frac{1}{3}\alpha & 0 & -\frac{1}{6}\alpha \\ -\frac{1}{3}\beta & 0 & \frac{1}{3}\beta & 0 & -\frac{1}{6}\beta & 0 & \frac{1}{6}\beta & 0 \\ 0 & \frac{1}{6}\alpha & 0 & \frac{1}{3}\alpha & 0 & -\frac{1}{6}\alpha & 0 & -\frac{1}{3}\alpha \\ \frac{1}{6}\beta & 0 & -\frac{1}{6}\beta & 0 & \frac{1}{3}\beta & 0 & -\frac{1}{3}\beta & 0 \\ 0 & -\frac{1}{3}\alpha & 0 & -\frac{1}{6}\alpha & 0 & \frac{1}{3}\alpha & 0 & \frac{1}{6}\alpha \\ -\frac{1}{6}\beta & 0 & \frac{1}{6}\beta & 0 & -\frac{1}{3}\beta & 0 & \frac{1}{3}\beta & 0 \\ 0 & -\frac{1}{6}\alpha & 0 & -\frac{1}{3}\alpha & 0 & \frac{1}{6}\alpha & 0 & \frac{1}{3}\alpha \end{bmatrix} \begin{Bmatrix} u_{x1} \\ u_{y1} \\ u_{x2} \\ u_{y2} \\ u_{x3} \\ u_{y3} \\ u_{x4} \\ u_{y4} \end{Bmatrix}$$

This refined stiffness matrix for the contribution of n_{xx} and n_{yy} is now combined with the same stiffness matrix for the contribution of n_{xy} as was used in "approximation 2" (with constant shear). The total refined element stiffness matrix now reads:

$$\begin{Bmatrix} F_{x1} \\ F_{y1} \\ F_{x2} \\ F_{y2} \\ F_{x3} \\ F_{y3} \\ F_{x4} \\ F_{y4} \end{Bmatrix} = E\,t \begin{bmatrix} \frac{\alpha}{8}+\frac{\beta}{3} & \frac{1}{8} & \frac{\alpha}{8}-\frac{\beta}{3} & -\frac{1}{8} & -\frac{\alpha}{8}+\frac{\beta}{6} & \frac{1}{8} & -\frac{\alpha}{8}-\frac{\beta}{6} & -\frac{1}{8} \\ \frac{1}{8} & \frac{\alpha}{3}+\frac{\beta}{8} & \frac{1}{8} & \frac{\alpha}{6}-\frac{\beta}{8} & -\frac{1}{8} & -\frac{\alpha}{3}+\frac{\beta}{8} & -\frac{1}{8} & -\frac{\alpha}{6}-\frac{\beta}{8} \\ \frac{\alpha}{8}-\frac{\beta}{3} & \frac{1}{8} & \frac{\alpha}{8}+\frac{\beta}{3} & -\frac{1}{8} & -\frac{\alpha}{8}-\frac{\beta}{6} & \frac{1}{8} & -\frac{\alpha}{8}+\frac{\beta}{6} & -\frac{1}{8} \\ -\frac{1}{8} & \frac{\alpha}{6}-\frac{\beta}{8} & -\frac{1}{8} & \frac{\alpha}{3}+\frac{\beta}{8} & \frac{1}{8} & -\frac{\alpha}{6}-\frac{\beta}{8} & \frac{1}{8} & -\frac{\alpha}{3}+\frac{\beta}{8} \\ -\frac{\alpha}{8}+\frac{\beta}{6} & -\frac{1}{8} & -\frac{\alpha}{8}-\frac{\beta}{6} & \frac{1}{8} & \frac{\alpha}{8}+\frac{\beta}{3} & -\frac{1}{8} & \frac{\alpha}{8}-\frac{\beta}{3} & \frac{1}{8} \\ \frac{1}{8} & -\frac{\alpha}{3}+\frac{\beta}{8} & \frac{1}{8} & -\frac{\alpha}{6}-\frac{\beta}{8} & -\frac{1}{8} & \frac{\alpha}{3}+\frac{\beta}{8} & -\frac{1}{8} & \frac{\alpha}{6}-\frac{\beta}{8} \\ -\frac{\alpha}{8}-\frac{\beta}{6} & -\frac{1}{8} & -\frac{\alpha}{8}+\frac{\beta}{6} & \frac{1}{8} & \frac{\alpha}{8}-\frac{\beta}{3} & -\frac{1}{8} & \frac{\alpha}{8}+\frac{\beta}{3} & \frac{1}{8} \\ -\frac{1}{8} & \frac{\alpha}{6}-\frac{\beta}{8} & -\frac{1}{8} & -\frac{\alpha}{3}+\frac{\beta}{8} & \frac{1}{8} & \frac{\alpha}{6}-\frac{\beta}{8} & \frac{1}{8} & \frac{\alpha}{3}+\frac{\beta}{8} \end{bmatrix} \begin{Bmatrix} u_{x1} \\ u_{y1} \\ u_{x2} \\ u_{y2} \\ u_{x3} \\ u_{y3} \\ u_{x4} \\ u_{y4} \end{Bmatrix}$$

This refined element produces numerical results as shown in Fig. 2.17 (same problem as the previous).

In "approximation 1" the membrane force n_{xx} varies linearly in the *x*-direction, and stepwise in the *y*-direction. In "approximation 2" the distribution is stepwise in both directions. Now, in the "refined approximation 2" n_{xx} has a linear distribution in the *y*-direction, and is stepwise constant in the *x*-direction! This element can be referred to as an application of the Finite Element Method.

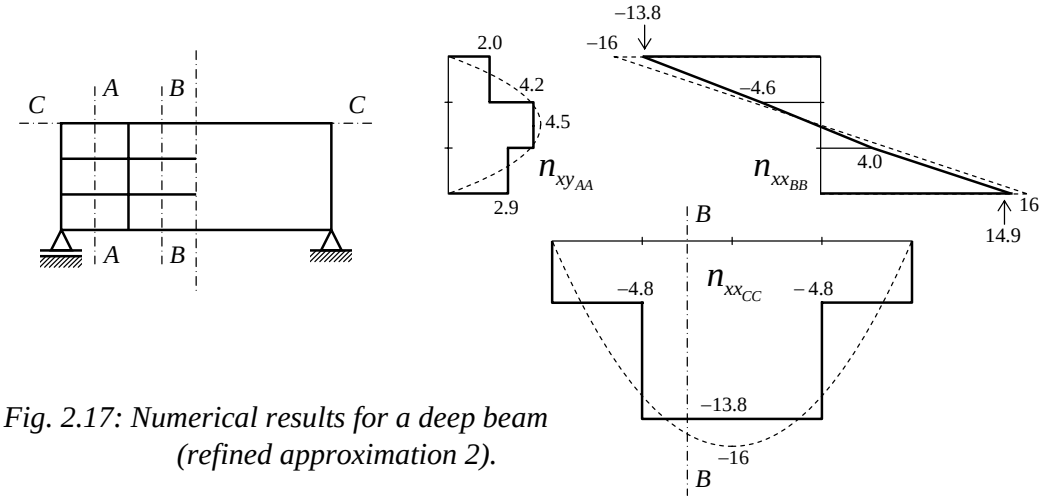

Fig. 2.17: Numerical results for a deep beam (refined approximation 2).

3 Plates. Finite Element Method (FEM)

In the preceding chapter 2 a finite plate element was derived, using insight, engineering judgement and experience in a more or less practical way. This approach has to its advantage that the approximations made are well understood, but there are too some large disadvantages. For instance, it is not easy to see how the deal with the effects of the lateral contraction ($\upsilon \neq 0$). In addition, it is not clear in this approach how to solve problems for elements of another shape, such as triangles and quadrilaterals. Moreover, no general method was developed with which elements for other types of structures can be derived, like slabs, shells and solid structures. Therefore, now a general approach will be discussed which is applicable in all situations and circumstances.

3.1 Truss Element (introduction)

Before moving to the finite element method for plates loaded in-plane, the finite element strategy is shown for a very simple case, the truss element. All the necessary steps will occur, without straying into confusing mathematical details. After that, the extension to plate elements is easily made.

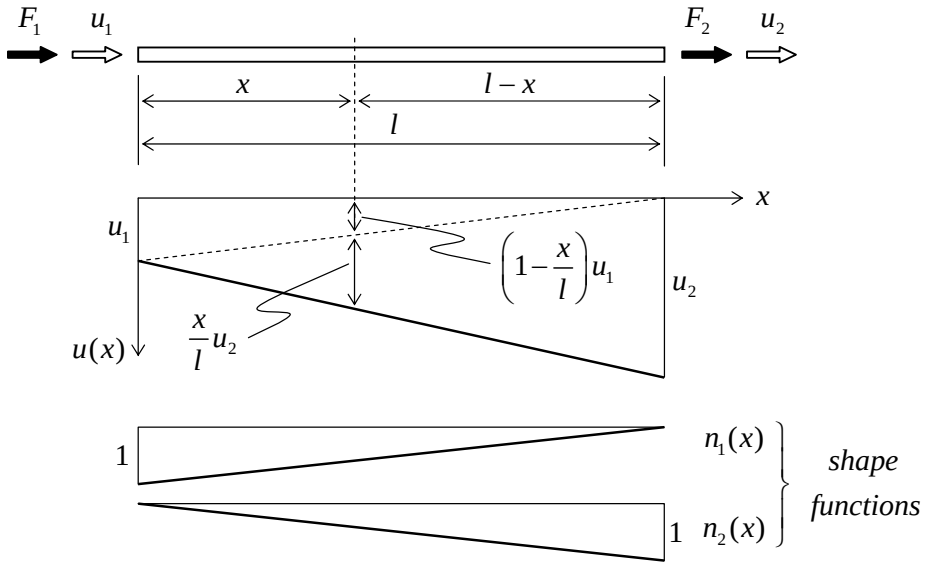

Fig. 3.1: Definitions and shape functions for the truss element.

Fig. 3.1 defines the truss element. The length is l, the cross-sectional area is A, the modulus of elasticity (Young's' modulus) is E. The truss element is loaded at its ends with forces F_1 and F_2 respectively. The displacements u_1 and u_2 of the truss ends are the degrees of freedom of the element. We introduce a displacement vector $\boldsymbol{u}$ and a force vector $\boldsymbol{f}$:

$$\boldsymbol{u} = \begin{Bmatrix} u_1 \\ u_2 \end{Bmatrix} \quad ; \quad \boldsymbol{f} = \begin{Bmatrix} F_1 \\ F_2 \end{Bmatrix}$$

and want to determine the stiffness matrix ***K*** which relates the two vectors to each other:

$$\boldsymbol{f} = \boldsymbol{K}\,\boldsymbol{u} \tag{3.1}$$

Matrix $\boldsymbol{K}$ has two rows and two columns. An x-axis is chosen along the element with its origin in the left-hand end. The first step in the method is to assume a displacement field, i.e. to interpolate the displacement $u_c(x)$ at any position x. The subscript c denotes formation of a continuous displacement field, to be distinguished from the discrete values u_1 and u_2. For the interpolation function, a linear distribution is chosen. (Later on, we will discuss the rules to be followed for selecting a function. It will become clear that we cannot use any arbitrary distribution). In Fig. 3.1 a dashed auxiliary line is drawn dividing u_c into two parts:

$$\frac{l-x}{l}u_1 \qquad (\textit{upper part})$$

$$\frac{x}{l}u_2 \qquad (\textit{lower part})$$

If we introduce the shape functions:

$$n_1(x) = \left(1 - \frac{x}{l}\right) \quad ; \quad n_2(x) = \left(\frac{x}{l}\right)$$

we may write:

$$u_c(x) = n_1(x)\,u_1 + n_2(x)\,u_2$$

One can note this differently:

$$u_c(x) = \begin{bmatrix} n_1(x) & n_2(x) \end{bmatrix} \begin{Bmatrix} u_1 \\ u_2 \end{Bmatrix}$$

In short this can be written as:

$$u_c(x) = \boldsymbol{N}\,\boldsymbol{u} \tag{3.2}$$

In case of the truss element, only one row occurs in matrix ***N***, but more rows may occur in other elements. Shape function $n_1(x)$ is related to displacement u_1 and $n_2(x)$ to u_2. It is a property that the shape function has the value 1 in the node where its relative degree of freedom is defined and is zero for the other degree(s) of freedom. The next step is to derive the strain $\varepsilon(x)$ in the element by using the kinematic relation $\varepsilon = du/dx$ *:*

$$\varepsilon = \begin{bmatrix} b_1(x) & b_2(x) \end{bmatrix} \begin{Bmatrix} u_1 \\ u_2 \end{Bmatrix}$$

abridged as:

$$\boxed{\boldsymbol{\varepsilon} = \boldsymbol{B}\,\boldsymbol{u}} \tag{3.3}$$

in which:

$$b_1(x) = \frac{dn_1}{dx} \quad ; \quad b_2(x) = \frac{dn_2}{dx}$$

In the example of the truss element, just one component occurs in the vector $\boldsymbol{\varepsilon}$, but for other elements more strain components may be considered. Note that matrix $\boldsymbol{B}$ cannot be chosen completely independent of $\boldsymbol{N}$. Instead, it follows from the matrix with the shape functions.
The third step is to bring in the constitutive relation:

$$\boxed{\boldsymbol{\sigma} = \boldsymbol{D}\,\boldsymbol{\varepsilon}} \tag{3.4}$$

where $\boldsymbol{D}$ is the extensional stiffness EA and $\boldsymbol{\sigma}$ is the normal force N.
The next step is to consider the equilibrium of the element, i.e. the relations between the external forces $\boldsymbol{f}$ and the normal force N in the element. The essential aspect of the method is to replace equilibrium conditions by a virtual work equation. Let u_1 and u_2 have values, which yield a normal force N that is in equilibrium with the forces $\boldsymbol{f}$. A variation $\delta\boldsymbol{u}$ of the displacements will be accompanied by a small variation $\delta\boldsymbol{\varepsilon}$ of the strain and the virtual work of the forces $\boldsymbol{f}$ will be equal to the virtual work of the normal force N.

$$\delta\boldsymbol{u}^T\boldsymbol{f} = \int_0^l \delta\boldsymbol{\varepsilon}^T\boldsymbol{\sigma}\,dx$$

As we did for ε we will consider the normal force as a vector, to keep this analysis general. The superscript T denotes transposition of the vector.
The variation $\delta u_c(x)$ of $u_c(x)$ is interpolated in the same way as $u_c(x)$ itself, applying the same matrix of shape functions $\boldsymbol{N}$. This means that the matrix $\boldsymbol{B}$ occurs in the relation between $\delta\boldsymbol{\varepsilon}$ and $\delta\boldsymbol{u}$:

$$\delta\boldsymbol{\varepsilon} = \boldsymbol{B}\,\delta\boldsymbol{u}$$

By substituting this in the virtual work equation one obtains:

$$\delta\boldsymbol{u}^T\boldsymbol{f} = \delta\boldsymbol{u}^T\int_0^l \boldsymbol{B}^T\boldsymbol{\sigma}\,dx$$

Note that the rule of transposing of the product of two matrices is achieved by changing the order of the matrices in the product and transposing each of them is used here.
In the right-hand member of the equation $\delta\boldsymbol{u}^T$ is not a function of x and is brought outside the integral. Both members of the equation start with $\delta\boldsymbol{u}^T$ and we conclude:

$$\boxed{\boldsymbol{f} = \int_0^l \boldsymbol{B}^T \boldsymbol{\sigma}\, dx} \tag{3.5}$$

This is the wanted relation between the external forces $\boldsymbol{f}$ and the internal normal force N that is denoted by $\boldsymbol{\sigma}$.
Working out this relation for the truss element we obtain:

$$\boldsymbol{B} = \begin{bmatrix} -\frac{1}{l} & \frac{1}{l} \end{bmatrix}$$

$$\begin{Bmatrix} F_1 \\ F_2 \end{Bmatrix} = \int_0^l \begin{bmatrix} -\frac{1}{l} \\ \\ \frac{1}{l} \end{bmatrix} [N]\, dx = \begin{Bmatrix} -\int_0^l \frac{N}{l} dx \\ \int_0^l \frac{N}{l} dx \end{Bmatrix} = \begin{Bmatrix} -N \\ \\ N \end{Bmatrix}$$

The result $F_1 = -N$ and $F_2 = N$ is the expected result for the sign convention that N is positive when a tensile force.

The relations (3.3), (3.4) and (3.5) are important results in the finite element method. In Fig. 3.2 they are listed in a relation scheme for memoria technica.

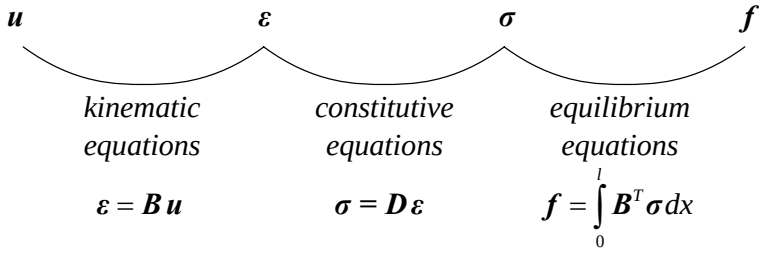

Fig. 3.2: Relation scheme for the truss element.

Substitution of (3.3) in (3.4) and finally in (3.5) yields:

$$\boldsymbol{f} = \int_0^l \boldsymbol{B}^T \boldsymbol{D}\, \boldsymbol{B}\, dx\, \boldsymbol{u}$$

from which it is concluded that:

$$\boxed{\boldsymbol{K} = \int_0^l \boldsymbol{B}^T \boldsymbol{D}\, \boldsymbol{B}\, dx} \tag{3.6}$$

This is the formal recipe to derive a stiffness matrix. The most important step is the choice of the shape functions, i.e. the matrix $\boldsymbol{N}$. After that no choices can be made anymore. Matrix $\boldsymbol{B}$ is derived from $\boldsymbol{N}$ on the basis of the kinematic relations and $\boldsymbol{D}$ is the constitutive law of the element. Elaborating (3.6) for the truss element one obtains:

$$\boldsymbol{B} = \begin{bmatrix} -\frac{1}{l} & \frac{1}{l} \end{bmatrix}$$

$$\boldsymbol{K} = \int_0^l \begin{bmatrix} -\frac{1}{l} \\ \frac{1}{l} \end{bmatrix} [EA] \begin{bmatrix} -\frac{1}{l} & \frac{1}{l} \end{bmatrix} dx \quad \rightarrow \quad \boldsymbol{K} = \begin{bmatrix} \int_0^l \frac{EA}{l^2} dx & \int_0^l \frac{-EA}{l^2} dx \\ \int_0^l \frac{-EA}{l^2} dx & \int_0^l \frac{EA}{l^2} dx \end{bmatrix} \quad \rightarrow \quad \boldsymbol{K} = \begin{bmatrix} \frac{EA}{l} & \frac{-EA}{l} \\ \frac{-EA}{l} & \frac{EA}{l} \end{bmatrix}$$

This stiffness matrix is the exact same one that has been used in the preceding chapters. In the case of the truss elements the terms in $\boldsymbol{B}$ are very simple, hence the integrations to obtain $\boldsymbol{K}$. For other elements more complexity may be involved.

3.2 Rectangular Element

The first step in this general approach is to choose a continuous displacement field $u_x(x, y)$ and $u_y(x, y)$. In the case of a rectangular element with four nodes (in the corners) the distributions of u_x and u_y should vary linearly along the edges (see Fig. 3.3). This allows for the displacement field to be written as follows:

$$u_x(x, y) = n_1(x, y)u_{x1} + n_2(x, y)u_{x2} + n_3(x, y)u_{x3} + n_4(x, y)u_{x4}$$
$$u_y(x, y) = n_1(x, y)u_{y1} + n_2(x, y)u_{y2} + n_3(x, y)u_{y3} + n_4(x, y)u_{y4}$$

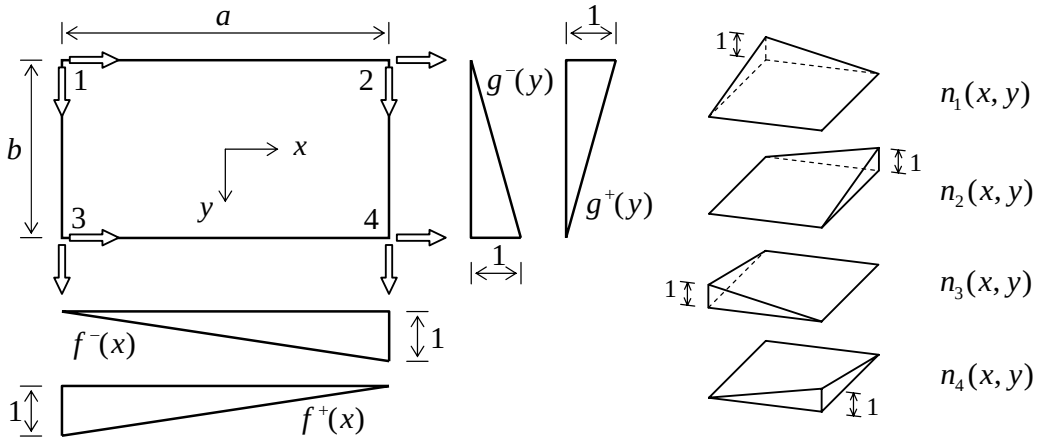

Fig. 3.3: Rectangular element with its shape functions.

The functions $n_1(x, y)$ up to $n_4(x, y)$ are called "shape functions". Function $n_1(x, y)$ takes a value 1 in node 1 and zero in the other three nodes. Along the edges $n_1(x, y)$ varies linearly.

Similarly, the other functions have a value 1 in the corresponding nodes and so on. To construct these functions four additional functions $f^-(x)$, $f^+(x)$, $g^-(y)$ and $g^+(y)$ are used. The equation $f^-(x)=0$ is the equation of the vertical edge in the negative x-domain. Outside of this edge $f^-(x)$ defines a plane. The coefficients in the equation $f^-(x)=0$ are scaled in such a way that $f^-(x)$ has a value 1 in the other vertical edge. This way $f^-(x)$ has become a coordinate that varies from 0 to 1 in the positive x-direction. Similarly $f^+(x)$ varies from 0 to 1 in the negative x-direction, and $g^-(y)$ and $g^+(y)$ have a corresponding role of area coordinates in the y-direction.
The functions are:

$$f^-(x)=\frac{1}{2}+\frac{x}{a} \quad ; \quad g^-(y)=\frac{1}{2}+\frac{y}{b}$$

$$f^+(x)=\frac{1}{2}-\frac{x}{a} \quad ; \quad g^+(y)=\frac{1}{2}-\frac{y}{b}$$

Now, the n-functions can be taken down using the f- and g-functions:

$$n_1(x,y)=f^+(x)\cdot g^+(y)$$

$$n_2(x,y)=f^-(x)\cdot g^+(y)$$

$$n_3(x,y)=f^+(x)\cdot g^-(y)$$

$$n_4(x,y)=f^-(x)\cdot g^-(y)$$

To determine the strains, the displacements will have to be differentiated. This requires the following derivatives:

$$\frac{df^-}{dx}=\frac{1}{a} \quad ; \quad \frac{dg^-}{dy}=\frac{1}{b}$$

$$\frac{df^+}{dx}=-\frac{1}{a} \quad ; \quad \frac{dg^+}{dy}=-\frac{1}{b}$$

Now, the strains found are:

$$\varepsilon_{xx}=\frac{\partial u_x}{\partial x} = -\frac{g^+}{a}u_{x1}+\frac{g^+}{a}u_{x2}-\frac{g^-}{a}u_{x3}+\frac{g^-}{a}u_{x4}$$

$$\varepsilon_{yy}=\frac{\partial u_y}{\partial y} = -\frac{f^+}{b}u_{y1}-\frac{f^-}{b}u_{y2}+\frac{f^+}{b}u_{y3}+\frac{f^-}{b}u_{y4}$$

$$\gamma_{xy}=\frac{\partial u_x}{\partial y}+\frac{\partial u_y}{\partial x}=-\frac{f^+}{b}u_{x1}-\frac{f^-}{b}u_{x2}+\frac{f^+}{b}u_{x3}+\frac{f^-}{b}u_{x4}+$$

$$-\frac{g^+}{a}u_{y1}+\frac{g^+}{a}u_{y2}-\frac{g^-}{a}u_{y3}+\frac{g^-}{a}u_{y4}$$

The constitutive relations define the relation between the stresses and the strains. In a state of plane stress (in Dutch: vlakke spanningstoestand):

$$n_{xx} = \frac{E\,t}{1-\upsilon^2}\left(\varepsilon_{xx} + \upsilon\,\varepsilon_{yy}\right)$$

$$n_{yy} = \frac{E\,t}{1-\upsilon^2}\left(\upsilon\,\varepsilon_{xx} + \varepsilon_{yy}\right) \qquad \text{(}\textit{rigidity relations}\text{)}$$

$$n_{xy} = \frac{E\,t}{2\left(1+\upsilon\right)}\,\gamma_{xy}$$

It is convenient to use matrix and vector notation to define the displacement field, strain field and stress field. We introduce:

$$\left.\begin{aligned} \boldsymbol{u}^T &= \left\{u_{x1} \quad u_{y1} \quad u_{x2} \quad u_{y2} \quad u_{x3} \quad u_{y3} \quad u_{x4} \quad u_{y4}\right\} \\ \boldsymbol{f}^T &= \left\{F_{x1} \quad F_{y1} \quad F_{x2} \quad F_{y2} \quad F_{x3} \quad F_{y3} \quad F_{x4} \quad F_{y4}\right\} \end{aligned}\right\} \textit{ in nodes}$$

$$\left.\begin{aligned} \boldsymbol{\varepsilon}(x,y)^T &= \left\{\varepsilon_{xx}(x,y) \quad \varepsilon_{yy}(x,y) \quad \gamma_{xy}(x,y)\right\} \\ \boldsymbol{\sigma}(x,y)^T &= \left\{n_{xx}(x,y) \quad n_{yy}(x,y) \quad n_{xy}(x,y)\right\} \\ \boldsymbol{u}_c(x,y)^T &= \left\{u_x(x,y) \quad u_y(x,y)\right\} \\ \boldsymbol{p}(x,y)^T &= \left\{p_x(x,y) \quad p_y(x,y)\right\} \end{aligned}\right\} \textit{ over element area}$$

The following relation exists:

$$\boldsymbol{u}_c = \boldsymbol{N}(x,y)\,\boldsymbol{u} \qquad \text{(}\textit{interpolation}\text{)}$$

$$\boldsymbol{\varepsilon} = \boldsymbol{B}(x,y)\,\boldsymbol{u} \qquad \text{(}\textit{kinematic relation}\text{)}$$

$$\boldsymbol{\sigma} = \boldsymbol{D}(x,y)\,\boldsymbol{\varepsilon} \qquad \text{(}\textit{rigidity relation}\text{)}$$

Summarizing (from now on the dependencies on x and y will not be written anymore):

$$\begin{Bmatrix} u_x \\ u_y \end{Bmatrix} = \begin{bmatrix} n_1 & 0 & n_2 & 0 & n_3 & 0 & n_4 & 0 \\ 0 & n_1 & 0 & n_2 & 0 & n_3 & 0 & n_4 \end{bmatrix} \begin{Bmatrix} u_{x1} \\ u_{y1} \\ u_{x2} \\ u_{y2} \\ u_{x3} \\ u_{y3} \\ u_{x4} \\ u_{y4} \end{Bmatrix}$$

Written in short:

$$\boxed{\boldsymbol{u}_c = \boldsymbol{N}\,\boldsymbol{u}} \tag{3.7}$$

From this the kinematic relation can be derived:

$$\begin{Bmatrix} \varepsilon_{xx} \\ \varepsilon_{yy} \\ \gamma_{xy} \end{Bmatrix} = \left[\begin{array}{cccccccc} -g^+/a & 0 & g^+/a & 0 & -g^-/a & 0 & g^-/a & 0 \\ 0 & -f^+/b & 0 & -f^-/b & 0 & f^+/b & 0 & f^-/b \\ -f^+/b & -g^+/a & -f^-/b & g^+/a & f^+/b & -g^-/a & f^-/b & g^-/a \end{array}\right] \begin{Bmatrix} u_{x1} \\ u_{y1} \\ u_{x2} \\ u_{y2} \\ u_{x3} \\ u_{y3} \\ u_{x4} \\ u_{y4} \end{Bmatrix}$$

or in short:

$$\boxed{\boldsymbol{\varepsilon} = \boldsymbol{B}\,\boldsymbol{u}} \tag{3.8}$$

in which $\boldsymbol{B}$ is the *kinematic matrix*.

The constitutive equation is:

$$\begin{Bmatrix} n_{xx} \\ n_{yy} \\ n_{xy} \end{Bmatrix} = \frac{E\,t}{1-\upsilon^2} \begin{bmatrix} 1 & \upsilon & 0 \\ \upsilon & 1 & 0 \\ 0 & 0 & \dfrac{1-\upsilon}{2} \end{bmatrix} \begin{Bmatrix} \varepsilon_{xx} \\ \varepsilon_{yy} \\ \gamma_{xy} \end{Bmatrix}$$

in short:

$$\boxed{\boldsymbol{\sigma} = \boldsymbol{D}\,\boldsymbol{\varepsilon}} \tag{3.9}$$

By substituting (3.8) into (3.9) a relation can be derived between the membrane forces $\boldsymbol{\sigma}$ and the element degrees of freedom $\boldsymbol{u}$. The result is:

$$\boxed{\boldsymbol{\sigma} = \boldsymbol{D}\,\boldsymbol{B}\,\boldsymbol{u}} \tag{3.10}$$

Written out in full this reads:

$$\begin{Bmatrix} n_{xx} \\ n_{yy} \\ n_{xy} \end{Bmatrix} = \frac{E\,t}{1-\upsilon^2} \left[\begin{array}{cccc|cccc} -\frac{1}{a}g^+ & -\frac{\upsilon}{b}f^+ & \frac{1}{a}g^+ & -\frac{\upsilon}{b}f^- & -\frac{1}{a}g^- & \frac{\upsilon}{b}f^+ & \frac{1}{a}g^- & \frac{\upsilon}{b}f^- \\ -\frac{\upsilon}{a}g^+ & -\frac{1}{b}f^+ & \frac{\upsilon}{a}g^+ & -\frac{1}{b}f^- & -\frac{\upsilon}{a}g^- & \frac{1}{b}f^+ & \frac{\upsilon}{a}g^- & \frac{1}{b}f^- \\ \hline -\frac{1-\upsilon}{2b}f^+ & -\frac{1-\upsilon}{2a}g^+ & -\frac{1-\upsilon}{2b}f^- & \frac{1-\upsilon}{2a}g^+ & \frac{1-\upsilon}{2b}f^+ & -\frac{1-\upsilon}{2a}g^- & \frac{1-\upsilon}{2b}f^- & \frac{1-\upsilon}{2a}g^- \end{array}\right] \begin{Bmatrix} u_{x1} \\ u_{y1} \\ u_{x2} \\ u_{y2} \\ u_{x3} \\ u_{y3} \\ u_{x4} \\ u_{y4} \end{Bmatrix}$$

Now, the final step is to look for a relation between the membrane forces (the stress resultants) and the generalised forces $\boldsymbol{f}$. In chapter 2, equilibrium considerations were used. Instead, a virtual work equation will be used now. The generalised element forces and the stress resultants are statically equivalent if they produce an equal amount of virtual work, when a virtual variation of the displacement field is applied. Suppose the virtual displacement field to be:

$$\delta \boldsymbol{u}_c = \boldsymbol{N}(x, y)\, \delta \boldsymbol{u}$$

and the virtual strains following from this:

$$\delta \boldsymbol{\varepsilon} = \boldsymbol{B}(x, y)\, \delta \boldsymbol{u}$$

Then the virtual work reads:

$$\delta \boldsymbol{u}^T \boldsymbol{f} = \iint_A \delta \boldsymbol{\varepsilon}^T \boldsymbol{\sigma}\, dA$$

Introducing $\delta \boldsymbol{\varepsilon}^T = \delta \boldsymbol{u}^T \boldsymbol{B}^T(x, y)$, the sought for equilibrium equation for loads and stresses is achieved:

$$\boxed{\boldsymbol{f} = \iint_A \boldsymbol{B}^T \boldsymbol{\sigma}\, dA} \qquad (3.11)$$

The corresponding relation scheme is shown in Fig. 3.4.
Successive substitution from left to right yields the stiffness relation between $\boldsymbol{f}$ and $\boldsymbol{u}$:

$$\boxed{\boldsymbol{f} = \boldsymbol{K}\, \boldsymbol{u}} \qquad (3.12)$$

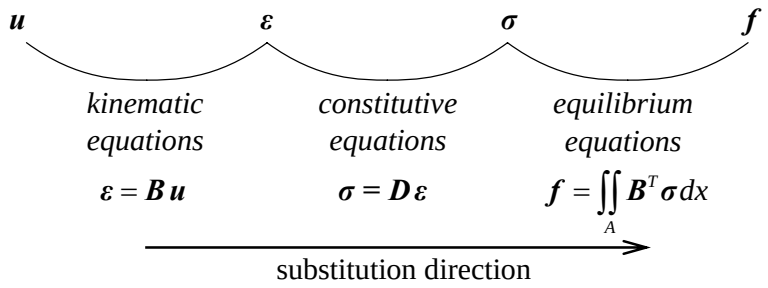

Fig. 3.4: Relation scheme for the rectangular (standard) plate element.

in which the stiffness matrix $\boldsymbol{K}$ is calculated according to the formula:

$$\boldsymbol{K} = \iint_A \boldsymbol{B}^T(x,y)\,\boldsymbol{D}(x,y)\,\boldsymbol{B}(x,y)\,dA \tag{3.13}$$

The matrix $\boldsymbol{B}$ has 8 columns and 3 rows and $\boldsymbol{D}$ has 3 rows and 3 columns. Consequently, the stiffness matrix $\boldsymbol{K}$ is square with 8 rows and 8 columns. In general $\boldsymbol{D}(x,y)$ can be a function of x and y, which occurs for a tapered element for instance. Here it is assumed that E, t and υ are kept constant across the area A of the rectangle. Multiplication of the matrices yields Table 3.1, except the factor $E\,t/(1-\upsilon^2)$. After integration of each term across the area A, Table 3.2 is found. For that purpose the factors α and β have been introduced defined by $\alpha = \beta^{-1} = a/b$ (also see Fig 3.5) and use has been made of the following integrals:

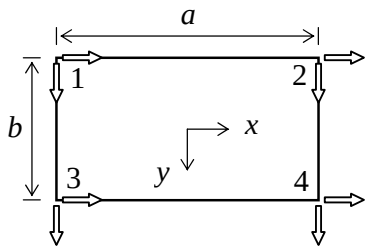

$$\alpha = \beta^{-1} = \frac{a}{b}$$

Fig. 3.5: Rectangular plate element with definition of α and β.

$$\iint_A \left(f^+\right)^2 dA = \iint_A \left(f^-\right)^2 dA = \iint_A \left(g^+\right)^2 dA = \iint_A \left(g^-\right)^2 dA = \frac{1}{3}ab$$

$$\iint_A f^- f^+ dA = \iint_A g^- g^+ dA = \frac{1}{6}ab$$

$$\iint_A f^- g^+ dA = \iint_A f^- g^- dA = \iint_A f^+ g^- dA = \iint_A f^+ g^+ dA = \frac{1}{4}ab$$

A close inspection of the strains reveals that:

$\frac{(g^+)^2}{a^2}+\frac{1-\upsilon}{2}\frac{(f^+)^2}{b^2}$	$\frac{\upsilon f^+g^+}{ab}+\frac{1-\upsilon}{2}\frac{f^+g^+}{ab}$	$-\frac{(g^+)^2}{a^2}+\frac{1-\upsilon}{2}\frac{f^-f^+}{b^2}$	$\frac{\upsilon f^-g^+}{ab}+\frac{1-\upsilon}{2}\frac{f^+g^+}{ab}$	$\frac{g^-g^+}{a^2}+\frac{1-\upsilon}{2}\frac{(f^+)^2}{b^2}$	$-\frac{\upsilon f^+g^+}{ab}+\frac{1-\upsilon}{2}\frac{f^+g^-}{ab}$	$-\frac{g^-g^+}{a^2}+\frac{1-\upsilon}{2}\frac{f^-f^+}{b^2}$	$-\frac{\upsilon f^-g^+}{ab}+\frac{1-\upsilon}{2}\frac{f^+g^-}{ab}$
	$\frac{(f^+)^2}{b^2}+\frac{1-\upsilon}{2}\frac{(g^+)^2}{a^2}$	$-\frac{\upsilon f^+g^+}{ab}+\frac{1-\upsilon}{2}\frac{f^-g^+}{ab}$	$\frac{f^-f^+}{b^2}+\frac{1-\upsilon}{2}\frac{(g^+)^2}{a^2}$	$\frac{\upsilon f^+g^+}{ab}+\frac{1-\upsilon}{2}\frac{f^+g^+}{ab}$	$-\frac{(f^+)^2}{b^2}+\frac{1-\upsilon}{2}\frac{g^-g^+}{a^2}$	$-\frac{\upsilon f^+g^-}{ab}+\frac{1-\upsilon}{2}\frac{f^-g^+}{ab}$	$-\frac{f^-f^+}{b^2}+\frac{1-\upsilon}{2}\frac{g^-g^+}{a^2}$
		$\frac{(g^+)^2}{a^2}+\frac{1-\upsilon}{2}\frac{(f^-)^2}{b^2}$	$-\frac{\upsilon f^-g^+}{ab}+\frac{1-\upsilon}{2}\frac{f^-g^+}{ab}$	$-\frac{g^-g^+}{a^2}+\frac{1-\upsilon}{2}\frac{f^-f^+}{b^2}$	$\frac{\upsilon f^+g^+}{ab}+\frac{1-\upsilon}{2}\frac{f^-g^-}{ab}$	$\frac{g^-g^+}{a^2}+\frac{1-\upsilon}{2}\frac{(f^-)^2}{b^2}$	$\frac{\upsilon f^-g^+}{ab}+\frac{1-\upsilon}{2}\frac{f^-g^-}{ab}$
			$\frac{(f^-)^2}{b^2}+\frac{1-\upsilon}{2}\frac{(g^+)^2}{a^2}$	$\frac{\upsilon f^-g^-}{ab}+\frac{1-\upsilon}{2}\frac{f^+g^+}{ab}$	$-\frac{f^-f^+}{b^2}+\frac{1-\upsilon}{2}\frac{g^-g^+}{a^2}$	$-\frac{\upsilon f^-g^-}{ab}+\frac{1-\upsilon}{2}\frac{f^-g^+}{ab}$	$-\frac{(f^-)^2}{b^2}+\frac{1-\upsilon}{2}\frac{g^-g^+}{a^2}$
				$\frac{(g^-)^2}{a^2}+\frac{1-\upsilon}{2}\frac{(f^+)^2}{b^2}$	$-\frac{\upsilon f^+g^-}{ab}+\frac{1-\upsilon}{2}\frac{f^+g^-}{ab}$	$-\frac{(g^-)^2}{a^2}+\frac{1-\upsilon}{2}\frac{f^-f^+}{b^2}$	$-\frac{\upsilon f^-g^-}{ab}+\frac{1-\upsilon}{2}\frac{f^+g^-}{ab}$
					$\frac{(f^+)^2}{b^2}+\frac{1-\upsilon}{2}\frac{(g^-)^2}{a^2}$	$\frac{\upsilon f^+g^-}{ab}+\frac{1-\upsilon}{2}\frac{f^-g^-}{ab}$	$\frac{f^-f^+}{b^2}+\frac{1-\upsilon}{2}\frac{(g^-)^2}{a^2}$
symmetric						$\frac{(g^-)^2}{a^2}+\frac{1-\upsilon}{2}\frac{(f^-)^2}{b^2}$	$\frac{\upsilon f^-g^-}{ab}+\frac{1-\upsilon}{2}\frac{f^-g^-}{ab}$
Each term must be multiplied by: $\frac{Et}{1-\upsilon^2}$							$\frac{(f^-)^2}{b^2}+\frac{1-\upsilon}{2}\frac{(g^-)^2}{a^2}$

Table 3.1: Stiffness matrix of rectangular element before execution of integration.

$\frac{\beta}{3}+\frac{(1-\upsilon)\alpha}{6}$	$\frac{\upsilon}{4}+\frac{(1-\upsilon)}{8}$	$-\frac{\beta}{3}+\frac{(1-\upsilon)\alpha}{12}$	$\frac{\upsilon}{4}-\frac{(1-\upsilon)}{8}$	$\frac{\beta}{6}-\frac{(1-\upsilon)\alpha}{6}$	$-\frac{\upsilon}{4}+\frac{(1-\upsilon)}{8}$	$-\frac{\beta}{6}-\frac{(1-\upsilon)\alpha}{12}$	$-\frac{\upsilon}{4}-\frac{(1-\upsilon)}{8}$
	$\frac{\alpha}{3}+\frac{(1-\upsilon)\beta}{6}$	$-\frac{\upsilon}{4}+\frac{(1-\upsilon)}{8}$	$\frac{\alpha}{6}-\frac{(1-\upsilon)\beta}{6}$	$\frac{\upsilon}{4}-\frac{(1-\upsilon)}{8}$	$-\frac{\alpha}{3}+\frac{(1-\upsilon)\beta}{12}$	$-\frac{\upsilon}{4}-\frac{(1-\upsilon)}{8}$	$-\frac{\alpha}{6}-\frac{(1-\upsilon)\beta}{12}$
		$\frac{\beta}{3}+\frac{(1-\upsilon)\alpha}{6}$	$-\frac{\upsilon}{4}-\frac{(1-\upsilon)}{8}$	$-\frac{\beta}{6}-\frac{(1-\upsilon)\alpha}{12}$	$\frac{\upsilon}{4}+\frac{(1-\upsilon)}{8}$	$\frac{\beta}{6}-\frac{(1-\upsilon)\alpha}{6}$	$\frac{\upsilon}{4}-\frac{(1-\upsilon)}{8}$
			$\frac{\alpha}{3}+\frac{(1-\upsilon)\beta}{6}$	$\frac{\upsilon}{4}+\frac{(1-\upsilon)}{8}$	$-\frac{\alpha}{6}-\frac{(1-\upsilon)\beta}{12}$	$-\frac{\upsilon}{4}+\frac{(1-\upsilon)}{8}$	$-\frac{\alpha}{3}+\frac{(1-\upsilon)\beta}{12}$
				$\frac{\beta}{3}+\frac{(1-\upsilon)\alpha}{6}$	$-\frac{\upsilon}{4}-\frac{(1-\upsilon)}{8}$	$-\frac{\beta}{3}+\frac{(1-\upsilon)\alpha}{12}$	$-\frac{\upsilon}{4}+\frac{(1-\upsilon)}{8}$
symmetric					$\frac{\alpha}{3}+\frac{(1-\upsilon)\beta}{6}$	$\frac{\upsilon}{4}-\frac{(1-\upsilon)}{8}$	$\frac{\alpha}{6}-\frac{(1-\upsilon)\beta}{6}$
						$\frac{\beta}{3}+\frac{(1-\upsilon)\alpha}{6}$	$\frac{\upsilon}{4}+\frac{(1-\upsilon)}{8}$
Each term must be multiplied by: $\frac{Et}{1-\upsilon^2}$							$\frac{\alpha}{3}+\frac{(1-\upsilon)\beta}{6}$

Table 3.2: Stiffness matrix of rectangular (standard) plate element after integration.

ε_{xx} : – linear in the *y*-direction
– constant in the *x*-direction

ε_{yy} : – linear in the *x*-direction
– constant in the *y*-direction

γ_{xy} : – linear in the *x*-direction
– linear in the *y*-direction

If $\upsilon = 0$, the same distributions are found for n_{xx}, n_{yy} and n_{xy} as are found for the strains. When $\upsilon \neq 0$, all stress resultants vary linearly in two directions. So, in general different values are found in the four nodes. The nodal values are calculated from the relation:

$$\boldsymbol{\sigma} = \boldsymbol{D}\,\boldsymbol{B}\,\boldsymbol{u}$$

By substituting the proper values of f^-, f^+, g^- and g^+. This then leads to a relation between the nodal stress resultants and the degrees of freedom as is shown in Table 3.3. Fig. 3.6 shows the used sign convention for n_{xx}, n_{yy} and n_{xy}.

$$\begin{Bmatrix} n_{xx_1} \\ n_{yy_1} \\ n_{xy_1} \\ \hline n_{xx_2} \\ n_{yy_2} \\ n_{xy_2} \\ \hline n_{xx_3} \\ n_{yy_3} \\ n_{xy_3} \\ \hline n_{xx_4} \\ n_{yy_4} \\ n_{xy_4} \end{Bmatrix} = \frac{Et}{1-\upsilon^2} \left[\begin{array}{cccccccc} -\frac{1}{a} & -\frac{\upsilon}{b} & \frac{1}{a} & 0 & 0 & \frac{\upsilon}{b} & 0 & 0 \\ -\frac{\upsilon}{a} & -\frac{1}{b} & \frac{\upsilon}{a} & 0 & 0 & \frac{1}{b} & 0 & 0 \\ -\frac{1-\upsilon}{2b} & -\frac{1-\upsilon}{2a} & 0 & \frac{1-\upsilon}{2a} & \frac{1-\upsilon}{2b} & 0 & 0 & 0 \\ \hline -\frac{1}{a} & 0 & \frac{1}{a} & -\frac{\upsilon}{b} & 0 & 0 & 0 & \frac{\upsilon}{b} \\ -\frac{\upsilon}{a} & 0 & \frac{\upsilon}{a} & -\frac{1}{b} & 0 & 0 & 0 & \frac{1}{b} \\ 0 & -\frac{1-\upsilon}{2a} & -\frac{1-\upsilon}{2b} & \frac{1-\upsilon}{2a} & 0 & 0 & \frac{1-\upsilon}{2b} & 0 \\ \hline 0 & -\frac{\upsilon}{b} & 0 & 0 & -\frac{1}{a} & \frac{\upsilon}{b} & \frac{1}{a} & 0 \\ 0 & -\frac{1}{b} & 0 & 0 & -\frac{\upsilon}{a} & \frac{1}{b} & \frac{\upsilon}{a} & 0 \\ -\frac{1-\upsilon}{2b} & 0 & 0 & 0 & \frac{1-\upsilon}{2b} & -\frac{1-\upsilon}{2a} & 0 & \frac{1-\upsilon}{2a} \\ \hline 0 & 0 & 0 & -\frac{\upsilon}{b} & -\frac{1}{a} & 0 & \frac{1}{a} & \frac{\upsilon}{b} \\ 0 & 0 & 0 & -\frac{1}{b} & -\frac{\upsilon}{a} & 0 & \frac{\upsilon}{a} & \frac{1}{b} \\ 0 & 0 & -\frac{1-\upsilon}{2b} & 0 & 0 & -\frac{1-\upsilon}{2a} & \frac{1-\upsilon}{2b} & \frac{1-\upsilon}{2a} \end{array}\right] \begin{Bmatrix} u_{x1} \\ u_{y1} \\ u_{x2} \\ u_{y2} \\ u_{x3} \\ u_{y3} \\ u_{x4} \\ u_{y4} \end{Bmatrix}$$

Table 3.3: Relation between the stress resultants in the nodes and the degrees of freedom for the rectangular standard element.

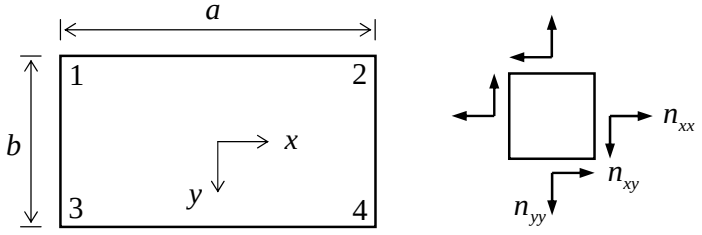

Fig. 3.6: Sign convention for n_{xx}, n_{yy} and n_{xy}.

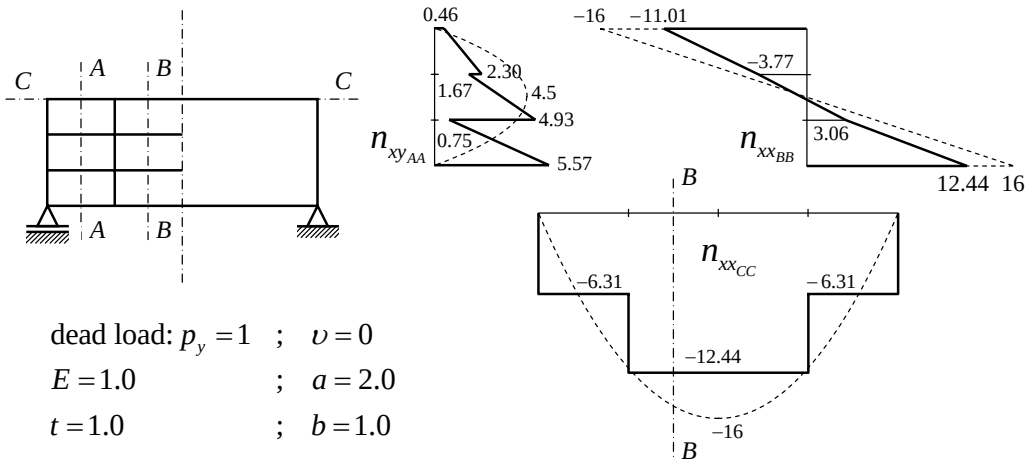

Fig. 3.7: Numerical results for the deep beam of chapter 2.

In Fig. 3.7, the found results are shown for the examples analysed in chapter 2. In this case, the shear stress varies linearly.

3.3 Constant Shear Element

In the general approach of the finite element method as will be discussed in this section, a constant shear element can be created. This can only be done when the values of the integrals in Table 3.1 are adapted. To do this, it is assumed that the value for the shear strain in the centre of the element applies to the whole element. The value in the centre is:

$$f^- = f^+ = g^- = g^+ = \frac{1}{2}$$

Consequently, all integrals associated to shear (identifiable through the factor $(1-\upsilon)/2$) become $ab/4$:

$$\iint_A \left(f^+\right)^2 dA = \iint_A \left(f^-\right)^2 dA = \iint_A \left(g^+\right)^2 dA = \iint_A \left(g^-\right)^2 dA = \frac{1}{4}ab$$

$$\iint_A f^- f^+ dA = \iint_A g^- g^+ dA = \frac{1}{4}ab$$

$$\iint_A f^- g^+ dA = \iint_A f^- g^- dA = \iint_A f^+ g^- dA = \iint_A f^+ g^+ dA = \frac{1}{4}ab$$

This leads to Table 3.4 instead of Table 3.2. Calculating the stresses we arrive at Table 3.5 instead of Table 3.3. When no lateral contraction is present (so $\upsilon = 0$), these results are completely identical to the outcome of the “refined approximation 2” in section 2.3. The general approach of section 3.2 has handed us the generalisation for values of υ not equal to zero.

$$\boldsymbol{K} = \frac{E\,t}{1-\upsilon^2}$$

$\frac{\beta}{3}+\frac{(1-\upsilon)\alpha}{8}$	$\frac{\upsilon}{4}+\frac{(1-\upsilon)}{8}$	$-\frac{\beta}{3}+\frac{(1-\upsilon)\alpha}{8}$	$\frac{\upsilon}{4}-\frac{(1-\upsilon)}{8}$	$\frac{\beta}{6}-\frac{(1-\upsilon)\alpha}{8}$	$-\frac{\upsilon}{4}+\frac{(1-\upsilon)}{8}$	$-\frac{\beta}{6}-\frac{(1-\upsilon)\alpha}{8}$	$-\frac{\upsilon}{4}-\frac{(1-\upsilon)}{8}$
	$\frac{\alpha}{3}+\frac{(1-\upsilon)\beta}{8}$	$-\frac{\upsilon}{4}+\frac{(1-\upsilon)}{8}$	$\frac{\alpha}{6}-\frac{(1-\upsilon)\beta}{8}$	$\frac{\upsilon}{4}-\frac{(1-\upsilon)}{8}$	$-\frac{\alpha}{3}+\frac{(1-\upsilon)\beta}{8}$	$-\frac{\upsilon}{4}-\frac{(1-\upsilon)}{8}$	$-\frac{\alpha}{6}-\frac{(1-\upsilon)\beta}{8}$
		$\frac{\beta}{3}+\frac{(1-\upsilon)\alpha}{8}$	$-\frac{\upsilon}{4}-\frac{(1-\upsilon)}{8}$	$-\frac{\beta}{6}-\frac{(1-\upsilon)\alpha}{8}$	$\frac{\upsilon}{4}+\frac{(1-\upsilon)}{8}$	$\frac{\beta}{6}-\frac{(1-\upsilon)\alpha}{8}$	$\frac{\upsilon}{4}-\frac{(1-\upsilon)}{8}$
			$\frac{\alpha}{3}+\frac{(1-\upsilon)\beta}{8}$	$\frac{\upsilon}{4}+\frac{(1-\upsilon)}{8}$	$-\frac{\alpha}{6}-\frac{(1-\upsilon)\beta}{8}$	$-\frac{\upsilon}{4}+\frac{(1-\upsilon)}{8}$	$-\frac{\alpha}{3}+\frac{(1-\upsilon)\beta}{8}$
				$\frac{\beta}{3}+\frac{(1-\upsilon)\alpha}{8}$	$-\frac{\upsilon}{4}-\frac{(1-\upsilon)}{8}$	$-\frac{\beta}{3}+\frac{(1-\upsilon)\alpha}{8}$	$-\frac{\upsilon}{4}+\frac{(1-\upsilon)}{8}$
					$\frac{\alpha}{3}+\frac{(1-\upsilon)\beta}{8}$	$\frac{\upsilon}{4}-\frac{(1-\upsilon)}{8}$	$\frac{\alpha}{6}-\frac{(1-\upsilon)\beta}{8}$
		symmetric				$\frac{\beta}{3}+\frac{(1-\upsilon)\alpha}{8}$	$\frac{\upsilon}{4}+\frac{(1-\upsilon)}{8}$
							$\frac{\alpha}{3}+\frac{(1-\upsilon)\beta}{8}$

Table 3.4: Stiffness matrix of the constant shear element.

$$\begin{Bmatrix} n_{xx_1} \\ n_{yy_1} \\ n_{xy_1} \\ \hline n_{xx_2} \\ n_{yy_2} \\ n_{xy_2} \\ \hline n_{xx_3} \\ n_{yy_3} \\ n_{xy_3} \\ \hline n_{xx_4} \\ n_{yy_4} \\ n_{xy_4} \end{Bmatrix} = \frac{E\,t}{1-\upsilon^2} \left[\begin{array}{cccccccc} -\frac{1}{a} & -\frac{\upsilon}{b} & \frac{1}{a} & 0 & 0 & \frac{\upsilon}{b} & 0 & 0 \\ -\frac{\upsilon}{a} & -\frac{1}{b} & \frac{\upsilon}{a} & 0 & 0 & \frac{1}{b} & 0 & 0 \\ -\frac{1-\upsilon}{4b} & -\frac{1-\upsilon}{4a} & -\frac{1-\upsilon}{4b} & \frac{1-\upsilon}{4a} & \frac{1-\upsilon}{4b} & -\frac{1-\upsilon}{4a} & \frac{1-\upsilon}{4b} & \frac{1-\upsilon}{4a} \\ \hline -\frac{1}{a} & 0 & \frac{1}{a} & -\frac{\upsilon}{b} & 0 & 0 & 0 & \frac{\upsilon}{b} \\ -\frac{\upsilon}{a} & 0 & \frac{\upsilon}{a} & -\frac{1}{b} & 0 & 0 & 0 & \frac{1}{b} \\ -\frac{1-\upsilon}{4b} & -\frac{1-\upsilon}{4a} & -\frac{1-\upsilon}{4b} & \frac{1-\upsilon}{4a} & \frac{1-\upsilon}{4b} & -\frac{1-\upsilon}{4a} & \frac{1-\upsilon}{4b} & \frac{1-\upsilon}{4a} \\ \hline 0 & -\frac{\upsilon}{b} & 0 & 0 & -\frac{1}{a} & \frac{\upsilon}{b} & \frac{1}{a} & 0 \\ 0 & -\frac{1}{b} & 0 & 0 & -\frac{\upsilon}{a} & \frac{1}{b} & \frac{\upsilon}{a} & 0 \\ -\frac{1-\upsilon}{4b} & -\frac{1-\upsilon}{4a} & -\frac{1-\upsilon}{4b} & \frac{1-\upsilon}{4a} & \frac{1-\upsilon}{4b} & -\frac{1-\upsilon}{4a} & \frac{1-\upsilon}{4b} & \frac{1-\upsilon}{4a} \\ \hline 0 & 0 & 0 & -\frac{\upsilon}{b} & -\frac{1}{a} & 0 & \frac{1}{a} & \frac{\upsilon}{b} \\ 0 & 0 & 0 & -\frac{1}{b} & -\frac{\upsilon}{a} & 0 & \frac{\upsilon}{a} & \frac{1}{b} \\ -\frac{1-\upsilon}{4b} & -\frac{1-\upsilon}{4a} & -\frac{1-\upsilon}{4b} & \frac{1-\upsilon}{4a} & \frac{1-\upsilon}{4b} & -\frac{1-\upsilon}{4a} & \frac{1-\upsilon}{4b} & \frac{1-\upsilon}{4a} \end{array}\right] \begin{Bmatrix} u_{x1} \\ u_{y1} \\ u_{x2} \\ u_{y2} \\ u_{x3} \\ u_{y3} \\ u_{x4} \\ u_{y4} \end{Bmatrix}$$

Table 3.5: Relation between the stress resultants in the nodes and the degrees of freedom for the constant shear element.

The constant shear element has advantages when used for beams that are loaded in bending. When using only one element over the total depth of the beam, the standard element is far too stiff to produce states of constant moment (only normal stresses varying linearly) without also producing simultaneous shear stresses. The constant shear element is capable of this. The standard element can only be applied, when a large amount of elements is used over the total depth of the beam.

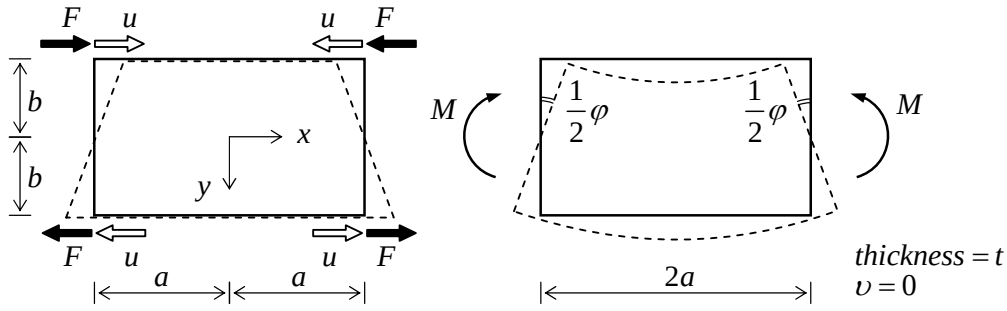

Fig. 3.8: Standard element subjected to bending.

To demonstrate that the standard element is too stiff a special case will be considered with one degree of freedom and $\upsilon = 0$. This case (left side of Fig. 3.8) is a model of a beam under a constant bending moment M (right side of Fig. 3.8). A given fact of this beam is:

$$M = \frac{EI}{2a}\varphi$$

Using $M = 2bF$, $\varphi = 2u/b$ and $EI = t(2b)^3/12$ this transforms into:

$$\boxed{F = \frac{1}{3}E\frac{tb}{a}u} \quad \rightarrow \quad \boxed{K_{exact} = \frac{1}{3}E\frac{tb}{a}}$$

The stiffness K_{exact} should also be found for the element (left side of Fig. 3.8).
In this specific case the displacement field is:

$$u_x(x,y) = \frac{x}{a}\frac{y}{b}u \quad ; \quad u_y(x,y) = 0$$

The strains now are:

$$\varepsilon_{xx} = \frac{\partial u_x}{\partial x} = \frac{y}{ab}u$$
$$\varepsilon_{yy} = \frac{\partial u_y}{\partial y} = 0$$
$$\gamma_{xy} = \frac{\partial u_x}{\partial y} + \frac{\partial u_y}{\partial x} = \frac{x}{ab}u$$

The matrices $\boldsymbol{B}(x,y)$ and $\boldsymbol{D}$ are:

$$\boldsymbol{B}(x,y) = \begin{bmatrix} \frac{y}{ab} \\ \\ \frac{x}{ab} \end{bmatrix} \quad ; \quad \boldsymbol{D} = \begin{bmatrix} E & 0 & 0 \\ 0 & E & 0 \\ 0 & 0 & \frac{E}{2} \end{bmatrix}$$

Hence:

$$\boldsymbol{K} = t\iint \boldsymbol{B}^T \boldsymbol{D}\, \boldsymbol{B}\, dx\, dy \quad \rightarrow \quad \boldsymbol{K} = t\int_{-a}^{a}\int_{-b}^{b} \begin{bmatrix} \frac{y}{a\,b} & 0 & \frac{x}{a\,b} \end{bmatrix} \begin{bmatrix} E & 0 & 0 \\ 0 & E & 0 \\ 0 & 0 & \frac{E}{2} \end{bmatrix} \begin{bmatrix} \frac{y}{a\,b} \\ 0 \\ \frac{x}{a\,b} \end{bmatrix} dy\, dx \quad \rightarrow$$

$$\boldsymbol{K} = E\,t\int_{-a}^{a}\int_{-b}^{b} \left(\frac{y^2}{a^2 b^2} + \frac{1}{2}\frac{x^2}{a^2 b^2} \right) dy\, dx = \frac{4}{3} E \frac{t\,b}{a}\left(1 + \frac{1}{2}\frac{a^2}{b^2} \right)$$

The virtual work equation now is:

$$4\,F\,\delta u = \delta u\, \boldsymbol{K}\, u$$

So, now we find that:

$$F = \frac{1}{3} E \frac{t\,b}{a}\left(1 + \frac{1}{2}\frac{a^2}{b^2} \right) u \quad \rightarrow \quad K_{approx} = \frac{1}{3} E \frac{t\,b}{a}\left(1 + \frac{1}{2}\frac{a^2}{b^2} \right)$$

When compared to the exact value, it can be seen that the stiffness is too large by a factor $1 + a^2/2b^2$. Only for cases in which $a \ll b$ is true, good results are found, see Fig. 3.9.

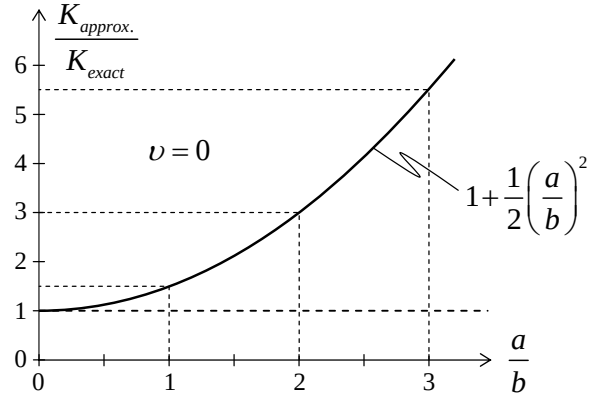

Fig. 3.9: Deviation in stiffness due to the contribution of shear stresses.

Following the derivation, it becomes obvious that the contribution $a^2/2b^2$ follows from the shear stresses. It occurs due to the displacement field used being different from the actual displacement field. In reality no shear stresses occur. The contribution disappears in a constant shear element, and so the correct stiffness is found (at least for $\upsilon = 0$).

3.4 Comparison of elements

Here, four elements which all use the same degrees of freedom are compared. The four elements are (all have $\upsilon = 0$):

- the “approximation 2” element
- the “refined approximation 2” element
- the standard element
- the general constant shear element

The comparison is made as follows. All the element types are deformed in the same way and the 8 generalised element forces in the 4 nodes will be inspected. The deformation is chosen such that $u_{x2} = 1$ and all other displacements are zero. The 8 element forces are found in the third column of the stiffness matrix. The 8 forces are presented in Fig. 3.10 in such a way it is clear which contribution is due to the normal strains and which is due to the shear strains.

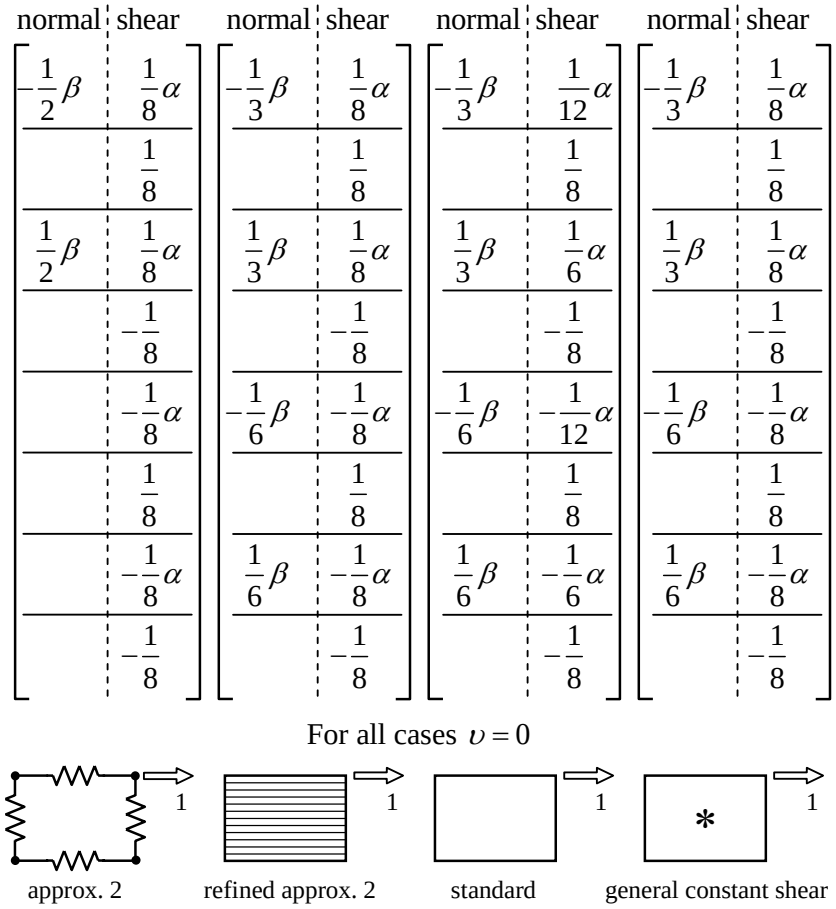

Fig. 3.10: Comparison of the element forces of the several elements.

Notice:

- The standard element has a deviating contribution of the shear strains. All other elements produce constant shear strains and consequently an equal contribution of the shear strains in the element forces.

– The “approximation 2” element has a deviating contribution of the normal strains (discrete springs). All other elements produce the same linearly varying normal strains and consequently an equal contribution of normal strains in the element forces.

The four element types used in the preceding sections were used to compute the stresses in a short simply supported beam due to dead weight. In all computation $\upsilon = 0$ was used.
In Table 3.6 the results are compared from three points of view:

– The sum of all shear stresses in section *AA* is taken and then divided by the exact value of the shear force in that position.
– The stress σ_{xx} in the bottom fibre of the beam is divided by the exact value at that position. In all four cases, the stress was calculated in line *BB*.
– The maximum vertical displacement is taken and then divided by the exact value.

	shear force in *AA*	$\sigma_{xx_{BB}}$ (max)	vertical displacement (max)
approximation 2	1.00	0.81	0.52
refined approx. 2	1.00	0.99	0.64
standard	0.87	0.83	0.55
general const. shear	1.00	0.99	0.64
exact (very fine mesh)	1.00	1.00	1.00

Table 3.6: Comparison of the several elements with respect to shear force, stress resultant and vertical displacement.

For the exact value the results of a calculation with 12 elements over the height and 16 elements in the horizontal direction (half span) are used.

As for the shear force, all approximations are correct except for the standard finite element. The constant shear element (which is equal to the “refined approximation 2”) is the best element. It produces the most favourable stresses and displacement. Both the standard element and “approximation 2” are too stiff. In the standard element, too much strain energy is involved for the shear stresses. Therefore, the displacements are smaller, and so are the stresses σ_{xx}. If the mesh is refined, the results of the standard element as well as the constant shear element will converge to the exact solution.
“Approximation 2” is also too stiff, which in this case is caused by the coarse discretization. Consequently, the stresses σ_{xx} are too small.

In this special example, the observed stresses have a far better result than the displacements. Moreover, of the four elements it is the constant shear element that deserves recommendation.

3.5 Convergence criteria

Discrete models that approximate exact solutions have to meet specific requirements. Deviation from the exact solution in the case of a course finite mesh is acceptable. However,

with increased refinement of the mesh the results of the model should converge more and more towards the exact solution (consistency requirement).
Two major requirements are:

- rigid body displacements are possible with zero strains;
- states of homogeneous strains can be described.

The first of these two requirements is self-evident and valid for all possible models, also those that use differential equations. The second requirement can be easily understood when the real strain state in an element of ever decreasing size is considered. The state of strain approaches a state of constant strains when the element sizes decrease. Consequently, the discrete model has to exactly describe homogeneous strain states. Otherwise, convergence will lead to a wrong result.
All preceding plate models meet the two above-mentioned requirements.

In the formal and general approach of the FEM another demand is made, namely:

- compatibility of displacements has to be preserved between elements

Particularly in the early days of FEM this was considered a rigorous condition. The continuity of displacements between two adjacent elements is achieved in the following way. A displacement field is adopted such that the displacements on one element edge are uniquely defined by only the degrees of freedom that occur on that edge.
When this requirement is met, convergence to the exact solution is more likely. Because in that case, the solution is approached in a specific way. If the mesh is refined, the stored strain energy will decrease and consequently so will the stiffness, see the Fig. 3.11. In the literature such elements are called *conforming elements*.

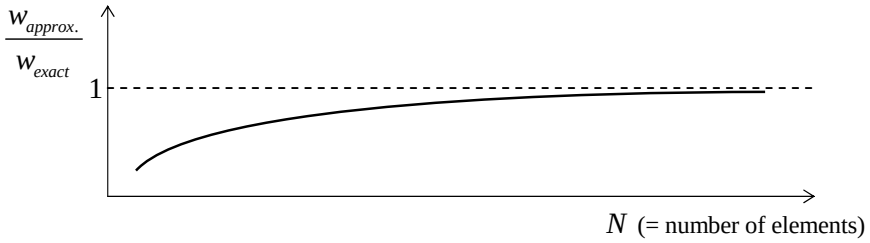

Fig. 3.11: Convergence to exact solution due to mesh refinement.

In this chapter, four elements were discussed of which only one, the standard element, meets the third requirement. All four element can be used though and converge to the correct solution.
The most rigorous one, the standard element, even appears to produce abominable results in the special case of beams in bending. The non-conforming constant shear element performs better.

3.6 Implicit interpolation method

In section 3.2, shape functions $n_1(x, y)$ to $n_4(x, y)$ were constructed in which the displacement field directly can be expressed. A rectangular plate element is a simple one and it is easy to define its shape functions. However, this is not always the case, which is why

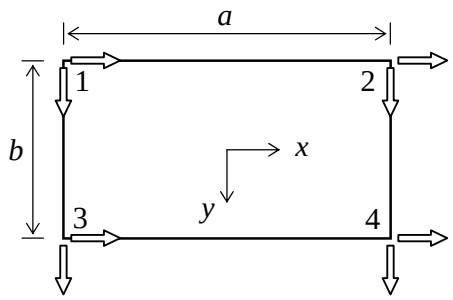

Fig. 3.12: Rectangular plate element.

often the shape functions are obtained in an indirect way, the so-called *implicit interpolation method*. The method will be illustrated using a rectangular element (Fig. 3.12).
Expressions are assumed for $u_x(x,y)$ and $u_y(x,y)$ of the following type:

$$u_x(x,y) = \alpha_1 + \alpha_2 x + \alpha_3 y + \alpha_4 x y$$
$$u_y(x,y) = \alpha_5 + \alpha_6 x + \alpha_7 y + \alpha_8 x y$$

Here, the quantities α_1 to α_8 are generalised displacement coordinates. From these field displacements the strains are derived:

$$\varepsilon_{xx} = \frac{\partial u_x}{\partial x} = \alpha_2 + \alpha_4 y$$
$$\varepsilon_{yy} = \frac{\partial u_y}{\partial y} = \alpha_7 + \alpha_8 y$$
$$\gamma_{xy} = \frac{\partial u_x}{\partial y} + \frac{\partial u_y}{\partial x} = \alpha_3 + \alpha_6 + \alpha_4 x + \alpha_8 y$$

The assumed displacement field meets the requirements of the strainless rigid body displacements and of homogeneous strain states. The rigid body displacements are:

- translation α_1 in x-direction $= u_x$
- translation α_5 in y-direction $= u_y$
- rotation $\frac{1}{2}(\alpha_6 - \alpha_3)$ $= \frac{1}{2}(\partial u_y / \partial x - \partial u_x / \partial y)$

The homogeneous strain states are:

- constant $\varepsilon_{xx} = \alpha_2$
- constant $\varepsilon_{yy} = \alpha_7$
- constant $\gamma_{xy} = \alpha_3 + \alpha_6$

The eight displacement coordinates α can mould themselves such that strainless rigid body displacements or homogeneous strains occur.

From the displacement field it is obvious that the additional third requirement is also complied with. Both u_x and u_y are bilinear, so a linear distribution is found along each edge. There are two degrees of freedom in each direction, so a unique interpolation occurs and full compatibility is assured.

From now on a more formal notation will be used:

$$\begin{Bmatrix} u_x(x,y) \\ u_y(x,y) \end{Bmatrix} = \begin{bmatrix} 1 & x & y & xy & 0 & 0 & 0 & 0 \\ 0 & 0 & 0 & 0 & 1 & x & y & xy \end{bmatrix} \begin{Bmatrix} \alpha_1 \\ \alpha_2 \\ \alpha_3 \\ \alpha_4 \\ \alpha_5 \\ \alpha_6 \\ \alpha_7 \\ \alpha_8 \end{Bmatrix}$$

Written in short:

$$\boldsymbol{u}_c = \boldsymbol{N}_\alpha(x,y)\,\boldsymbol{\alpha}$$

The strains are:

$$\begin{Bmatrix} \varepsilon_{xx}(x,y) \\ \varepsilon_{yy}(x,y) \\ \gamma_{xy}(x,y) \end{Bmatrix} = \begin{bmatrix} 0 & 1 & 0 & y & 0 & 0 & 0 & 0 \\ 0 & 0 & 0 & 0 & 0 & 0 & 1 & x \\ 0 & 0 & 1 & x & 0 & 1 & 0 & y \end{bmatrix} \begin{Bmatrix} \alpha_1 \\ \alpha_2 \\ \alpha_3 \\ \alpha_4 \\ \alpha_5 \\ \alpha_6 \\ \alpha_7 \\ \alpha_8 \end{Bmatrix}$$

Written in short:

$$\boldsymbol{\varepsilon} = \boldsymbol{B}_\alpha(x,y)\,\boldsymbol{\alpha}$$

The number of generalised coordinates $\boldsymbol{\alpha}$ is eight because the element has eight degrees of freedom $\boldsymbol{u}$. A geometrical relation between $\boldsymbol{\alpha}$ and $\boldsymbol{u}$ can be derived in a simple way. For each of the four nodes the value for x and y is introduced in $\boldsymbol{N}_\alpha(x,y)$.
This yields:

$$\begin{Bmatrix} u_{x1} \\ u_{y1} \\ u_{x2} \\ u_{y2} \\ u_{x3} \\ u_{y3} \\ u_{x4} \\ u_{y4} \end{Bmatrix} = \begin{bmatrix} 1 & -\frac{1}{2}a & -\frac{1}{2}b & \frac{1}{4}ab & 0 & 0 & 0 & 0 \\ 0 & 0 & 0 & 0 & 1 & -\frac{1}{2}a & -\frac{1}{2}b & \frac{1}{4}ab \\ 1 & \frac{1}{2}a & -\frac{1}{2}b & -\frac{1}{4}ab & 0 & 0 & 0 & 0 \\ 0 & 0 & 0 & 0 & 1 & \frac{1}{2}a & -\frac{1}{2}b & -\frac{1}{4}ab \\ 1 & -\frac{1}{2}a & \frac{1}{2}b & -\frac{1}{4}ab & 0 & 0 & 0 & 0 \\ 0 & 0 & 0 & 0 & 1 & -\frac{1}{2}a & \frac{1}{2}b & -\frac{1}{4}ab \\ 1 & \frac{1}{2}a & \frac{1}{2}b & \frac{1}{4}ab & 0 & 0 & 0 & 0 \\ 0 & 0 & 0 & 0 & 1 & \frac{1}{2}a & \frac{1}{2}b & \frac{1}{4}ab \end{bmatrix} \begin{Bmatrix} \alpha_1 \\ \alpha_2 \\ \alpha_3 \\ \alpha_4 \\ \alpha_5 \\ \alpha_6 \\ \alpha_7 \\ \alpha_8 \end{Bmatrix}$$

or in short:

$$\boldsymbol{u} = \boldsymbol{A}\,\boldsymbol{\alpha}$$

Inverting $\boldsymbol{A}$ results in:

$$\boldsymbol{\alpha} = \boldsymbol{A}^{-1}\,\boldsymbol{u}$$

So, the displacements $\boldsymbol{u}_c$ can be expresses in $\boldsymbol{u}$:

$$\boldsymbol{u}_c = \boldsymbol{N}_\alpha(x, y)\,\boldsymbol{A}^{-1}\,\boldsymbol{u}$$

Hence, the direct interpolation matrix $\boldsymbol{N}(x, y)$ is found:

$$\boldsymbol{N}(x, y) = \boldsymbol{N}_\alpha(x, y)\,\boldsymbol{A}^{-1}$$

and similarly, the strain matrix $\boldsymbol{B}(x, y)$ is derived:

$$\boldsymbol{B}(x, y) = \boldsymbol{B}_\alpha(x, y)\,\boldsymbol{A}^{-1}$$

From here on, section 3.2 is applicable again.
The implicit interpolation helps to understand that the finite element method provides an approximation in the sense that the internal equilibrium equations are violated. This will be shown for the case in which $\upsilon = 0$.
From the strains it is found:

$$\sigma_{xx} = E\,\varepsilon_{xx} = E\left(\alpha_2 + y\,\alpha_4\right)$$
$$\sigma_{yy} = E\,\varepsilon_{yy} = E\left(\alpha_7 + x\,\alpha_8\right)$$
$$\sigma_{xy} = \frac{E}{2}\gamma_{xy} = \frac{E}{2}\left(\alpha_3 + x\,\alpha_4 + \alpha_6 + y\,\alpha_8\right)$$

For the equilibrium it is required that:

$$\frac{\partial \sigma_{xx}}{\partial x} + \frac{\partial \sigma_{yx}}{\partial y} = 0$$
$$\frac{\partial \sigma_{yy}}{\partial y} + \frac{\partial \sigma_{xy}}{\partial x} = 0$$

Substituting the relations mentioned above, we find:

$$E\left(0 + \frac{1}{2}\alpha_8\right) \neq 0$$
$$E\left(0 + \frac{1}{2}\alpha_4\right) \neq 0$$

In general internal equilibrium does not occur. The use of the virtual work equation shows that equilibrium in the global is satisfied.
When the element mesh is refined, the generalised coordinates α_4 and α_8 will disappear, and so, the internal equilibrium is reached in the limit case.

3.7 Consistent load vector

In the preceding calculations, the distributed forces were lumped. In case of homogeneously distributed dead load, engineering judgement was used to determine which part of the load is related to each degree of freedom. The generalised nodal loads need a more solid definition method for more arbitrary distributions. This method will be derived here.

Generalised nodal loads, which are consistent with the distributed load and the assumed displacement field, need to be defined. The criterion is:

> *When a virtual displacement $\delta \boldsymbol{u}$ is applied, the virtual work of the generalised nodal loads must be equal to the virtual work done by the distributed loads.*

In general, a distributed load $p_x(x, y)$ per unit plate area acts in the x-direction and a distributed load $p_y(x, y)$ in the y-direction. For the distributed loads these will be combined in a vector $\boldsymbol{p}$:

$$\boldsymbol{p} = \begin{Bmatrix} p_x(x, y) \\ p_y(x, y) \end{Bmatrix}$$

The eight generalised nodal loads are joined in a vector $\boldsymbol{f}$:

$$\boldsymbol{f}^T = \begin{Bmatrix} F_{x1} & F_{y1} & F_{x2} & F_{y2} & F_{x3} & F_{y3} & F_{x4} & F_{y4} \end{Bmatrix}$$

The equivalence of virtual requires that:

$$\delta \boldsymbol{u}^T \boldsymbol{f} = \iint_A \delta \boldsymbol{u}_c^T \boldsymbol{p} \, dA$$

in which A is the area of the element.
Substitution of:

$$\delta \boldsymbol{u}_c^T = \delta \boldsymbol{u}^T \boldsymbol{N}^T$$

leads to:

$$\delta \boldsymbol{u}^T \boldsymbol{f} = \delta \boldsymbol{u}^T \iint_A \boldsymbol{N}^T \boldsymbol{p} \, dA$$

Hence:

$$\boldsymbol{f} = \iint_A \boldsymbol{N}^T \boldsymbol{p}\, dA$$

Written fully, the expression reads:

$$\begin{Bmatrix} F_{x1} \\ F_{y1} \\ F_{x2} \\ F_{y2} \\ F_{x3} \\ F_{y3} \\ F_{x4} \\ F_{y4} \end{Bmatrix} = \begin{Bmatrix} \iint_A n_1(x,y)\ p_x(x,y)\, dA \\ \iint_A n_1(x,y)\ p_y(x,y)\, dA \\ \iint_A n_2(x,y)\ p_x(x,y)\, dA \\ \iint_A n_2(x,y)\ p_y(x,y)\, dA \\ \iint_A n_3(x,y)\ p_x(x,y)\, dA \\ \iint_A n_3(x,y)\ p_y(x,y)\, dA \\ \iint_A n_4(x,y)\ p_x(x,y)\, dA \\ \iint_A n_4(x,y)\ p_y(x,y)\, dA \end{Bmatrix}$$

For a better understanding, this will be clarified a bit (see Fig. 3.13). The first term in $\boldsymbol{f}$ will be considered:

$$F_{x1} = \iint_A n_1(x,y)\ p_x(x,y)\, dA$$

The shape function acts as a weighing function and indicates the influence of p_x at a particular position (x,y) on the generalised nodal load F_{x1}.

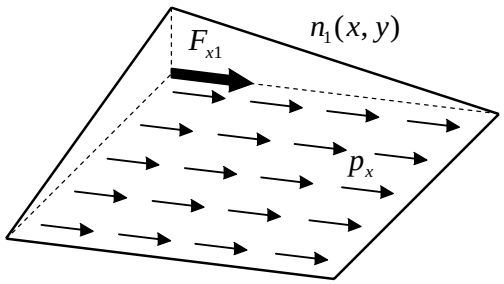

Fig. 3.13: Relation between nodal load F_{x1} and distributed load p_x.

In the case of a homogeneously distributed load $p_x = p$, the next four integrals are found:

$$\iint_A n_1(x,y)\, dA = \frac{1}{4}A \quad ; \quad \iint_A n_2(x,y)\, dA = \frac{1}{4}A$$

$$\iint_A n_3(x,y)\, dA = \frac{1}{4}A \quad ; \quad \iint_A n_4(x,y)\, dA = \frac{1}{4}A$$

The nodal load vector now is:

$$\begin{Bmatrix} F_{x1} \\ F_{y1} \\ F_{x2} \\ F_{y2} \\ F_{x3} \\ F_{y3} \\ F_{x4} \\ F_{y4} \end{Bmatrix} = \begin{Bmatrix} \frac{1}{4} pA \\ 0 \\ \frac{1}{4} pA \\ 0 \\ \frac{1}{4} pA \\ 0 \\ \frac{1}{4} pA \\ 0 \end{Bmatrix}$$

In this case, the same result is found as for the calculation based on sound engineering judgement.

3.8 Some other elements

Until now, the discussed methods were restricted to rectangular elements. Other element types are also used, that are different in shape and/or degrees of freedom.
All elements shown in Fig. 3.14 have two degrees of freedom per node. If mid-side nodes are used, higher order polynomials are necessary for the description of the displacement field.
Three-dimensional elements exist as well. Fig. 3.15 displays a number of these elements.

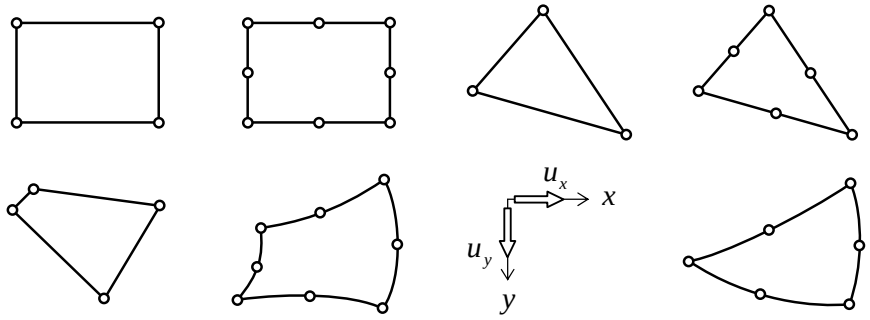

Fig. 3.14: Several two-dimensional elements.

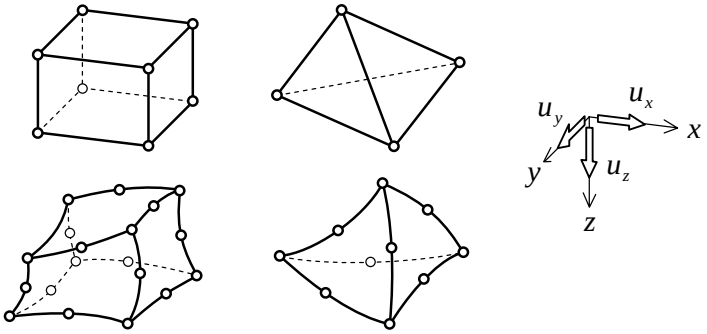

Fig. 3.15: Several three-dimensional elements.

3.9 Examples of plate structures loaded in-plane

On this and the next pages a number arbitrary selected finite element examples are listed of plate structures loaded in-plane.

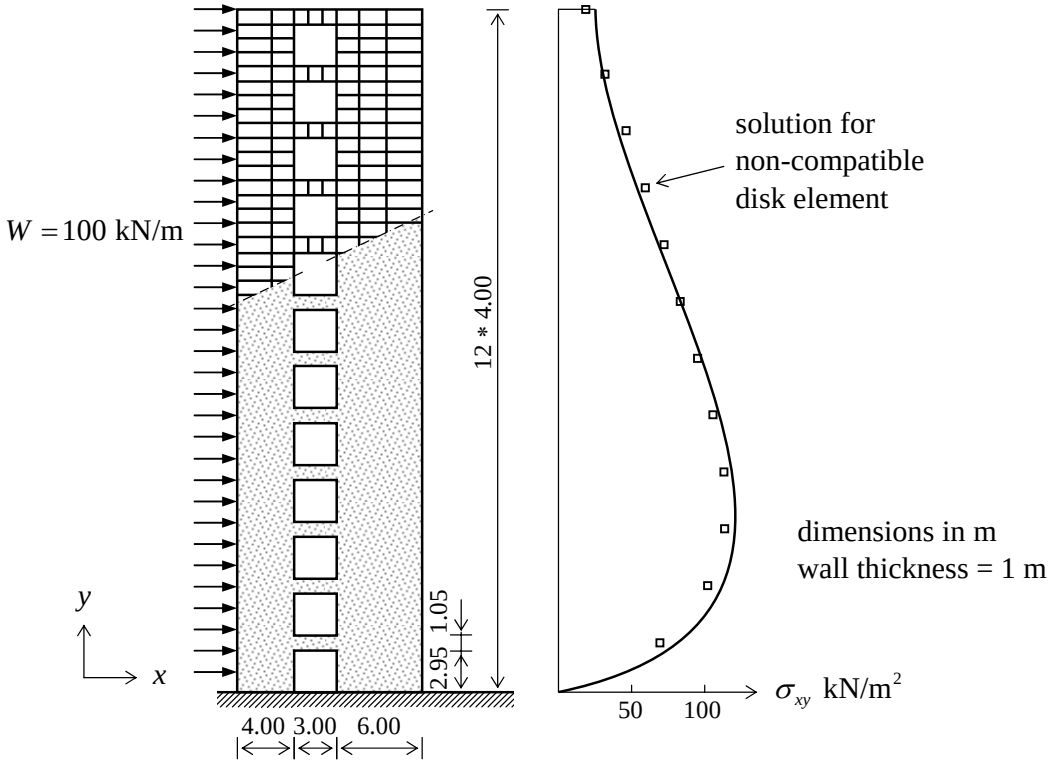

Fig. 3.16: Wall subjected to wind load; Average shear stress in the middle of the connecting beams.

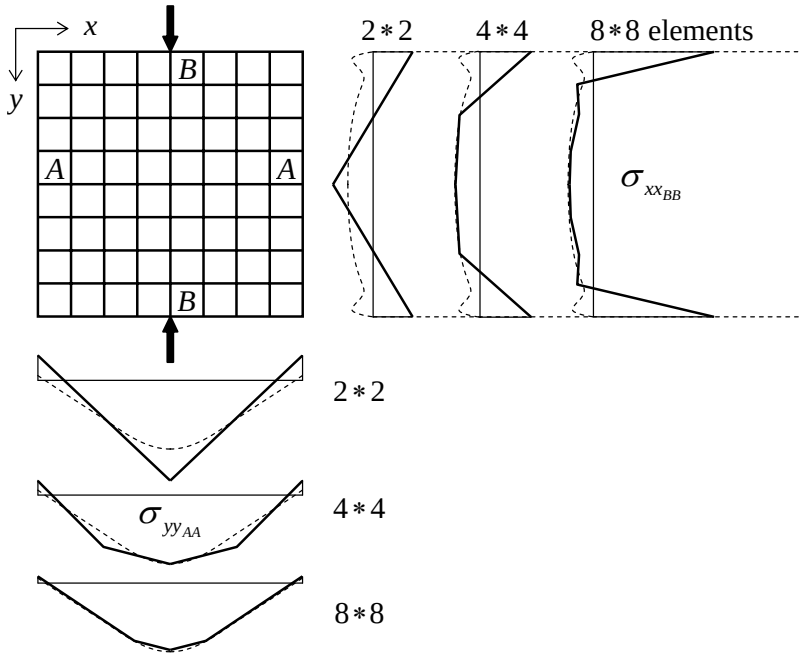

Fig. 3.17: Plane stress case; effect of mesh refinement (dashed line is the exact solution).

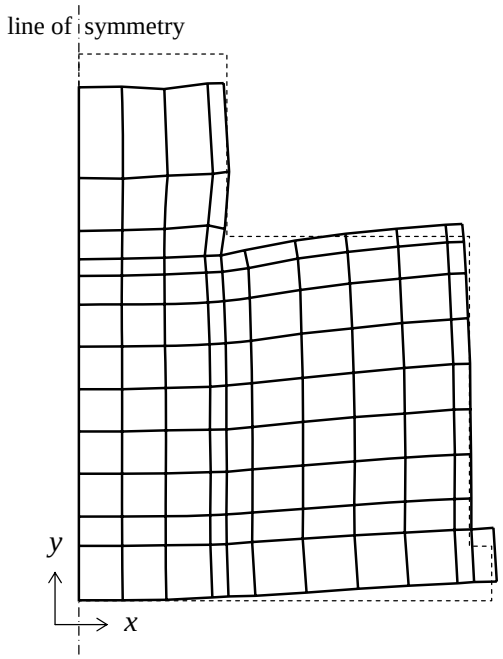

Fig. 3.18: Deformed mesh contours of Storebaelt West Bridge Caisson.

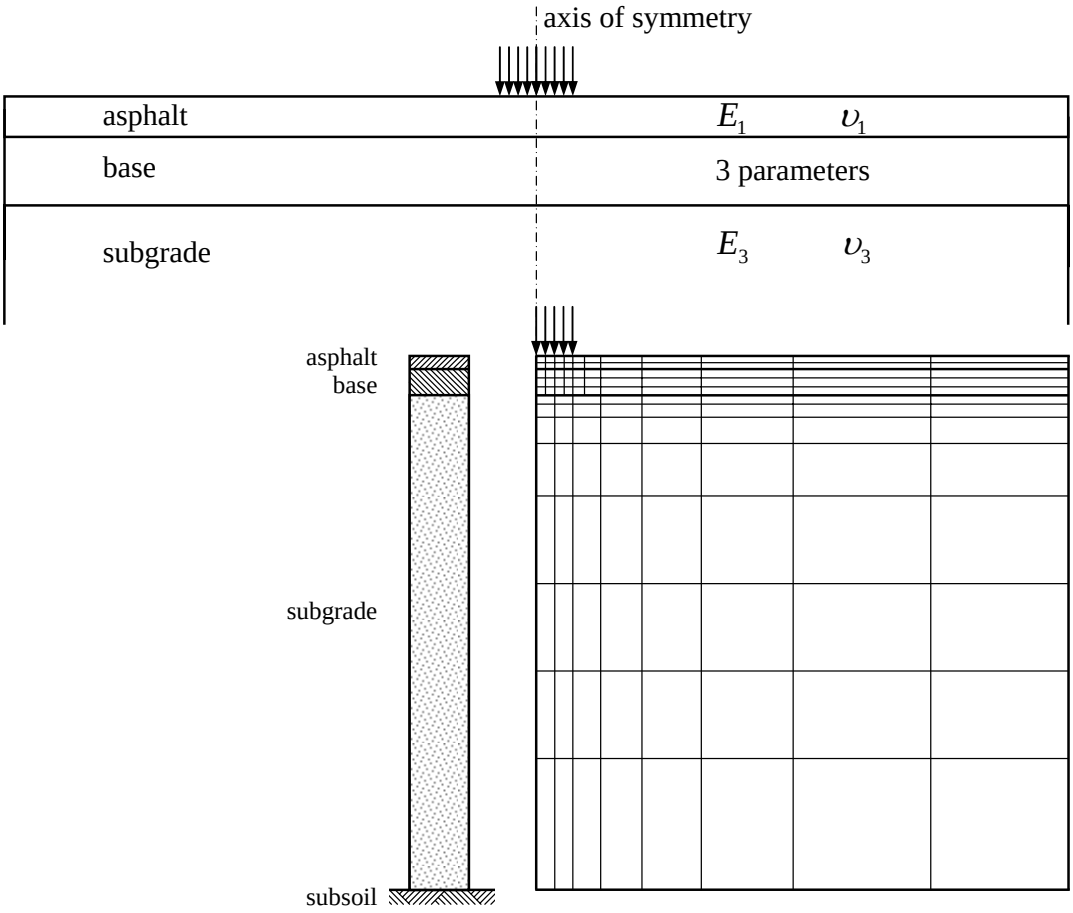

Fig. 3.19: Modelling of pavement subjected to a distributed load.

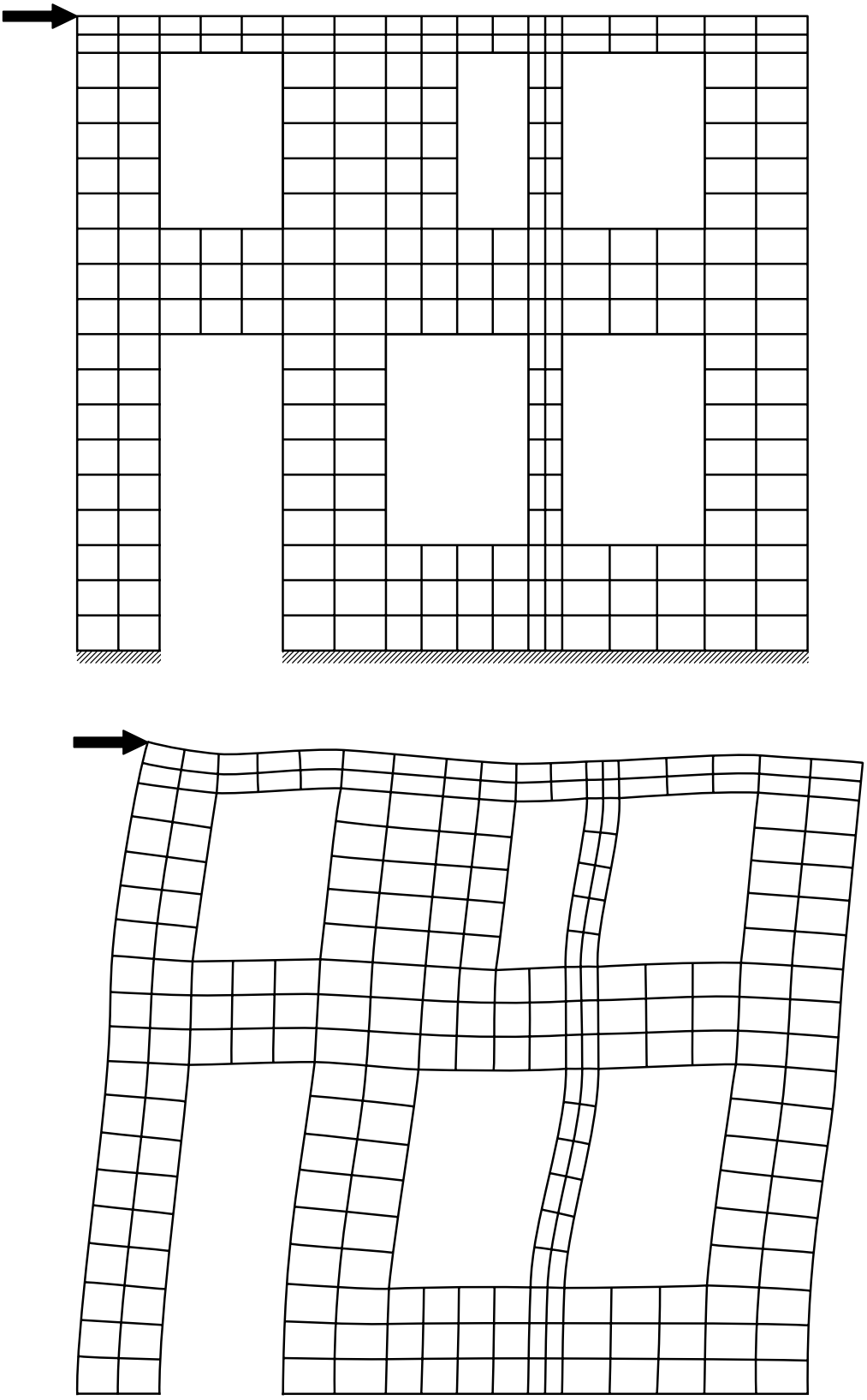

Fig.3.20: Brick wall with door and windows. Finite element mesh (top) and deformations due to concentrated horizontal load (bottom).

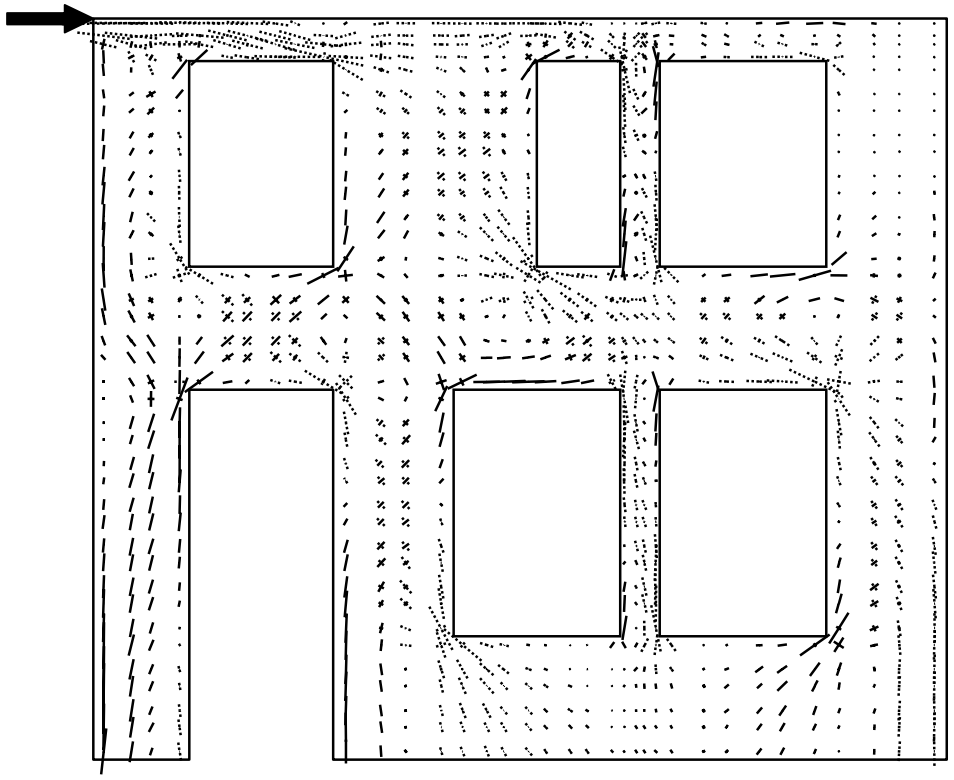

Fig.3.21: Brick wall with door and windows.
Principal stresses due to concentrated horizontal load.

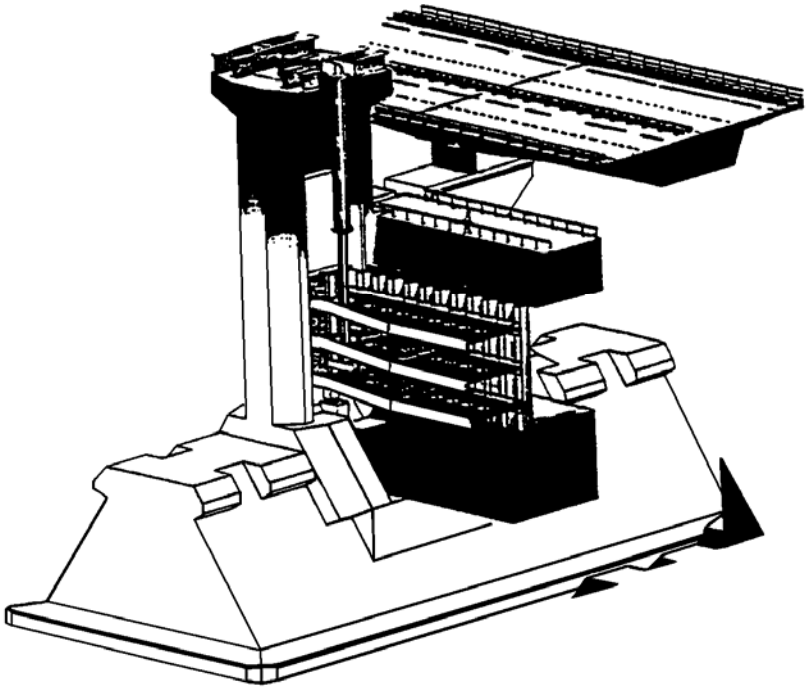

Fig. 3.22: Modelling of an early design of the Easter Scheld storm surge barrier; artist impression of the barrier.

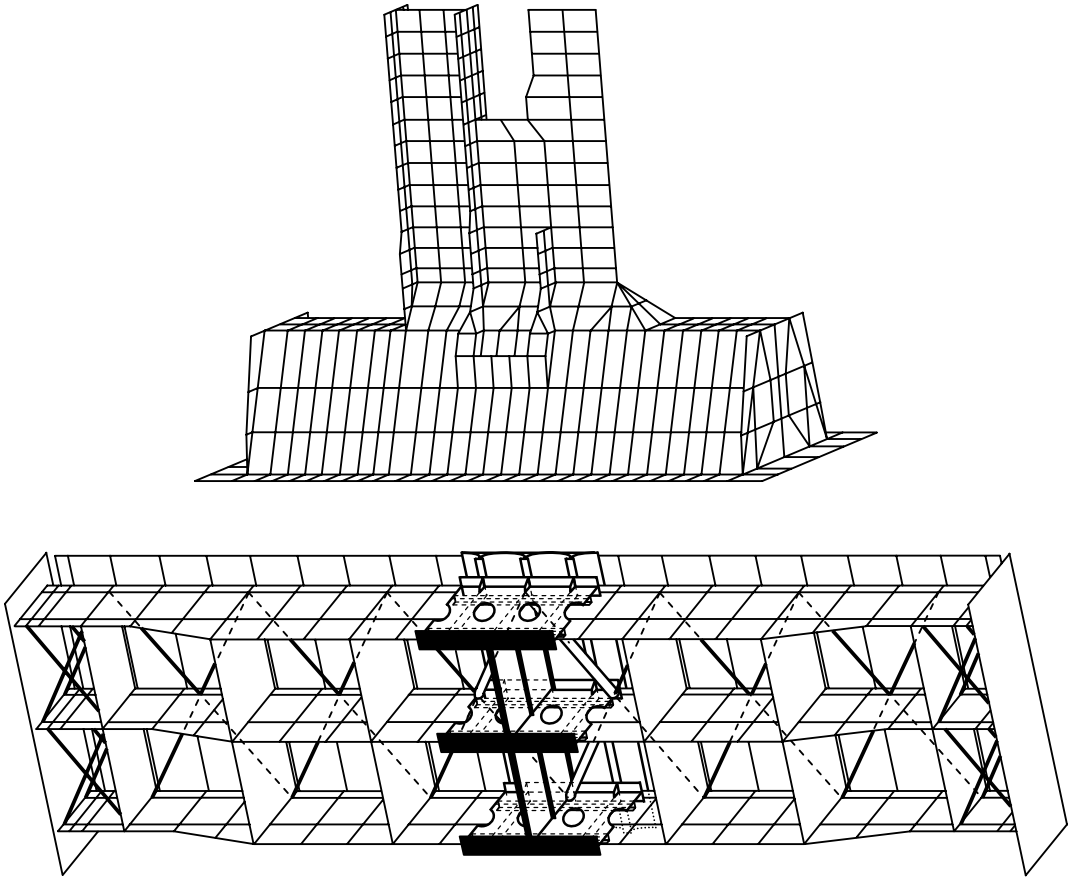

Fig. 3.23: Modelling of the Easter Scheld storm surge barrier; finite element models of the base and gate.

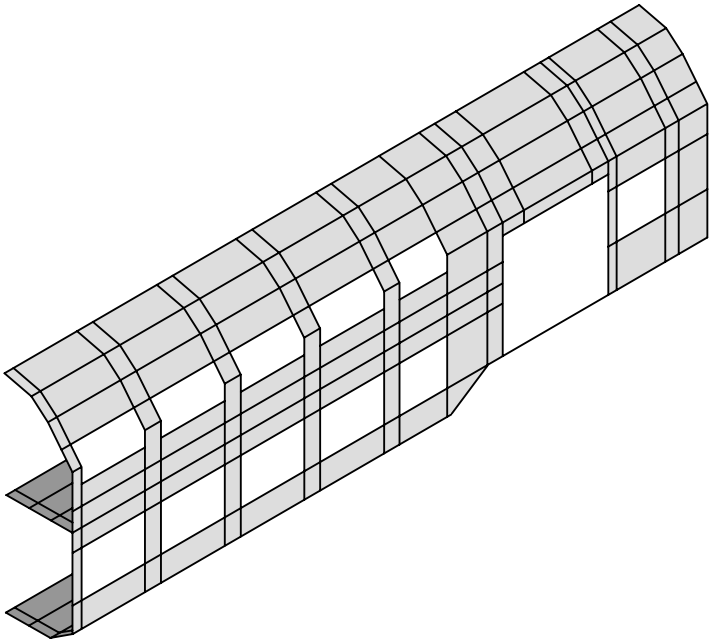

Fig. 3.24: Geometry of the body of a double-deck train (use is made of symmetry).

4 Plates. FEM for discrete elements

4.1 Derivation of the Spring Element

In chapter 2 the stiffness matrix was derived for two discrete elements, i.e. a spring element with two degrees of freedom and a shear panel with four degrees of freedom. To be able to do this derivation a kinematic relation, a constitutive relation and equilibrium considerations are needed.

Here the stiffness matrix will be derived in another more formal way. For this purpose, the distinction will be used between degrees of freedom and generalised deformations. An element with m degrees of freedom and l independent strainless rigid body motions is considered. The number m is always larger than the number l. This restricts the element to have only $m-l$ different independent modes of deformation. These different modes are called generalised deformations and their number is noted as n. So, the following is always true:

$$m = l + n$$

This fact will be of use later on.

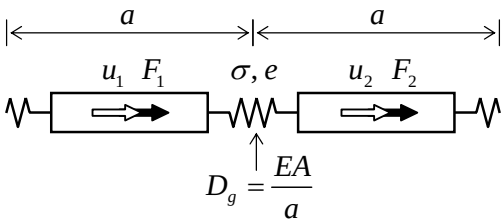

Fig. 4.1: Discrete spring element.

The discrete spring element as shown in Fig. 4.1 has 2 degrees of freedom u_1 and u_2, so $m = 2$. Two forces F_1 and F_2 can be applied in the direction of these degrees of freedom. The displacements form a vector $\boldsymbol{u}$ and the forces a vector $\boldsymbol{f}$. The element has one possible rigid body motions, so $l = 1$. This means one generalised deformation can occur, so $n = 1$. This deformation is the elongation (extension) of the spring. The corresponding generalised stress is the force σ in the spring. The relation scheme worked with is displayed in Fig. 4.2:

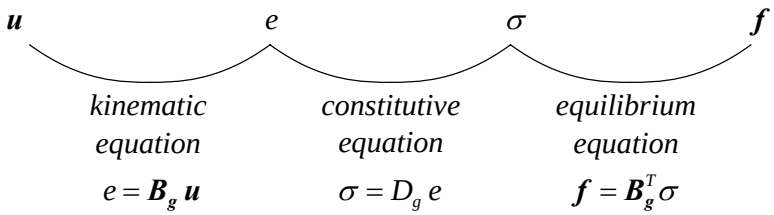

Fig. 4.2: Relation scheme for the discrete spring element.

The kinematic relation between the deformation e and the displacement vector $\boldsymbol{u}$ is determined by the kinematic matrix $\boldsymbol{B}_g$, which reads:

$$\boldsymbol{B}_g = \begin{bmatrix} -1 & 1 \end{bmatrix}$$

The same matrix, however transposed, occurs in the equilibrium equation for the generalised stress σ in the spring and the force vector $\boldsymbol{f}$. This can be proved by applying a small virtual displacement $\delta\boldsymbol{u}$ and equating the virtual work of external loading and internal stress:

$$\delta\boldsymbol{u}^T \boldsymbol{f} = \delta e \, \sigma$$

We know that:

$$\delta e = \boldsymbol{B}_g \, \delta\boldsymbol{u} \quad \text{or} \quad \delta e = \delta\boldsymbol{u}^T \boldsymbol{B}_g^T$$

Hence:

$$\delta\boldsymbol{u}^T \boldsymbol{f} = \delta\boldsymbol{u}^T \boldsymbol{B}_g^T \, \sigma$$

All this must be valid for all $\delta\boldsymbol{u} \neq 0$, therefore it can be concluded that:

$$\boldsymbol{f} = \boldsymbol{B}_g^T \, \sigma \qquad \text{q.e.d}$$

The constitutive relation is:

$$\sigma = D_g \, e$$

in which:

$$D_g = \frac{EA}{\Delta}$$

Now, a substitution towards the equilibrium equation will be made:

$$\begin{aligned} & e = \boldsymbol{B}_g \boldsymbol{u} && (\textit{kinematics}) \\ & \sigma = D_g e \quad ; \quad D_g = \frac{EA}{\Delta} && (\textit{constitution}) \\ & \boldsymbol{f} = \boldsymbol{B}_g^T \sigma && (\textit{equilibrium}) \end{aligned}$$

$$\downarrow$$

SUBSTITUTION

$$\boldsymbol{f} = \boldsymbol{B}_g^T D_g \boldsymbol{B}_g \boldsymbol{u}$$

The result is:

$$\boldsymbol{f} = \boldsymbol{K} \boldsymbol{u}$$

In which the expression for the stiffness matrix is:

$$\boxed{\boldsymbol{K} = \boldsymbol{B}_g^T \boldsymbol{D} \boldsymbol{B}}$$

Using: $\boldsymbol{B}_g = [-1 \quad 1]$, we find:

$$\boldsymbol{K} = \begin{bmatrix} -1 \\ 1 \end{bmatrix} D_g \begin{bmatrix} 1 & -1 \end{bmatrix} \rightarrow \boldsymbol{K} = D_g \begin{bmatrix} 1 & -1 \\ -1 & 1 \end{bmatrix}$$

This matrix was also found earlier on in chapter 1 for “approximation 1”.

4.2 Derivation of the Shear Panel

The element has four degrees of freedom $\boldsymbol{u}$, so $m = 4$ (Fig. 4.3). Likewise four forces $\boldsymbol{f}$ occur.
The element can move in three independent ways as a rigid body: a translation in the x-direction, a translation in the y-direction and a rotation about the z-axis. This leaves $l = 3$.

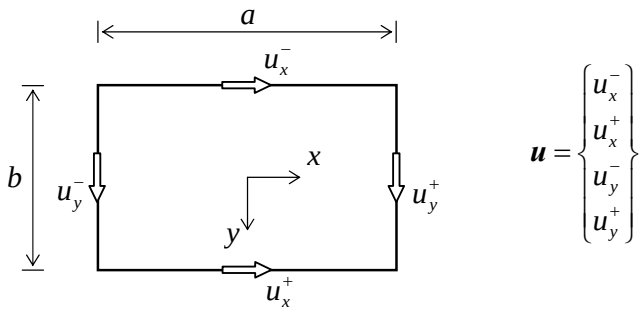

Fig. 4.3: Shear panel.

This allows for a conclusion that there is only one generalised stress, for $n = m - l = 1$. This conclusion confirms the fact that only a state of constant shear stress is possible. Again, the same scheme as shown in Fig. 4.4 applies.

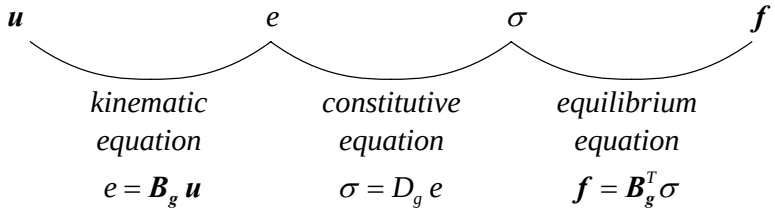

Fig. 4.4: Relation scheme for the shear panel.

Now the question arises of how to interpret σ and e. They should be chosen such that for a virtual displacement $\delta\boldsymbol{u}$, the product of δe and σ represents the total internal virtual work of the panel. This amount of internal virtual work, when stress and strain are constant, reads:

$$\iint_A \delta\gamma_{xy}\ n_{xy}\ dA = a\ b\ \delta\gamma_{xy}\ n_{xy} = \delta e\ \sigma$$

This justifies choosing:

$$\sigma = n_{xy}$$
$$e = a\ b\ \gamma$$

Consequently the rigidity D_g should be:

$$D_g = \frac{G\,t}{a\,b}$$

In section 2.2 a relation between γ_{xy} and $\boldsymbol{u}$ was introduced:

$$\gamma_{xy} = \frac{u_x^+ - u_x^-}{b} + \frac{u_y^+ - u_y^-}{a}$$

From this it can be derived:

$$\boldsymbol{B_g} = \begin{bmatrix} -a & a & -b & b \end{bmatrix}$$

So, the stiffness matrix is:

$$\boldsymbol{K} = \boldsymbol{B_g^T}\,\boldsymbol{D_g}\,\boldsymbol{B_g} \quad \rightarrow \quad \boldsymbol{K} = \begin{bmatrix} -a \\ a \\ -b \\ b \end{bmatrix} \frac{G\,t}{a\,b} \begin{bmatrix} -a & a & -b & b \end{bmatrix}$$

Introducing once again $\alpha = \beta^{-1} = a/b$ and $G = E/2$ the result is:

$$\boldsymbol{K} = \frac{1}{2} E\,t \begin{bmatrix} \alpha & -\alpha & 1 & -1 \\ -\alpha & \alpha & -1 & 1 \\ 1 & -1 & \beta & -\beta \\ -1 & 1 & -\beta & \beta \end{bmatrix}$$

This is the same result found in section 2.1.

Remark
Another possible choice could have been:

$$\sigma = n_y l$$
$$e = \gamma_{xy} \frac{a\,b}{l}$$

resulting in:

$$D_g = G\,t\,\frac{l^2}{a\,b}$$

Here l is a length that is characteristic for the element. It may be a or b or (if no preference is necessary for the x- or y-direction) $\sqrt{a\,b}$.

Now, e and the degrees of freedom $\boldsymbol{u}$ have the same dimension, and so do σ and the forces $\boldsymbol{f}$. This ensures comparability with the discrete spring element.

4.3 Derivation of the Constant Shear Element

In chapter 3 a four-noded rectangular element with 8 degrees of freedom was derived. This element produced membrane forces n_{xx} constant in the x-direction. Similarly, the membrane forces n_{yy} are constant in the y-direction, and vary linearly in the x-direction. In addition, the membrane forces n_{xy} are constant in both directions. Formally speaking, the element produces the following membrane forces:

$$n_{xx} = \beta_1 + \beta_4\, y$$
$$n_{yy} = \beta_2 + \beta_5\, x$$
$$n_{xy} = \beta_3$$

Similar distributions will be present for the strains:

$$\varepsilon_{xx} = \delta_1 + \delta_4\, y$$
$$\varepsilon_{yy} = \delta_2 + \delta_5\, x$$
$$\gamma_{xy} = \delta_3$$

The following constitutive equations were used to derive the element:

$$\begin{Bmatrix} n_{xx} \\ n_{yy} \\ n_{xy} \end{Bmatrix} = \frac{E\,t}{1-\upsilon^2} \begin{bmatrix} 1 & \upsilon & 0 \\ \upsilon & 1 & 0 \\ 0 & 0 & \dfrac{1-\upsilon}{2} \end{bmatrix} \begin{Bmatrix} \varepsilon_{xx} \\ \varepsilon_{yy} \\ \gamma_{xy} \end{Bmatrix} \tag{4.1}$$

or in short:

$$\boldsymbol{\sigma} = \boldsymbol{D}\,\boldsymbol{\varepsilon}$$

The element gives a relatively good result. It produces constant states of stress and strain and does not act extremely stiff when subjected to bending. When $\upsilon = 0$ the bending state is reproduced exactly, but when $\upsilon \neq 0$ the plate behaves a bit too stiff, because of the used elasticity modulus being $E/(1-\upsilon^2)$ instead of E. The reason is that in the element ε_{yy} is zero when the bending strains are $\varepsilon_{xx} = \delta_4\, y$. This also means that stresses $n_{yy} \neq 0$ will arise,

which have a value υ times n_{xx}. In reality these lateral stresses do not occur, because the appropriate strains ε_{yy} will develop. In case of bending the total change in length in the transverse direction of the element has to be zero, and not the strain in each position in that direction. The problem is that the constitutive relations mentioned before are necessary to exactly reproduce the constant strain states, but we want to use the relations:

$$\begin{aligned} n_{xx} &= E\,t\,\varepsilon_{xx} \\ n_{yy} &= E\,t\,\varepsilon_{yy} \end{aligned} \tag{4.2}$$

for the two bending modes. Applying the concept of generalised deformations used for the discrete elements can solve this dilemma.
The considered element has 8 degrees of freedom, so $m = 8$, and 3 independent rigid body motions are possible, so $l = 3$ (see Fig. 4.5).

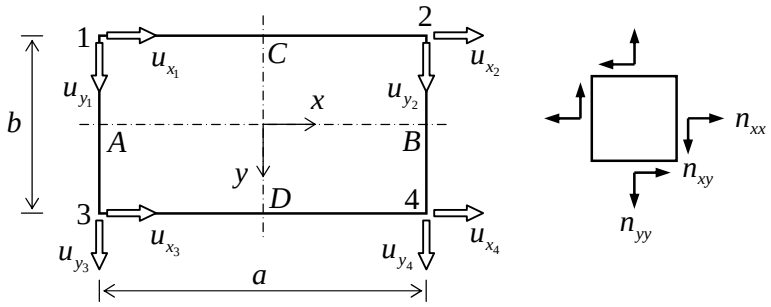

Fig. 4.5: Constant shear element.

Consequently 5 generalised deformations must exist, for $n = m - l = 5$. They shall be named e_1, e_2, e_3, e_4 and e_5. Each generalised deformation is connected to a deformation mode of the element. Deformation e_1 is related to constant strains ε_{xx}, deformation e_2 is to constant strains ε_{yy} and deformation e_3 is to constant strains γ_{xy}. Deformation e_4 is connected to bending strains ε_{xx} and e_5 to bending strains ε_{yy}.
Now, the scheme of Fig. 4.6 should be applied.

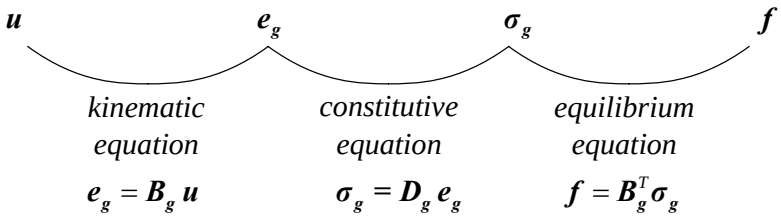

Fig. 4.6: Relation scheme for the constant shear element.

The kinematic matrix $\boldsymbol{B_g}$ has 5 rows and 8 columns. The rigidity matrix $\boldsymbol{D_g}$ is a square matrix of 5 rows and 5 columns.
The deformations e_1, e_2 and e_3 are chosen in a way that:

$$\begin{aligned} e_1 &= \varepsilon_{xx}\,a \\ e_2 &= \varepsilon_{yy}\,b \\ e_3 &= \gamma_{xy}\,b \end{aligned} \tag{4.3}$$

Here ε_{xx} and ε_{yy} represent the values in the centre of the element. In the definition for e_3, b has been used for the characteristic length l mentioned for the discrete shear panel.
The definitions of e_4 and e_5 are:

$$\begin{aligned} e_4 &= \left(\varepsilon_{xx}^{+} - \varepsilon_{xx}^{-}\right) a \\ e_5 &= \left(\varepsilon_{yy}^{+} - \varepsilon_{yy}^{-}\right) b \end{aligned} \tag{4.4}$$

This way, they are the measurements for the curvatures in x- and y-direction respectively. All 5 deformations have the dimension of length. The result is (for the positions A, B, C and D see Fig. 4.5):

$$\begin{aligned} e_1 &= u_{xB} - u_{xA} \\ e_2 &= u_{yD} - u_{yC} \\ e_3 &= b\left(\frac{u_{xD} - u_{xC}}{b} + \frac{u_{yB} - u_{yA}}{a}\right) \\ e_4 &= u_{x4} - u_{x1} + u_{x2} - u_{x3} \\ e_5 &= u_{y1} - u_{y2} + u_{y3} - u_{y4} \end{aligned}$$

Further expansion from here yields:

$$\begin{aligned} u_{xA} &= \frac{1}{2}\left(u_{x1} + u_{x3}\right) \\ u_{xB} &= \frac{1}{2}\left(u_{x2} + u_{x4}\right) \\ u_{xC} &= \frac{1}{2}\left(u_{x1} + u_{x2}\right) \\ u_{xD} &= \frac{1}{2}\left(u_{x3} + u_{x4}\right) \end{aligned} \qquad \text{etc.}$$

If x is replaced by y, the other 4 expressions are found. The final matrix formulation reads:

$$\begin{Bmatrix} e_1 \\ e_2 \\ e_3 \\ e_4 \\ e_5 \end{Bmatrix} = \begin{bmatrix} -\frac{1}{2} & 0 & \frac{1}{2} & 0 & -\frac{1}{2} & 0 & \frac{1}{2} & 0 \\ 0 & -\frac{1}{2} & 0 & -\frac{1}{2} & 0 & \frac{1}{2} & 0 & \frac{1}{2} \\ -\frac{1}{2} & -\frac{\beta}{2} & -\frac{1}{2} & \frac{\beta}{2} & \frac{1}{2} & \frac{\beta}{2} & \frac{1}{2} & -\frac{\beta}{2} \\ -1 & 0 & 1 & 0 & -1 & 0 & 1 & 0 \\ 0 & 1 & 0 & -1 & 0 & 1 & 0 & -1 \end{bmatrix} \begin{Bmatrix} u_{x1} \\ u_{y1} \\ u_{x2} \\ u_{y2} \\ u_{x3} \\ u_{y3} \\ u_{x4} \\ u_{y4} \end{Bmatrix}$$

or in short:

$$\boldsymbol{e}_g = \boldsymbol{B}_g \, \boldsymbol{u}$$

To derive the matrix $\boldsymbol{D}_g$ relation (4.1) is applied for the modes e_1, e_2 and e_3 and (4.2) for the bending modes e_4 and e_5. This way the correct results for bending with $\upsilon \neq 0$ will be achieved.
In case of a virtual displacement, the following must be valid:

$$\delta \boldsymbol{e}_g^T \boldsymbol{\sigma}_g = \iint_A \delta \boldsymbol{\varepsilon}^T \boldsymbol{\sigma} \, dA$$

and so:

$$\delta \boldsymbol{e}_g^T \boldsymbol{D}_g \boldsymbol{e}_g = \iint_A \delta \boldsymbol{\varepsilon}^T \boldsymbol{D} \, \boldsymbol{\varepsilon} \, dA$$

For the first three modes then it is known:

$$\begin{Bmatrix} \varepsilon_{xx} \\ \varepsilon_{yy} \\ \gamma_{xy} \end{Bmatrix} = \begin{bmatrix} \frac{1}{a} & 0 & 0 \\ 0 & \frac{1}{b} & 0 \\ 0 & 0 & \frac{1}{b} \end{bmatrix} \begin{Bmatrix} e_1 \\ e_2 \\ e_3 \end{Bmatrix}$$

or in short:

$$\boldsymbol{\varepsilon} = \boldsymbol{B} \, \boldsymbol{e}_g$$

So, the recipe for $\boldsymbol{D}_g$ using (4.1) is:

$$\boldsymbol{D}_g = \iint_A \boldsymbol{B}^T \boldsymbol{D} \, \boldsymbol{B} \, dxdy$$

Keep in mind that this equation only defines the top left-hand 3 by 3 sub-matrix of $\boldsymbol{D}_g$.
The other part of $\boldsymbol{D}_g$ exists of two diagonal terms. To calculate them, the following matrix expression is applied:

$$\begin{Bmatrix} \varepsilon_{xx} \\ \varepsilon_{yy} \end{Bmatrix} = \begin{bmatrix} \frac{y}{ab} & 0 \\ 0 & \frac{x}{ab} \end{bmatrix} \begin{Bmatrix} e_4 \\ e_5 \end{Bmatrix}$$

or in short:

$$\boldsymbol{\varepsilon} = \boldsymbol{B}\,\boldsymbol{e}_g$$

The same recipe is used for $\boldsymbol{D}_g$, only now with (4.2). The result is the 2 by 2 bottom right-hand sub matrix of $\boldsymbol{D}_g$.
The total result is:

$$\boldsymbol{D}_g = E\,t\begin{bmatrix} \frac{\beta}{1-\upsilon^2} & \frac{\upsilon}{1-\upsilon^2} & 0 & 0 & 0 \\ \frac{\upsilon}{1-\upsilon^2} & \frac{\alpha}{1-\upsilon^2} & 0 & 0 & 0 \\ 0 & 0 & \frac{\beta}{2(1+\upsilon)} & 0 & 0 \\ 0 & 0 & 0 & \frac{\beta}{12} & 0 \\ 0 & 0 & 0 & 0 & \frac{\alpha}{12} \end{bmatrix}$$

With:

$$\beta = \frac{b}{a}$$

The stiffness matrix $\boldsymbol{K}$ now becomes:

$$\boldsymbol{K} = \boldsymbol{B}_g^T\,\boldsymbol{D}_g\,\boldsymbol{B}_g$$

This element can predict the exact behaviour for two-dimensional homogeneous stress states, and for constant moments in the x- and y-direction too.

5 Case history of cable-stayed wide-box bridge

5.1 Introduction

The site plan and photograph of the considered cable-stayed bridge over the river Waal at Ewijk (nearby Nijmegen, The Netherlands) is given in Fig. 5.1. A longitudinal profile and a cross-sectional profile are shown in Fig. 5.2. The pylons are in the centre of the cross-section. The pylon distance is 270 meters. The span on the outside of the pylons at both ends is 105 meters.

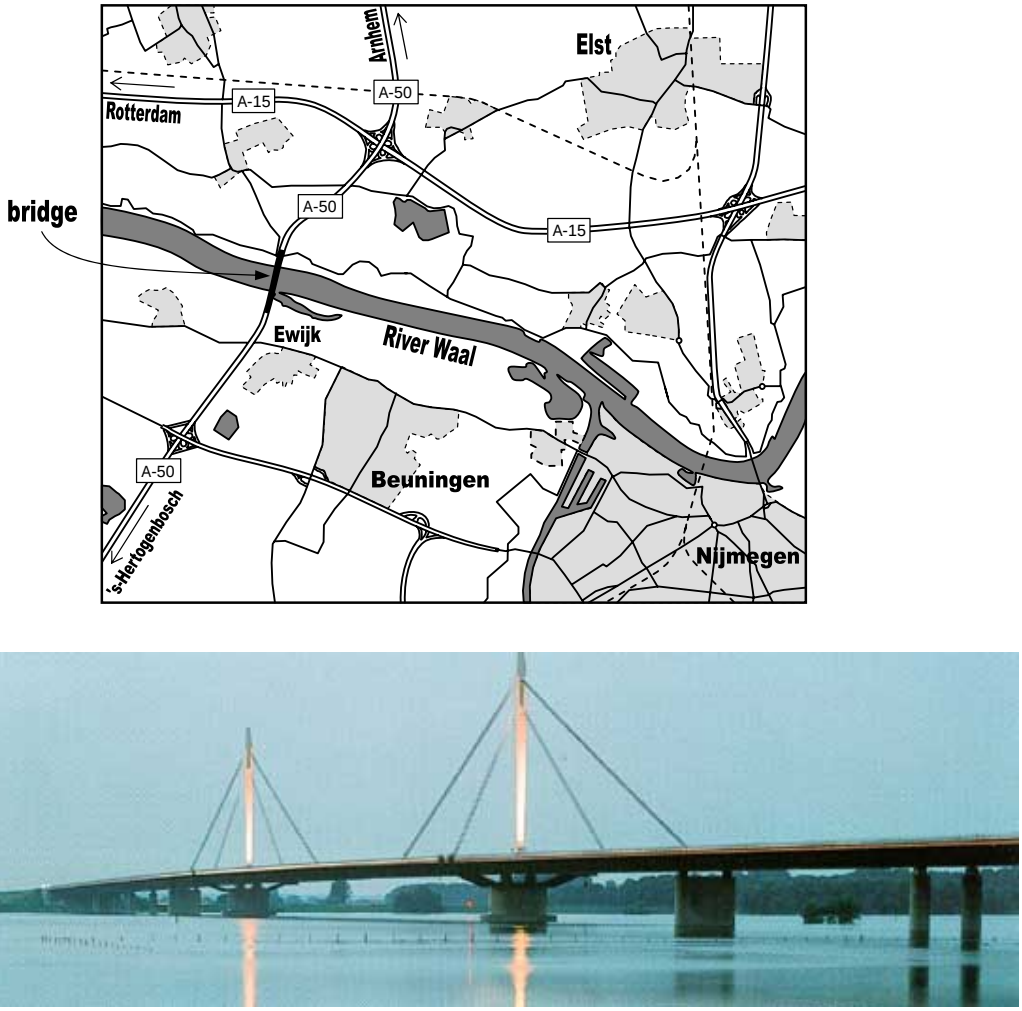

Fig. 5.1: Site plan and photo of the cable-stayed bridge over the river Waal at Ewijk.

The structural height of the box girder is 3.50 meters and the width of the box girder is approximately 26 meters. Including the overhangs, the width is about 36 meters. No longitudinal inner web is applied in the box girder, except where the stay cables are lead in. The shape of the box girder is determined partly by aerodynamic considerations.

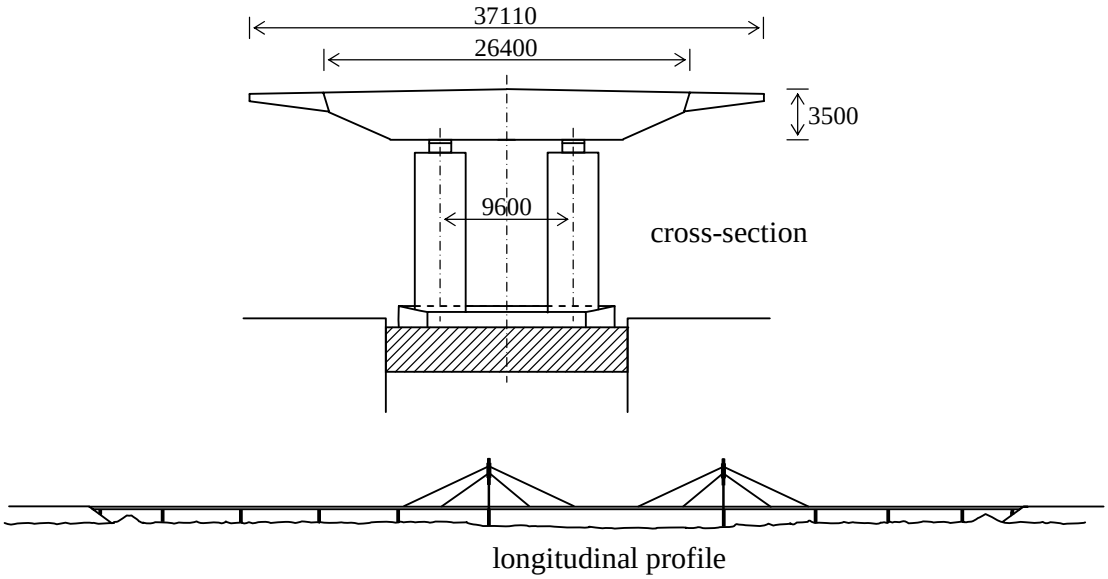

Fig. 5.2: Cross-section and longitudinal view of the bridge (dimensions in mm).

Fig. 5.3 shows the box girder that is composed of diaphragms and plate panels stiffened by hat sections (prefabricated). Every 5 meters a cross diaphragm is present. In Fig. 5.4 the situation at an end partition above the support is drawn on a larger scale. The bridge is extended at the front. Sections of 15 meters in length are added one by one using a specially developed auxiliary structure.

If all parts of the bridge were subdivided into elements, a very large system of equations would arise. Using three degrees of freedom per node for structures loaded in their plane, a cross-section would have about 200 nodes when taking into account all the hat sections. This

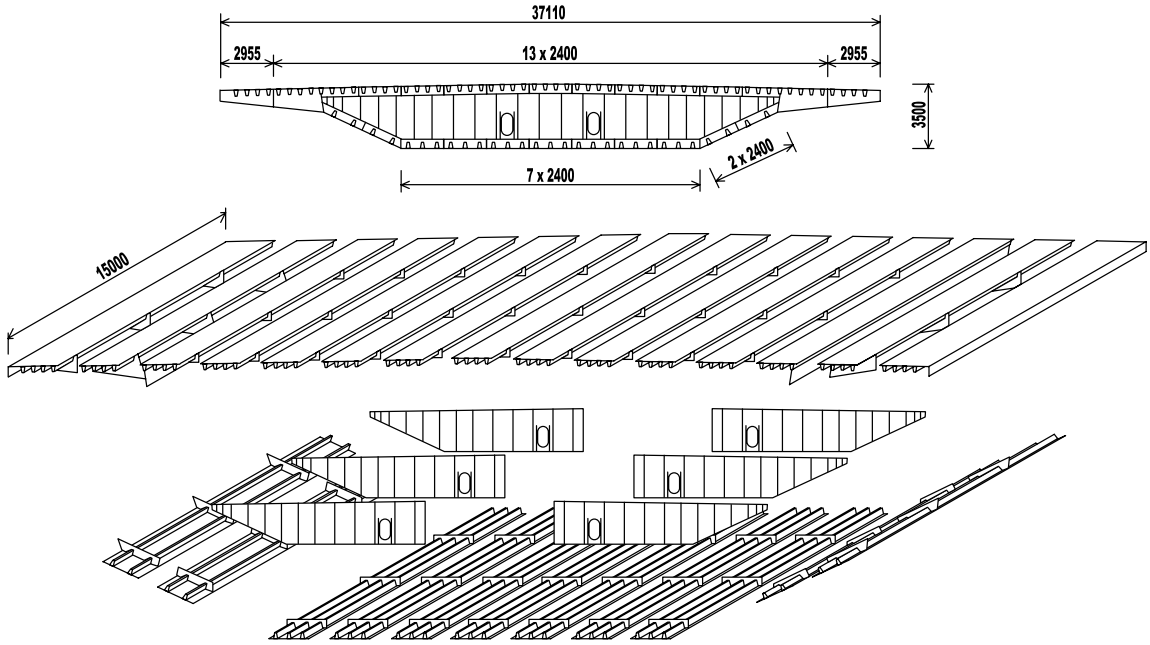

Fig. 5.3: Construction of the box girder, assemblage of sections (dimensions in mm).

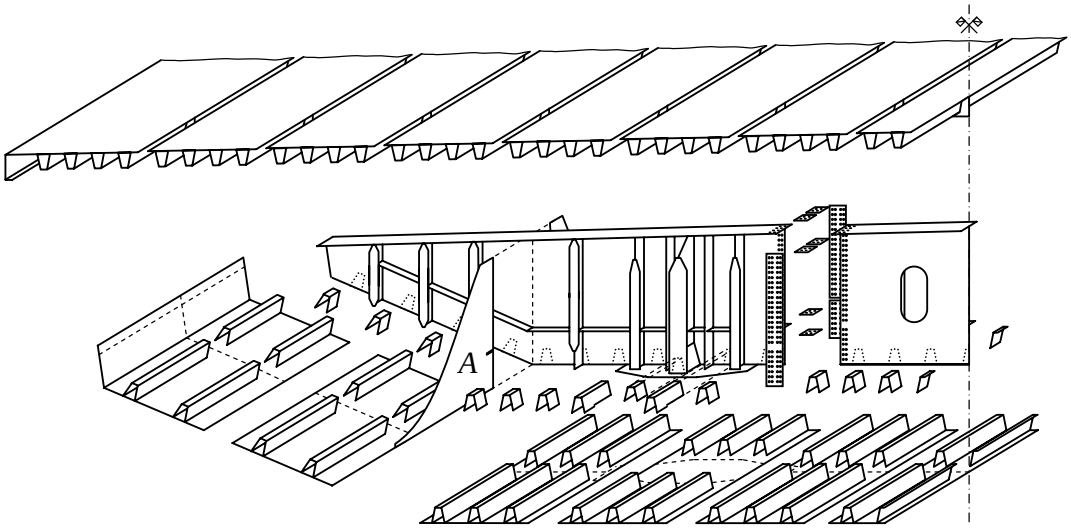

Fig. 5.4: Structural composition of the end partition and diaphragm above the support.

delivers about 600 degrees of freedom per cross-section. Lengthwise we can think of elements of 5 meters long (we will get elongated elements). The total bridge would make for approximately 100 cross-sections and therefore 50,000 degrees of freedom with half a bandwidth of about 600. In practice, this is a very large system.

Such a detailed overall calculation is not very useful for a bridge like this one. In the design stage a calculation with a program for flat bar structures is sufficient. Bridge parts of a limited size can be calculated with a finite element program, for example a critical extension phase.

The panels with hat-shaped stiffeners may be considered as orthotropic plates loaded in their plane, as if the contribution of the hat sections is smeared out.
Only for smaller details, a very fine mesh is meaningful. A meticulous analysis of the end diaphragm, that has to endure a large supporting reaction, or the analysis of a local introduction of the stay cables, may require such fine meshes.

5.2 Calculation of a construction phase

5.2.1 Problem definition and finite element mesh

Fig. 5.5 shows how the load case is simplified to that of a constant shear force. Because the vertical load is applied above the vertical walls, a calculation with elements that are only loaded in their plane is possible. The orthotropic constitutive relation reads:

$$\begin{Bmatrix} n_{xx} \\ n_{yy} \\ n_{xy} \end{Bmatrix} = \begin{bmatrix} S_{xx} & S_{\upsilon} & 0 \\ S_{\upsilon} & S_{yy} & 0 \\ 0 & 0 & S_{xy} \end{bmatrix} \begin{Bmatrix} \varepsilon_{xx} \\ \varepsilon_{yy} \\ 2\varepsilon_{xy} \end{Bmatrix}$$

The stiffnesses are computed from (see Fig. 5.6):

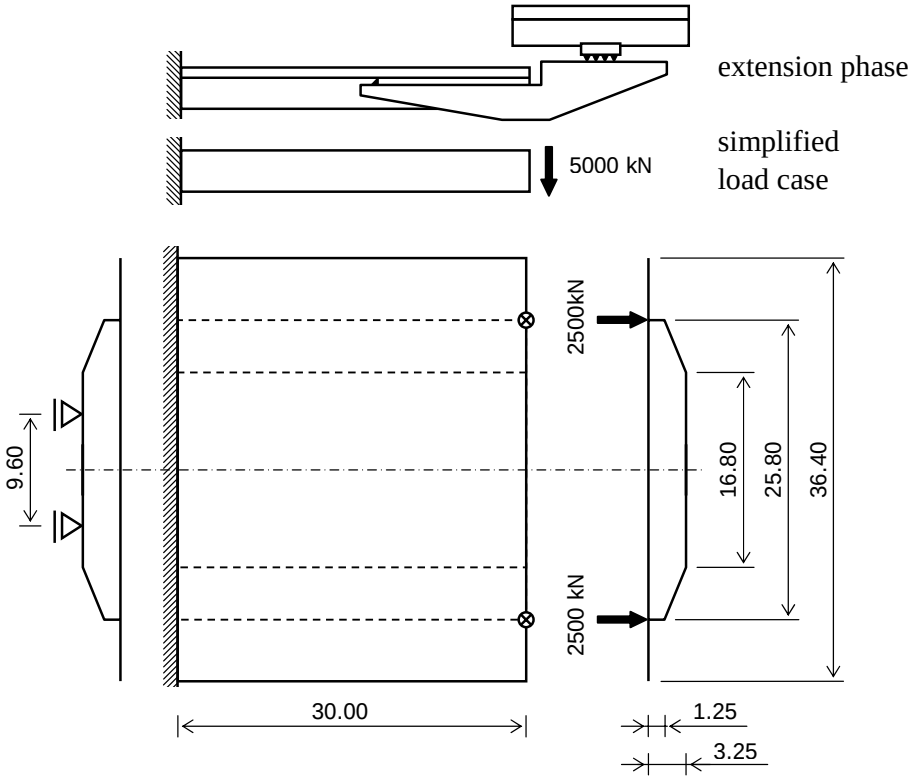

Fig. 5.5: Loading during a critical extension phase (dimensions in m).

$$S_{xx} = \frac{E\,t}{1-\upsilon^2} + E\,t'\frac{l}{b} \quad ; \quad S_{\upsilon} = E\,t\frac{\upsilon}{1-\upsilon^2}$$

$$S_{yy} = \frac{E\,t}{1-\upsilon^2} \quad ; \quad \frac{1}{S_{xy}} = \frac{1}{G\,t}\left\{\frac{b-e}{b} + \frac{e}{b}\,\frac{1}{1+\alpha}\right\}$$

The reader is encouraged to derive these stiffnesses her/himself.

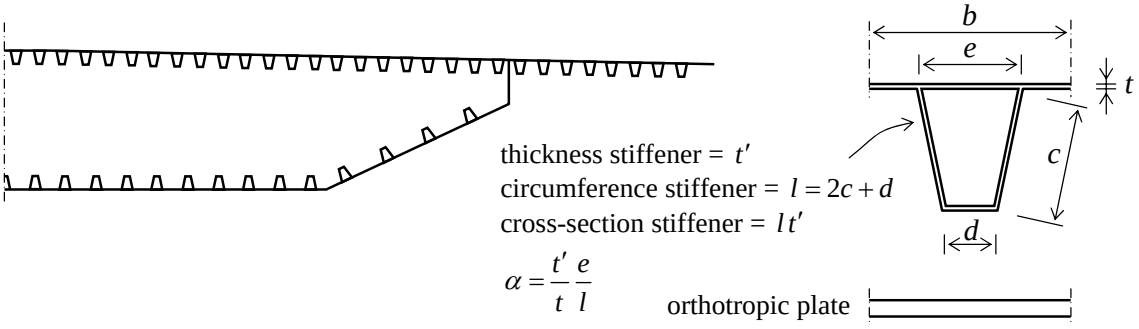

Fig. 5.6: Replacement of channel-stiffened sections by orthotropic plates.

The initial analysis is a calculation of the stresses based on the classic beam theory. These stresses have been drawn in Fig 5.7. Subsequently a calculation using the finite element method has been made. At the position where the vertical web meets the clamped end, stress concentrations are expected and the mesh is refined, as Fig. 5.8 shows.

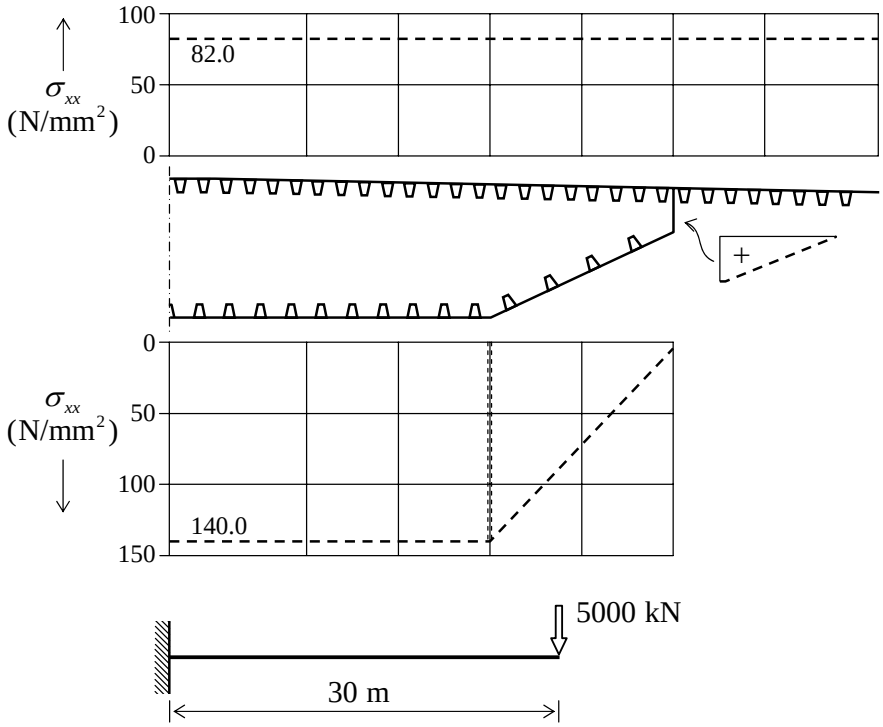

Fig. 5.7a: Stress σ_{xx} in top and bottom plate at the clamped end (beam theory).

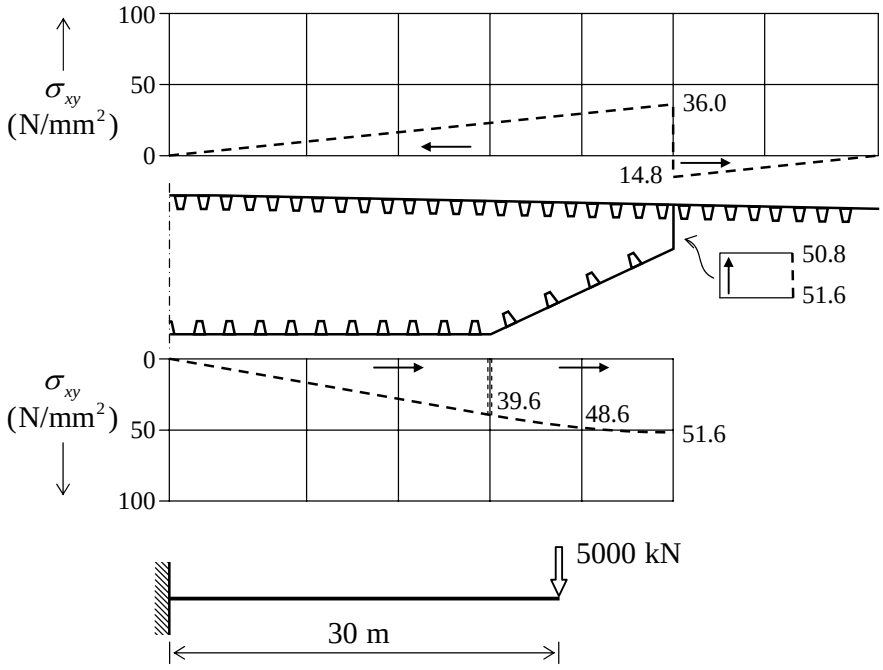

Fig. 5.7b: Stress σ_{xy} in top and bottom plate at the clamped end (beam theory).

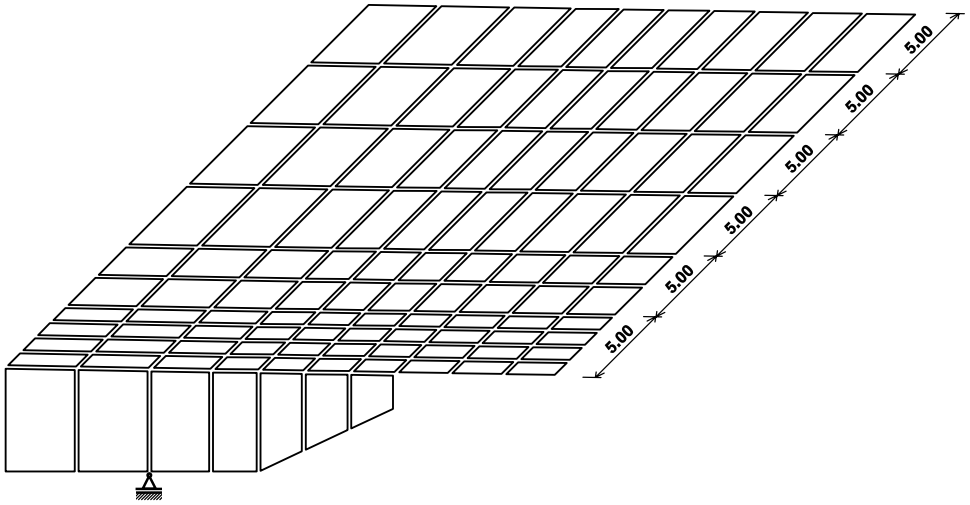

Fig. 5.8: Finite element mesh displaying shrunken elements.

5.2.2 Results of the finite element calculation

If the box girder were subjected to a constant moment over the length, the finite element method would deliver results that correspond quite closely with the beam theory. In the considered case of a linearly varying moment, this is not the case. The distribution of the stress σ_{xx} close to the clamped end in Fig. 5.9 shows large peaks close to the connections with the vertical and the sloping webs. The effective plate width to be chosen in an analysis-

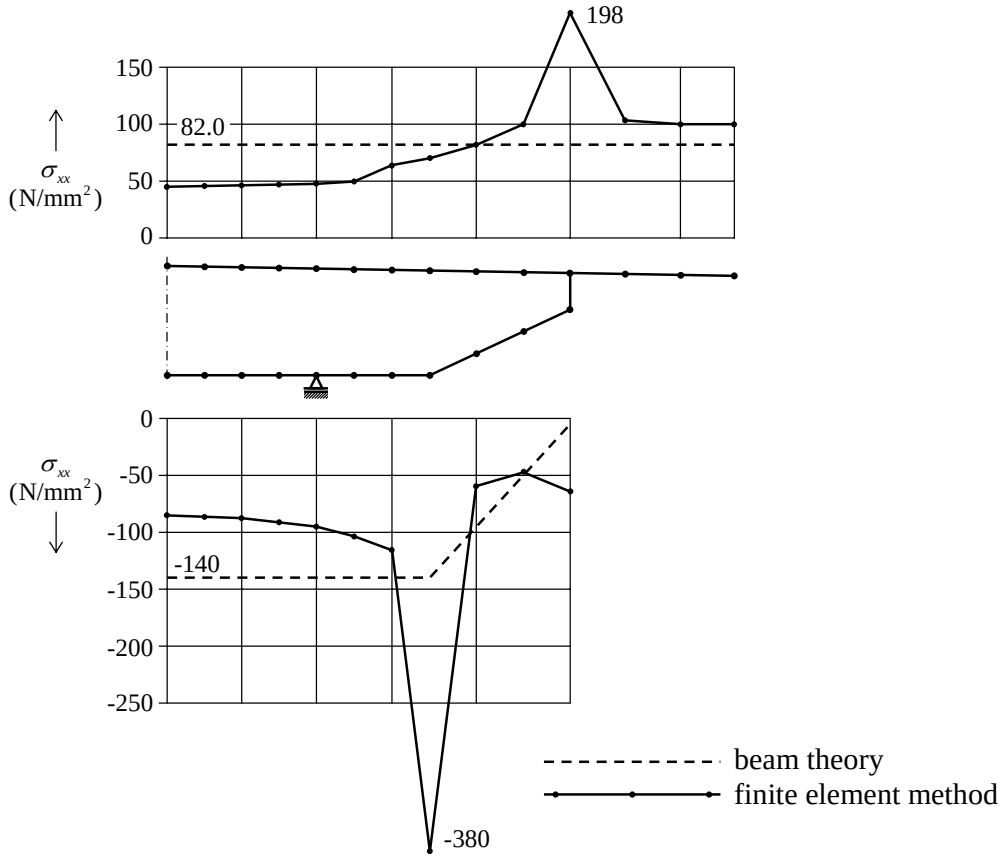

Fig. 5.9: Stress σ_{xx} in top and bottom plate at the clamped end.

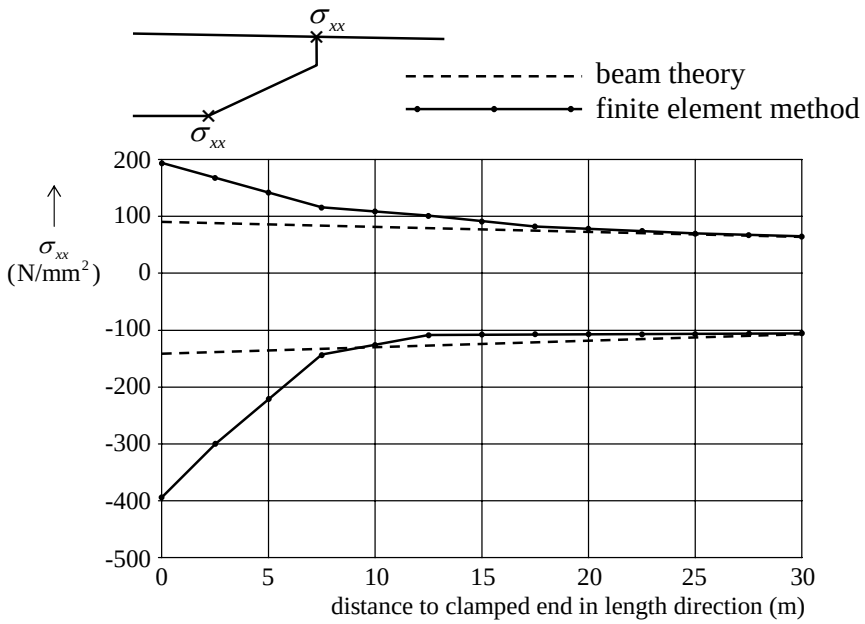

Fig. 5.10: Stress σ_{xx} in length direction.

as-beam is apparently much smaller than the box girder width. Fig. 5.10 displays the variation of σ_{xx} in length direction. It shows that the peak subdues rapidly.

The stress σ_{yy} in the circumferential direction is given in Fig. 5.11. At the centre of the cross-

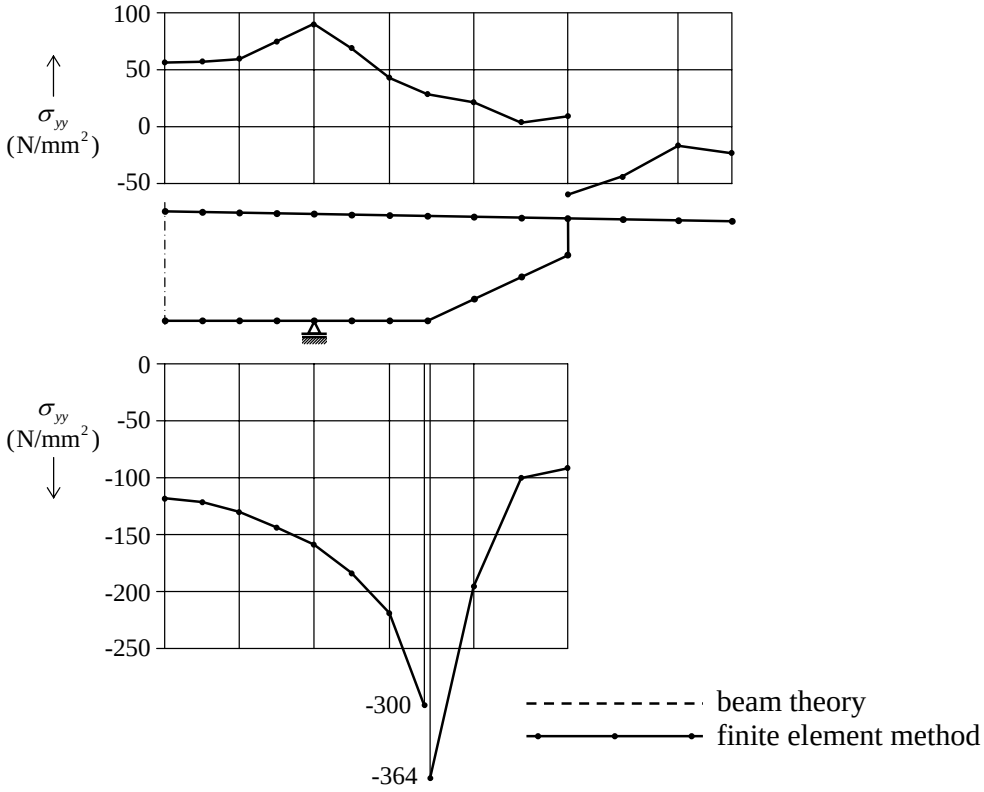

Fig. 5.11: Stress σ_{yy} next to the end diaphragm.

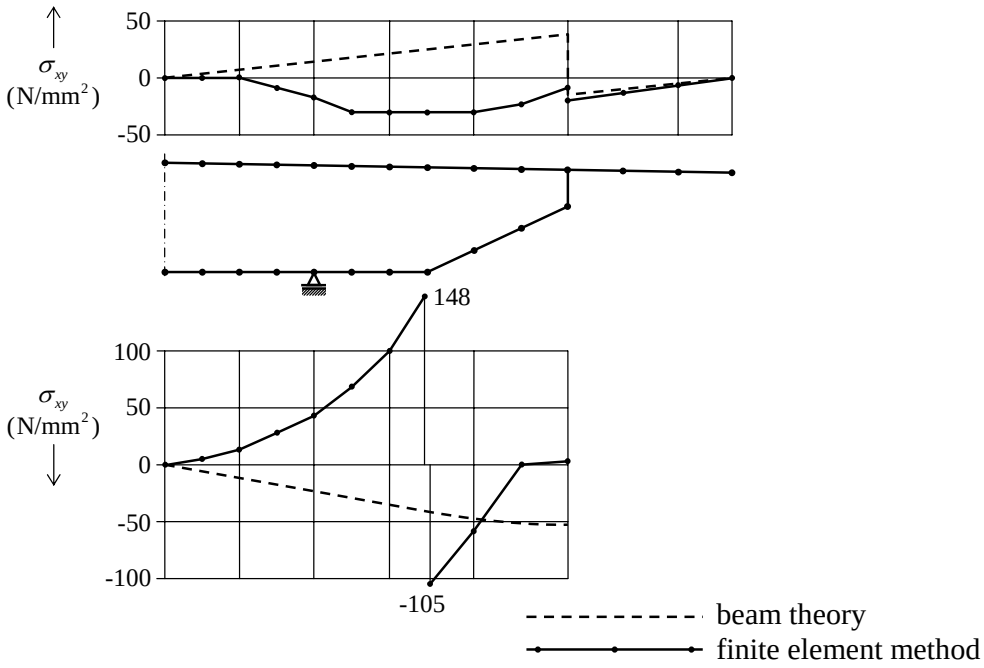

Fig. 5.12: Stress σ_{xy} next to the end diaphragm.

section, these stresses are of the same order of magnitude as σ_{xx}. According to the beam theory, these would be non-existing. Striking is the large peak close to the connection with the sloping wall in the bottom plate.
The distribution of the shear stress σ_{xy} is drawn in Fig. 5.12. The deviation from the results according to the beam theory is even larger now. Both in the upper plate and in the bottom plate the sign of the finite element result is opposite to the sign according to the beam theory. In the bottom plate the sudden change of sign and the large peak values close to the connection to the sloping web attract attention.

5.2.3 Comparison of the results with a model test

However, a few of the unexpected results can be explained at closer inspection, it has been decided to verify the finite element calculation with a model test. This was done because at the time of this bridge design (1971) there was no experience in calculating structures of this size and the structural engineer responsible for the design, appreciated a test for the reliability of this new computational method. In addition, the developers of the used finite element program were pleased with the verification check.

An elastic model made of perspex on a scale of 1:50 was built by the TNO Institute for Building Research. For the sake of simplicity, the model was made of isotropic plates, because a finite element calculation revealed that all the surprising outcomes appeared in that case as well. The model was subjected to strain gauge measurements and the deflection curve was measured.

In the Figs. 5.13, 5.14, 5.15, and 5.16 model measurements are compared to the finite element results. A large consistency was found for all the stresses. The largest difference occurs for σ_{xy} in the bottom plate and in the sloping web, but the measured values for σ_{xy} do not turn

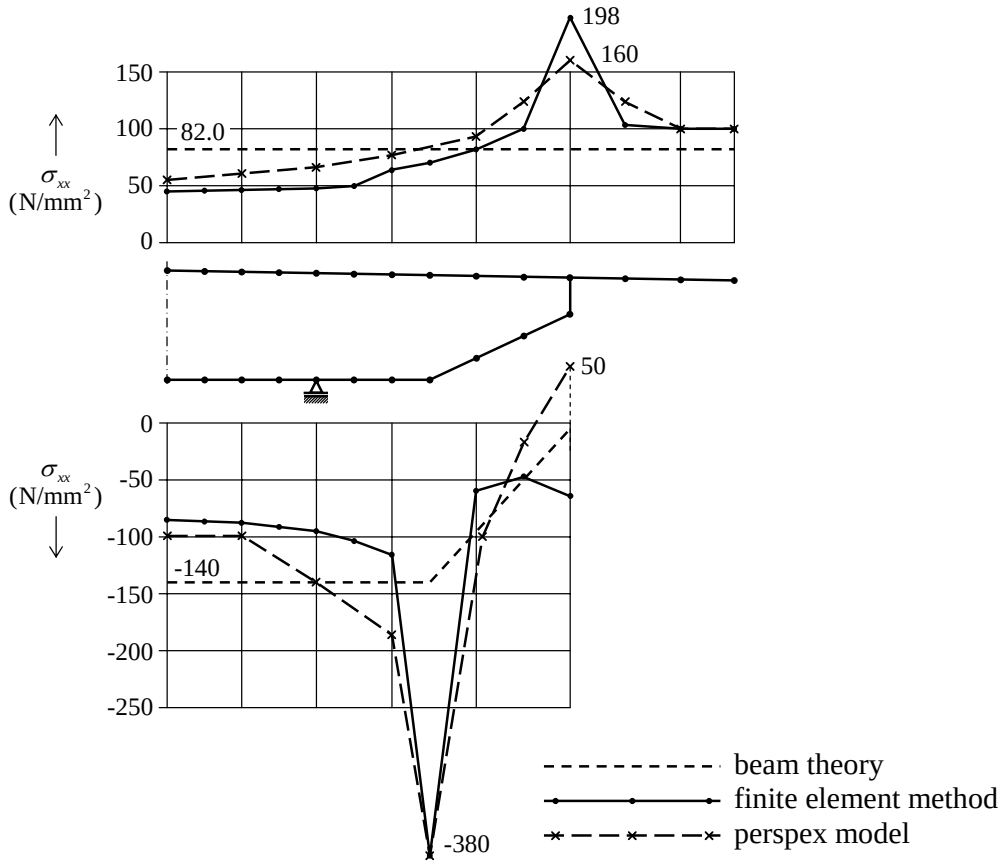

Fig. 5.13: Comparison with experiments of σ_{xx} in top and bottom plate at the clamped end.

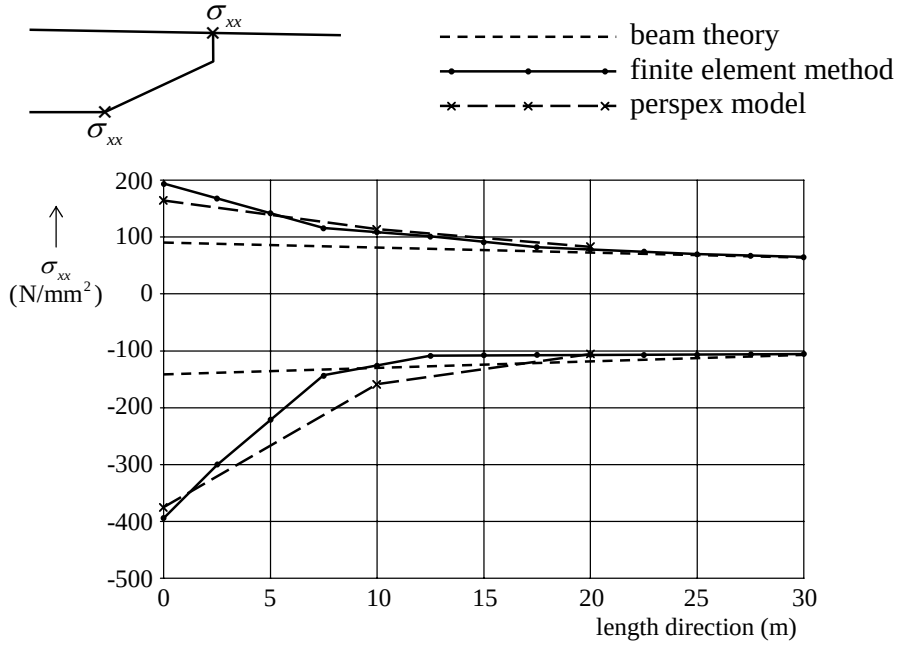

Fig. 5.14: Comparison with experiments of σ_{xx} in length direction.

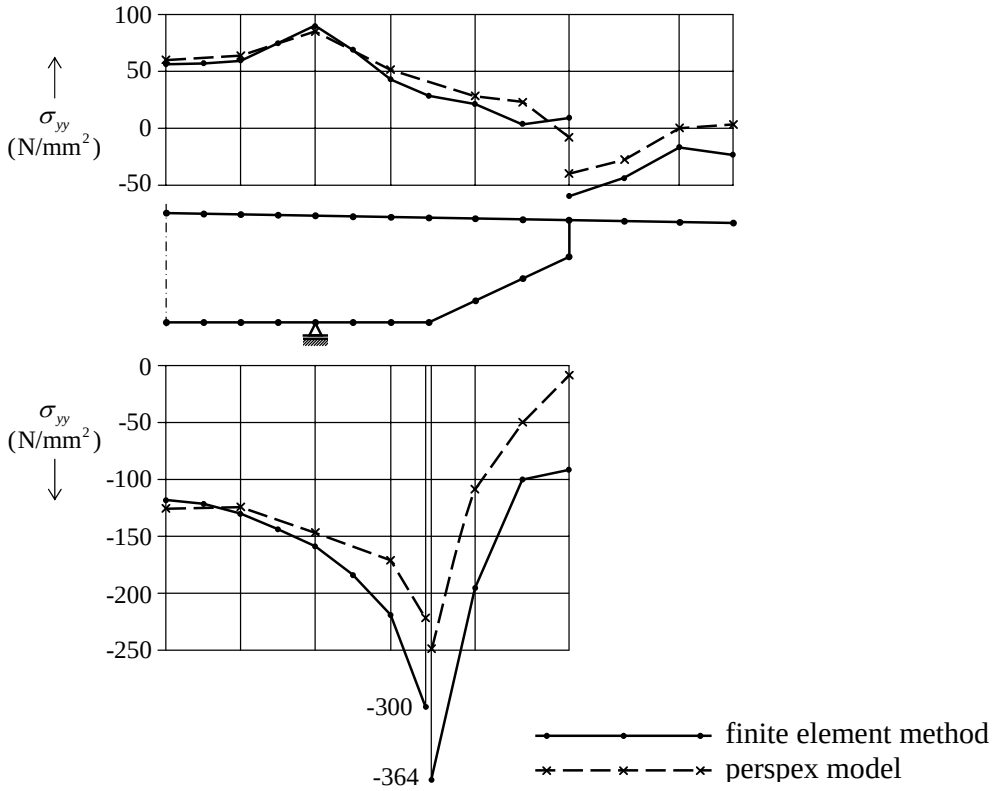

Fig. 5.15: Comparison with experiments of σ_{yy} next to the end diaphragm.

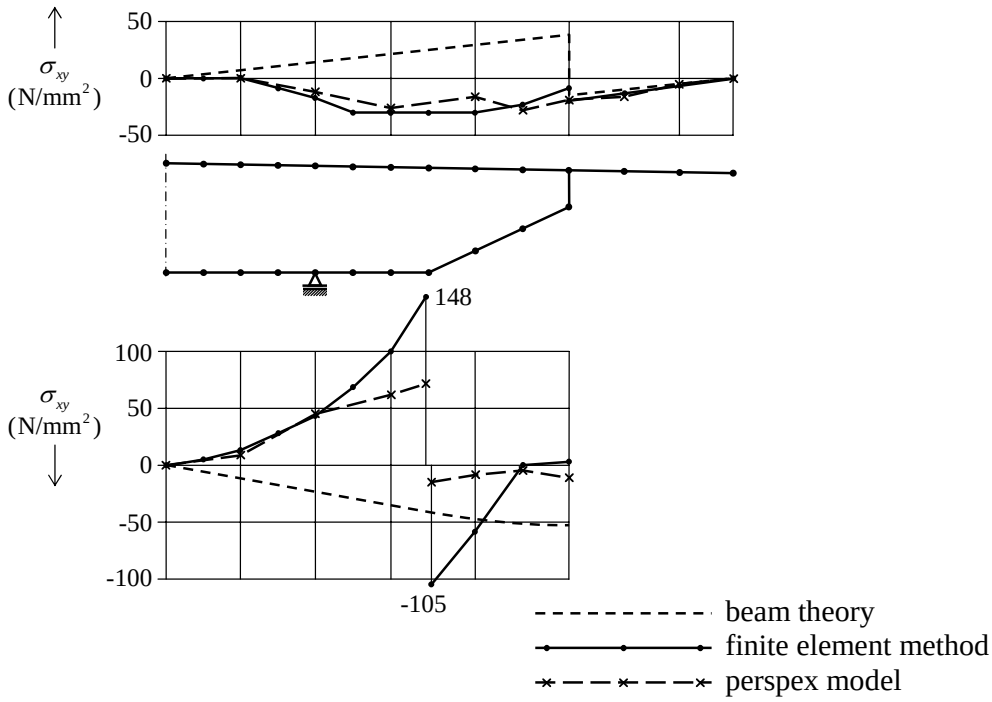

Fig. 5.16: Comparison with experiments σ_{xy} next to the end diaphragm.

out to be very reliable there. They are very hard to determine exactly from a rosette gauge measurement. Because of that, the vertical resultant of all measured shear stresses is not in equilibrium with the applied point load. However, in the finite element calculation the equilibrium is satisfied.

The performed comparison has made a substantial contribution to the acceptance of the finite element calculations with the responsible structural designers. Since this verification took place, the finite element method has become a generally accepted computational method and all important structures are checked in this fashion.

5.3 Interpretation of the results

Now that the results of the calculation have been proved reliable, it is desirable to see if the results can be explained. Perhaps it may be possible to reduce the stress peaks with local adaptations.

5.3.1 Stress σ_{xx}

The distribution of the stresses σ_{xx} does match the expectation according to the beam theory when the box girder is subjected to a constant moment, but not when the moment varies linearly. This indicates the influence of the deformation due to the shear force. The outcomes of the beam theory are only possible when the associated deformations can take place. The distribution of the shear stresses over the cross-section, however, involves a warping of this cross-section. On the spot of the restraint above the pylon there is a line of symmetry in which the warping cannot occur (clamped end in the analysis). Therefore, a local disturbance system of stresses σ_{xx} occurs to prevent the warping.

In the Figs. 5.17, 5.18, 5.19 and 5.20 the warping that takes place according to the beam

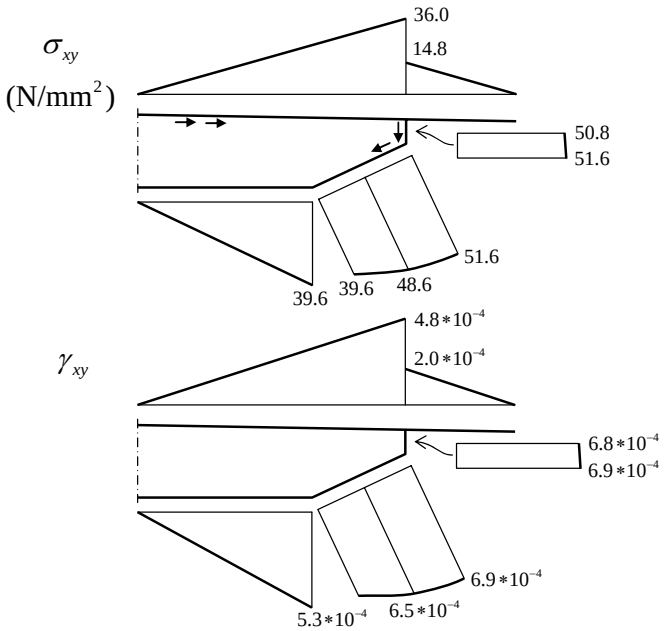

Fig. 5.17: Shear stress σ_{xy} and shear strain γ_{xy} according to the beam theory.

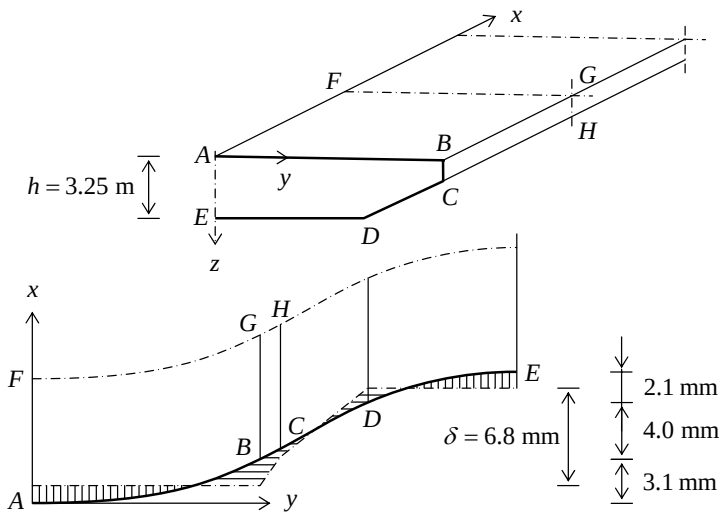

Fig. 5.18: Warping of the cross-section due to shear deformation in the beam theory.

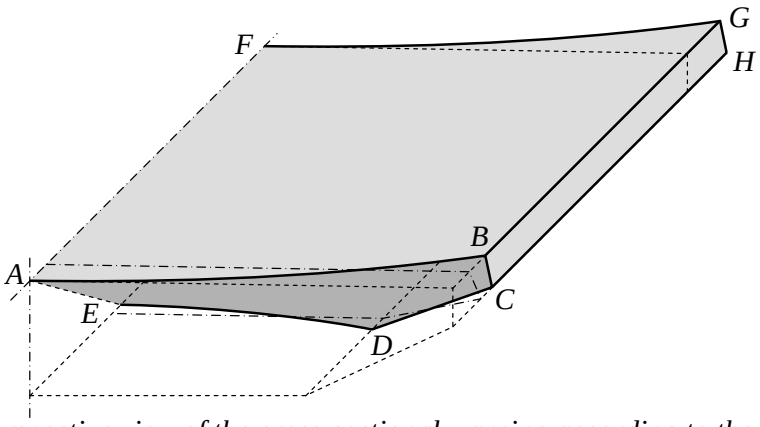

Fig. 5.19: Perspective view of the cross-sectional warping according to the beam theory.

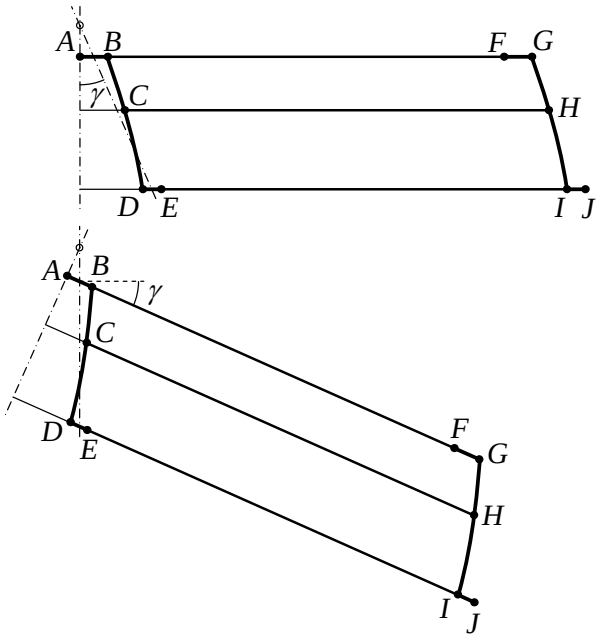

Fig. 5.20: Side view of the girder; warping due to shear deformation in the beam theory.

theory is depicted. Fig. 5.17 shows the distribution of σ_{xy} and the corresponding shear angle γ_{xy} according to the beam theory. In Fig. 5.18 the box girder is opened out into a flat surface and the way of deformation due to the calculated γ_{xy} is drawn. If the plate parts are placed back in the shape of the box girder, the perspective sketch of Fig. 5.19 appears. The side view of the deformed box girder is finally given in Fig. 5.20. In the top part of Fig. 5.20 the straight chain line indicates where about the mean of the warped section is. After toppling over an angle γ, this chain line corresponds with the vertical plane of symmetry above the support. The vertical displacement involved with the toppling is the share in the deflection line of the shear deformation.

Furthermore, it appears directly how the equilibrium system of extra stresses σ_{xx} will look like, to bring back the warped section to the flat surface that delivers the chain line in the side view. In the top plate, compression is needed in point A and tension in point B. The constant tensile stress in the upper plate according to the beam theory will be reduced in point A and increased in point B. This corresponds with the findings for σ_{xx} in the top plate in Fig. 5.9. In the bottom plate according to Fig. 5.20, tension is needed in point E and compression in point D. According to the beam theory, the magnitude of the constant compressive force gets smaller in point E and larger in point D. This also corresponds with the calculations for the bottom plate in Fig. 5.9.

5.3.2 Stress σ_{yy}

The distribution of σ_{yy} in Fig. 5.11 requires the following comments. In the upper plate, a tensile stress σ_{yy} can be expected of magnitude υ (Poisson's ratio) times σ_{xx} if the end diaphragm were totally rigid and a stress σ_{yy} equal to zero if there were no end diaphragm at all. In reality the end partition has a finite stiffness, so an intermediate value for the tensile stress σ_{yy} will follow. This may be 20% of σ_{xx}. Founded on the same principles a compressive stress σ_{yy} can be expected in the bottom plate.

However, there is more. Because the supporting points of the box girder are positioned relatively far inside, the end diaphragm starts to act as a cross girder. This cross girder has co-acting flanges being the upper and bottom plate. At the ends of this cross girder vertical forces act downwards. These are the vertical resultants of the shear stresses in the webs of the box. The cross girder is bended upwards between the supports. This delivers extra tensile stresses in the top and extra compressive stresses in the bottom. This way stresses σ_{yy} can arise in lateral direction, that are in the same order of magnitude as the longitudinal stresses σ_{xx}.

Another explanation can be found for the stress peak for σ_{yy} in the bottom plate, at the point of connection to the sloping web. We already mentioned that the cross beam has co-acting flange parts from the top plate and bottom plate. On the considered point the bottom flange of the beam abruptly gets another slope as shown in Fig. 5.21. If we assume that the bottom flange continues its function in that position, compressive stresses will work in the horizontal flange part and in the sloping flange part. However, on the slope discontinuity these cannot reach equilibrium. After all, no vertical component can be absorbed. That means the stresses in the flanges have to be zero in the slope discontinuity. The active width of flange is subsequently zero, so the stresses σ_{yy} rise sharply in that area.

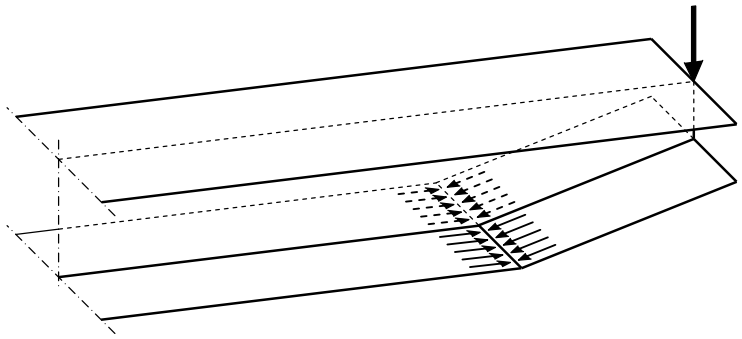

Fig. 5.21: Situation at the connection of the sloping and horizontal flange.

This calculated result has lead to the addition of a local vertical plate in longitudinal direction in this slope discontinuity. In Fig. 5.4, this is the partition carrying the letter *A.* This action halved the peak stress, which result was very welcome, also with respect to buckling, because the bottom plate is under compression in two directions there.

5.3.3 Stress σ_{xy}

If no end diaphragm was present and the stress distribution of the beam theory would hold, the top plate would shorten in cross direction due to lateral contraction and the bottom plate would widen in cross direction. However, there is an end diaphragm and it is attached to the plates. So, a shear stream σ_{xy} has to act outwards along the upper plate and inwards on the bottom plate. This acts against the direction the shear stresses according to the beam theory for the box bridge.

In addition, this effect is amplified by the fact that the supports under the cross beam (and diaphragm) have been placed inwards. In order to get the co-acting top flange under strain of tension and the co-acting bottom flange under compression, the shear stresses are even more opposed to the direction of the beam theory for the box bridge. The final result indeed is a situation with shear stresses that have a different sign than initially found according to the beam theory.

Another thing happens close to the slope discontinuity in the bottom plate. There, the active flange width of the cross beam abruptly drops to zero. Already we noticed that the stress σ_{yy} rises sharply locally. Also, large shear stresses are generated locally. These are necessary to regenerate the stress σ_{yy} in the flanges. Left and right of the slope discontinuity these shear stresses have a different direction. This results in a sudden sign change in the distribution for σ_{xy} (see Fig. 5.22).
This was seen in Fig. 5.12 in the shear stresses in the bottom plate of the box girder. By applying the previously mentioned local vertical plate in longitudinal direction at the position of the slope discontinuity. The peaks in the shear stress distributions disappear altogether.

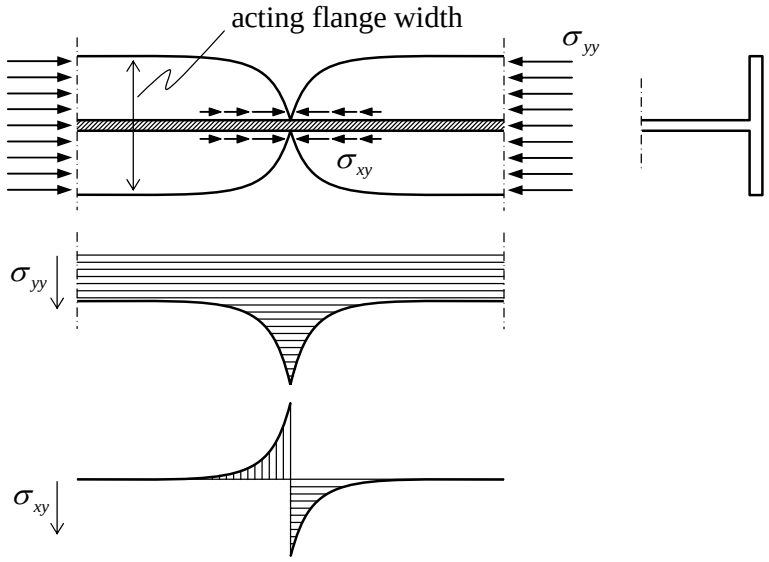

Fig. 5.22: Compressive and shear stresses due to slope discontinuity.

5.3.4 Deflection curve

To explain the calculated deflection curve first the case of pure bending is investigated. If no shear force occurs, the beam theory is in very good agreement with the finite element method, as appears from Fig. 5.23. Only at the free end of the overhanging box differences occur, but these can be explained by the way the constant moment is applied to the box bridge.

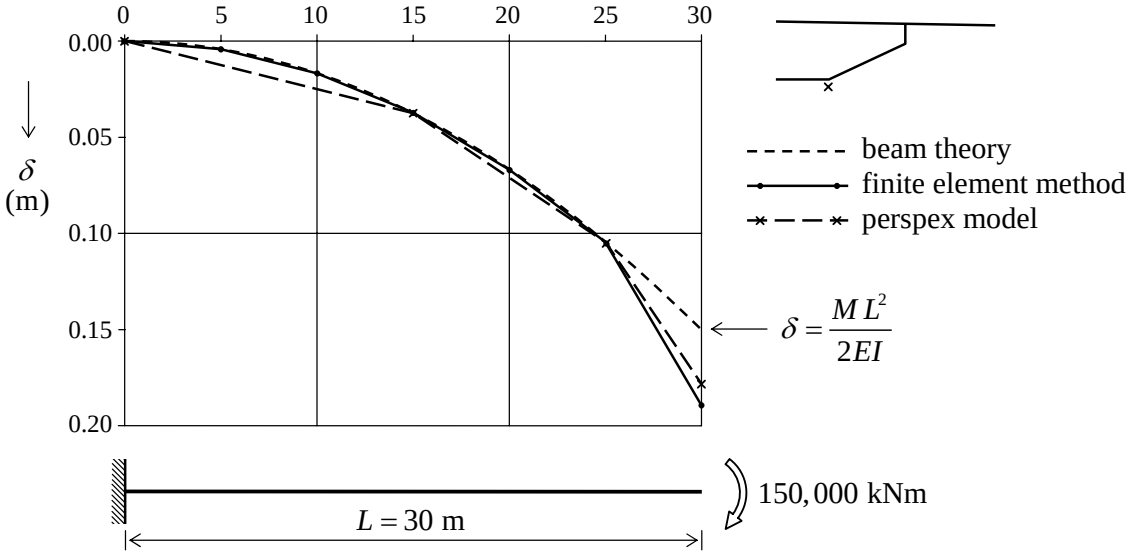

Fig. 5.23: Deflection curve for a constant moment.

Fig. 5.24 shows the deflection curve for the constant shear force due to a point load. The model measurement is once again in good agreement with the finite element calculation.

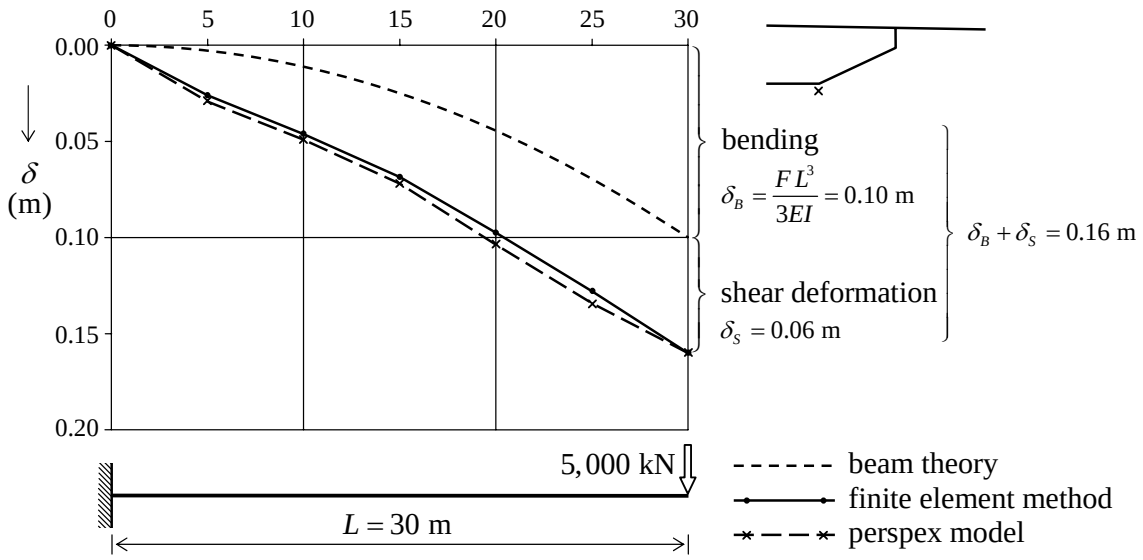

Fig. 5.24: Deflection curve for a constant shear force.

The beam theory, only taking into account bending, delivers a deflection δ_B that is much smaller. At the end this is $FL^3/3EI$. The difference with the finite element method result has to be due to the shear force deformation. If we use the average γ calculated in section 5.3.1 the δ_S can be calculated. It appears that the measured end value does correspond quite well with the sum of δ_B and δ_S .

Generally the average γ will be calculated in a different manner, namely with the well-known formula:

$$\gamma = \frac{V}{G\,A_s}$$

in which G is the shear modulus and A_s is the reduced cross-sectional area. A_s is sometimes also written as:

$$A_s = \frac{A}{\eta}$$

in which A is the actual cross-sectional area and η is a shape factor (6/5 for a rectangle). In the course CT 5141 " Theory of Elasticity" it is set forth that this replacing area A_s can be determined by equating the expressions for the work:

$$\frac{1}{2}\iint_A \frac{\sigma_{xy}^2}{G}\,dA = \frac{1}{2}\frac{V^2}{G\,A_s}$$

in which σ_{xy} are the shear stresses according to the beam theory for a shear force V as shown in Fig. 5.25

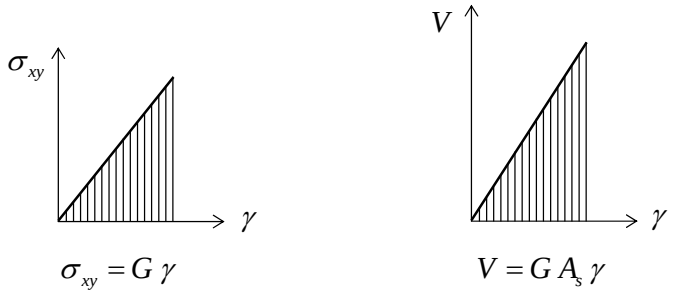

Fig. 5.25: Shear stress and shear force functions according to the beam theory.

5.4 Lessons from this case history

From the calculation and the interpretation two important lessons can be learnt. The first lesson is that *the shear force deformation is large*. If a cable-stayed bridge with this cross-sectional shape is designed using a computer program for beam structures, the program must be able to take into account the shear force deformation. The cross-sectional profile in Fig. 5.2 is deceiving in this respect. At a first glance it could concern a slender beam. The distance from the pylon to the first stay cable is 45 meters. If the height of structure is 3 meters, the ratio span to height is equal to 15. For the calculation of a solid rectangular cross-section, only the bending deformation would be required. However, this is not true for this wide box girder.

The second lesson is that *stress concentrations are important*. The considered case is actually a symmetrical problem, in which the shear force left and right of the support is of the same magnitude, but with an opposite sign as shown in Fig. 5.26. Actually there is a shear force

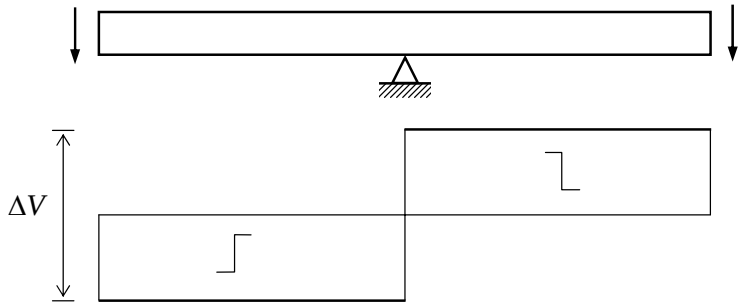

Fig. 5.26: Shear force distribution.

jump ΔV . Every place where this phenomenon occurs extra stresses have to be expected. So, this also takes place at the attachment points of the stay cables.

6 Beam loaded laterally (bending). Approximation

Chapter 1 discussed two different approximations for a bar loaded in extension. In approximation 1 the deformations were adjusted (lumped) and in approximation 2 the loads were adjusted (lumped). These two approaches may also be applied to beams in bending. Approximation 2 will not be discussed any further here, for it is treated at full length in all elementary textbooks on the Finite Element Method.

6.1 Stiffness Matrix of Discrete Bending Element

In approximation 1 for beams in bending, discrete springs are used to model the lumped bending deformation. A rigid element that has rotational springs at its ends replaces a beam part with a length a. This model is depicted in Fig. 6.1. The rotational spring is considered to

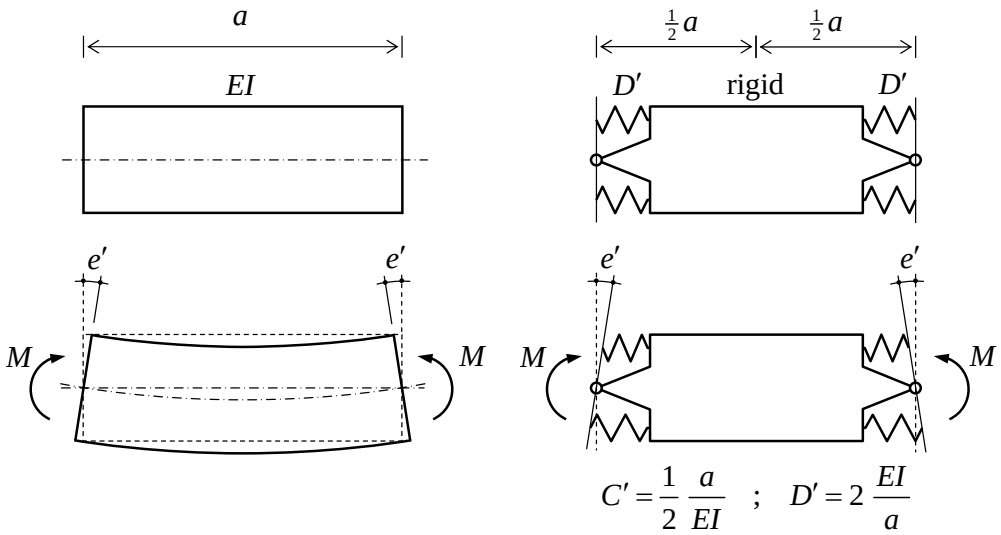

Fig. 6.1: Discrete bending element.

be composed of two horizontal extensional springs. The rotational stiffness at each end is D' and the compliance (flexibility) is C'.
It is required that the two beam-ends in both the model and the actual beam have the same rotation e'. This yields:

$$C' = \frac{1}{2}\frac{a}{EI} \quad ; \quad D' = 2\frac{EI}{a}$$

So, when two beam parts are joined together, the two rotational end springs are connected in series. The combined rotational spring has a C and D as follows:

$$C = C' + C' = \frac{a}{EI}$$

$$D = \frac{1}{C} = \frac{EI}{a}$$

Now a cantilever beam modelled by four beam parts with length a is considered as shown in Fig. 6.2. The homogeneous load is lumped in the hinges between the four sections. The deflections of the hinges are the actual unknowns.

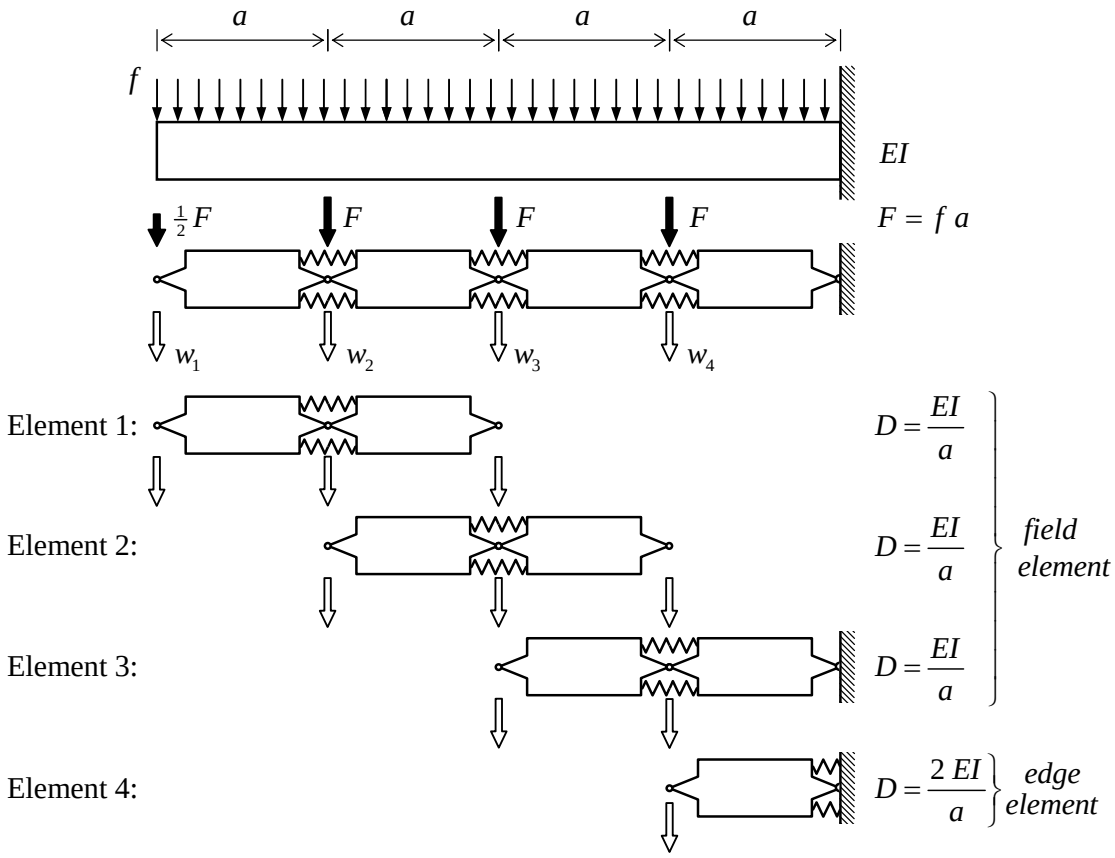

Fig. 6.2: Modelling of a cantilever beam.

The structure is considered an assembly of four discrete elements and four degrees of freedom. The elements 1, 2, and 3 each have three degrees of freedom, element 4 only has one. This last element is used at the clamped end. It may also be used in a line of symmetry, in which case the element has two degrees of freedom. Naturally, this element may occur with the rotational spring at the other end as well. First, the different stiffness matrices of the two element types are derived. The element types will be named “field element” and “edge element” respectively.

Field element

The angle e between the two rigid parts is the generalised deformation of the rotational spring. The stiffness relation is:

$$M = De$$

Here M is the moment in the spring and $D = EI/a$. Because of the geometry, it is true that (see Fig. 6.3):

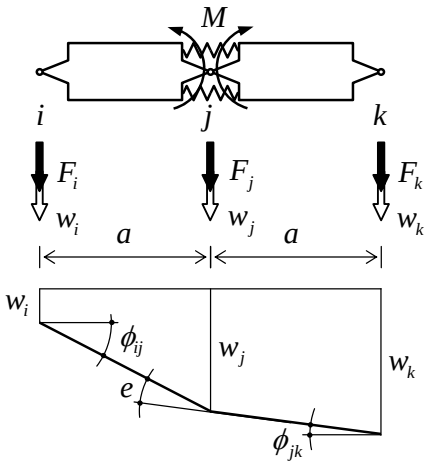

Fig. 6.3: Determination of the generalised deformation of a field element.

$$\left.\begin{aligned}\phi_{ij} &= \frac{1}{a}\left(w_j - w_i\right)\\ \phi_{jk} &= \frac{1}{a}\left(w_k - w_j\right)\end{aligned}\right\} \quad \rightarrow \quad e = \phi_{ij} - \phi_{jk} = \frac{1}{a}\left(-w_i + 2\,w_j - w_k\right)$$

Hence:

$$M = D\,e = \frac{D}{a}\left(-w_i + 2\,w_j - w_k\right)$$

The forces F_i, F_j and F_k are:

$$\begin{aligned}F_i &= -\frac{M}{a} = \frac{D}{a^2}\left(w_i - 2\,w_j + w_k\right)\\ F_j &= 2\frac{M}{a} = \frac{D}{a^2}\left(-2\,w_i + 4\,w_j - 2w_k\right)\\ F_k &= -\frac{M}{a} = \frac{D}{a^2}\left(w_i - 2\,w_j + w_k\right)\end{aligned}$$

In matrix notation this delivers:

$$\begin{Bmatrix}F_i\\ F_j\\ F_k\end{Bmatrix} = \frac{D}{a^2}\begin{bmatrix}1 & -2 & 1\\ -2 & 4 & -2\\ 1 & -2 & 1\end{bmatrix}\begin{Bmatrix}w_i\\ w_j\\ w_k\end{Bmatrix}$$

Edge element

For the element at the restrained end it holds (see Fig. 6.4): $M = D\,e$ in which $D = 2\,EI/a$.
The generalised deformation of the rotational spring becomes:

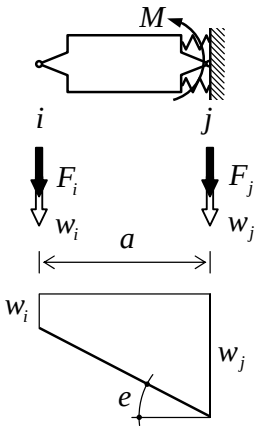

Fig. 6.4: Determination of the generalised deformation of an edge element.

$$e = \frac{1}{a}\left(w_j - w_i\right)$$

Hence:

$$M = \frac{D}{a}\left(w_j - w_i\right)$$

The forces F_i and F_j are:

$$F_i = -\frac{M}{a} = \frac{D}{a^2}\left(w_i - w_j\right)$$
$$F_j = \frac{M}{a} = \frac{D}{a^2}\left(w_j - w_i\right)$$

In matrix notation it reads:

$$\begin{Bmatrix} F_i \\ F_j \end{Bmatrix} = \frac{D}{a^2}\begin{bmatrix} 1 & -1 \\ -1 & 1 \end{bmatrix}\begin{Bmatrix} w_i \\ w_j \end{Bmatrix}$$

The same stiffness matrix results in case of the spring being at the other end i.

6.2 Global Stiffness Matrix of cantilever Beam

The stiffness matrix of the cantilever beam structure is an assembly of three field elements and one edge element. The result is shown in Fig. 6.5. The matrix needs to be multiplied by EI/a^3.
As can be seen in the figure, the displacements are not yet constrained. If displacements are prescribed, the corresponding rows and columns are skipped. In Fig. 6.6 a number of possibilities have been indicated.

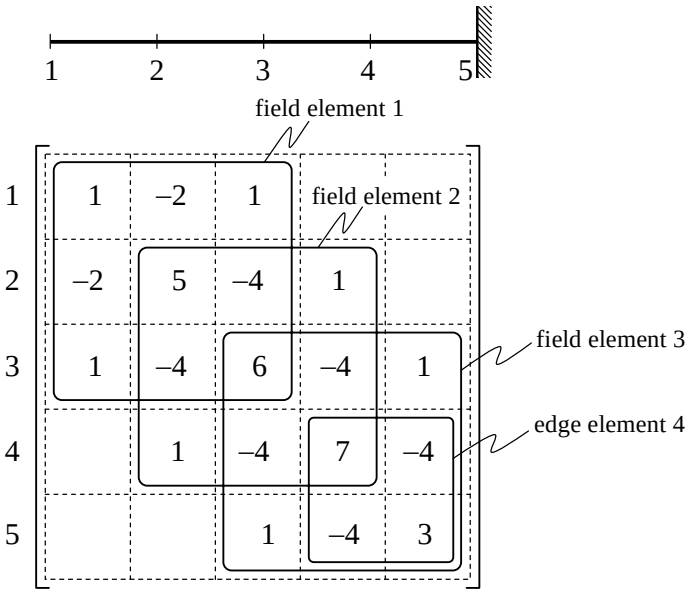

Fig. 6.5: Composition of the stiffness matrix.

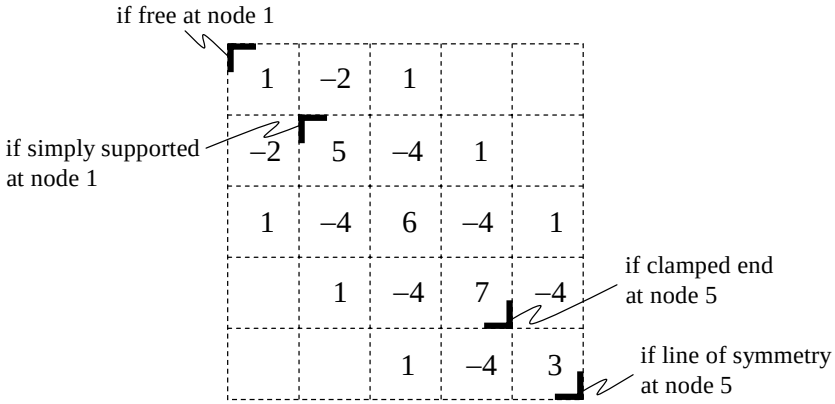

Fig. 6.6: Effect of several boundary conditions.

The third row of the stiffness matrix is complete. If more nodes were present, the row would appear more often. Apart from the multiplication factor EI/a^3, the "molecule" shown in Fig. 6.7 applies for nodes not affected by any edge conditions.

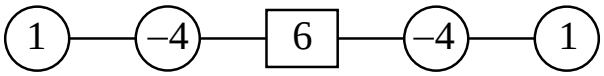

Fig. 6.7: "Molecule" in a complete field row.

Remark

As long as no boundary constraints have been applied, the sum of the terms in each row of the stiffness matrix must be zero. This can be verified by performing a rigid body translation with

all values for w equal. In that case, all the right-hand member terms of the stiffness equation $\boldsymbol{K}\,\boldsymbol{u} = \boldsymbol{f}$ have to be zero.

Example

The set of equation for the case of a cantilever beam has been solved. The nodal force F as shown in Fig. 6.8 can be obtained from:

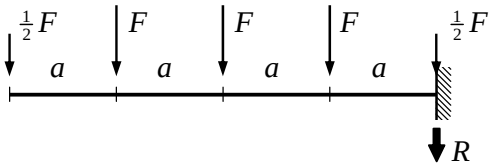

Fig. 6.8: Example of a Cantilever beam.

$$F = f\,a$$

The matrix equation reads:

$$\frac{EI}{a^3}\begin{bmatrix} 1 & -2 & 1 & & \\ -2 & 5 & -4 & 1 & \\ 1 & -4 & 6 & -4 & 1 \\ & 1 & -4 & 7 & -4 \\ & & 1 & -4 & 3 \end{bmatrix}\begin{Bmatrix} w_1 \\ w_2 \\ w_3 \\ w_4 \\ w_5 \end{Bmatrix} = \begin{Bmatrix} \tfrac{1}{2} f\,a \\ f\,a \\ f\,a \\ f\,a \\ \tfrac{1}{2} f\,a + R \end{Bmatrix}$$

The solution is:

$$\boldsymbol{u}^T = \frac{a^4 f}{EI}\left\{ 34 \quad 23 \quad 12\tfrac{1}{2} \quad 4 \right\} \quad 0$$

And from the fifth row, we can obtain:

$$\tfrac{1}{2} f\,a + R = f\,a\left(1*12\tfrac{1}{2} - 4*4 + 3*0\right) \quad \rightarrow \quad R = -4\,fa$$

which is correct.

The moments are determined from:

$$M = \frac{EI}{a^2}\left(-w_i + 2w_j - w_k\right) \qquad (\textit{for a field element})$$

$$M = 2\frac{EI}{a^2}\left(w_j - w_i\right) \qquad (\textit{for an edge element})$$

And so we find the results as depicted in Fig. 6.9.

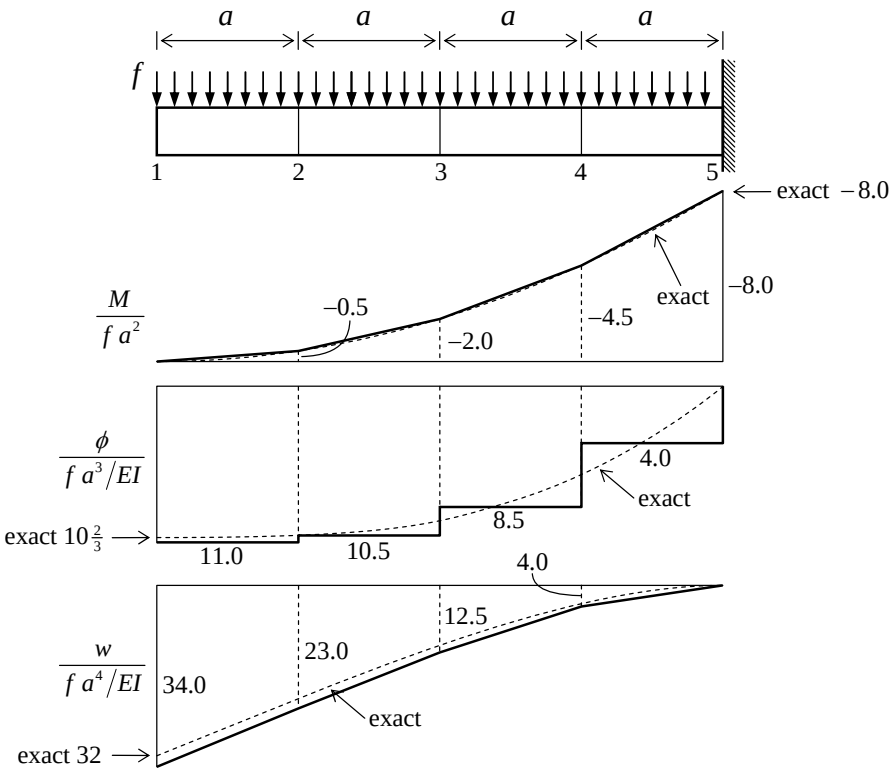

Fig. 6.9: Computed moments, rotations and displacements.

Remark

When the classical method of finite differences is applied, the governing differential equation is replaced by:

$$EI\frac{d^2H}{dx^2} = f \quad ; \quad H = \frac{d^2w}{dx^2} \tag{6.1}$$

In node 3 then the case is:

$$\frac{d^2H}{dx^2} = \frac{H_2 - 2H_3 + H_4}{a^2} \tag{6.2}$$

And H_2, H_3 and H_4 are:

$$H_i = \left[\frac{d^2w}{dx^2}\right]_i = \frac{w_{i-1} - 2w_i + w_{i+1}}{a^2} \qquad i = 2,3,4 \tag{6.3}$$

Substituting (6.2) and (6.3) in (6.1) yields:

$$\frac{EI}{a^3}\left(w_1 - 4w_2 + 6w_3 - 4w_4 + w_5\right) = f\,a$$

The coefficients seen above form the scheme as shown in Fig. 6.10, which was also found to be the third row of the stiffness matrix as indicated in Fig. 6.7. All rows not influenced by boundary conditions will have this same structure. The advantage to the method discussed in

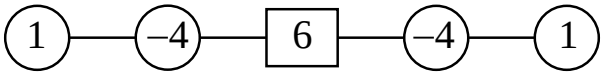

Fig. 6.10: Molecule in Finite Difference Method.

this chapter, is that it is also applicable to nodes that are at irregular distances, nodes close to or on the boundaries and to cases with abrupt changes of thickness.

Exercise

Consider two beam parts with lengths a_p and a_q and bending stiffnesses EI_p and EI_q respectively (see Fig. 6.11). The rotational spring of the element has stiffness D_{pq} and the stiffness matrix is $\boldsymbol{K}_{pq}$.

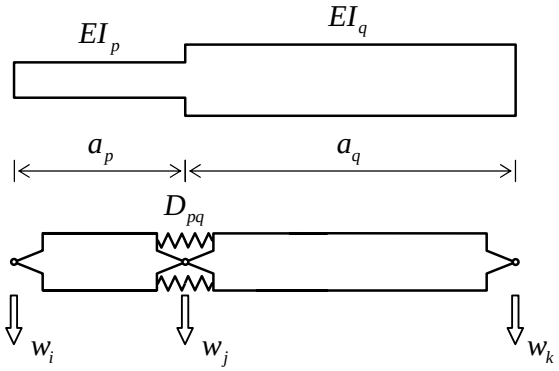

Fig. 6.11: Modelling of a beam with a sudden change in thickness.

Determine D_{pq} and $\boldsymbol{K}_{pq}$.

7 Slabs. Discrete Element Approximation

This chapter considers plates in bending (slabs). The distributed load $p(x, y)$ acts as a normal load on the plane. The plate depth is t, Young's modulus is E and Poisson's ratio is υ. This consideration is restricted to rectangular plates, and deformations due to shear forces are excluded.
The acting loads produce bending moments m_{xx} and m_{yy}, a torsional moment m_{xy} and shear forces q_x and q_y. The moments m_{xx}, m_{yy} and m_{xy} correspond with curvatures κ_{xx} and κ_{yy} and a torsional deformation ρ_{xy}, respectively. The sign convention is the same as in Volume 1, Theory.

The relation between these stress resultants and deformations is:

$$\begin{Bmatrix} m_{xx} \\ m_{yy} \\ m_{xy} \end{Bmatrix} = \frac{E t^3}{12\left(1-\upsilon^2\right)} \begin{bmatrix} 1 & \upsilon & 0 \\ \upsilon & 1 & 0 \\ 0 & 0 & \dfrac{1-\upsilon}{2} \end{bmatrix} \begin{Bmatrix} \kappa_{xx} \\ \kappa_{yy} \\ \rho_{xy} \end{Bmatrix}$$

or in short:

$$\boldsymbol{m} = \boldsymbol{D}\,\boldsymbol{\kappa}$$

Here E is the modulus of elasticity, υ is Poisson's ratio and t is the plate thickness. In the following part the plate bending stiffness (or flexural rigidity) D will be required:

$$D = \frac{E t^3}{12\left(1-\upsilon^2\right)}$$

The sign convention is shown in Fig. 7.1.

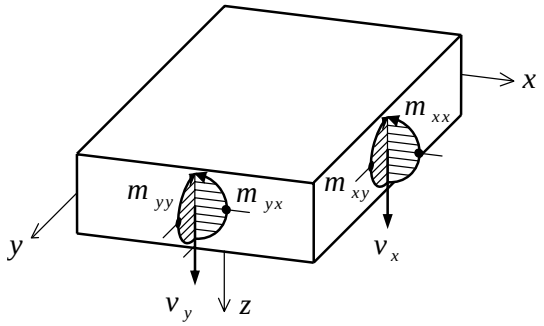

Fig. 7.1: Stress resultants in the slab; the drawn quantities are positive.

Similarly to plates loaded in their plane, lateral contractions are excluded to start with. So the input for Poisson's ratio is $\upsilon = 0$.
This section will elaborate on the results found in chapter 6 by making the extension to plates, once again called approximation 1. As was done previously, an approximation 2, a refined

approximation 2 and an approximation 3 will be considered. Then, the general FEM will be applied in section 7.2, which is valid also for values of υ that are not zero.

7.1 Assembly of Spring Elements and Torsion Panels. Approximation 1

A rectangular plate element with length a and width b is considered as shown in Fig. 7.2. The bending behaviour in the *x*- and *y*-direction is modelled with the spring elements derived in chapter 6. To take into account torsion, torsional panels are introduced. The contribution of bending part is analysed first.

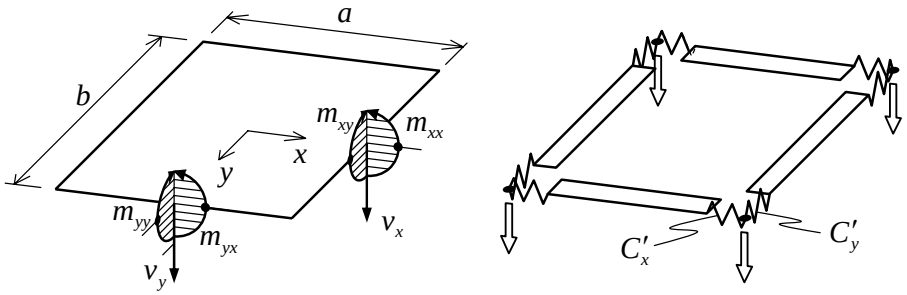

Fig. 7.2: Modelling of bending behaviour with spring elements.

In a state with homogeneous moments m_{xx} or m_{yy} the same deformation should be produced in the spring model. This yields compliances:

$$C'_x = \frac{\alpha}{D} \quad ; \quad C'_y = \frac{\beta}{D}$$

in which:

$$\alpha = \beta^{-1} = \frac{a}{b} \quad ; \quad D = \frac{E\,t^3}{12}$$

Exercise

When four elements are joined the resulting set of rotational springs in a particular node is as shown in Fig. 7.3.

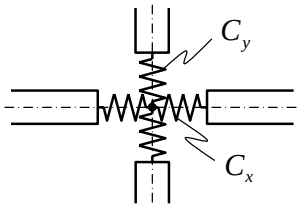

Fig. 7.3: Connection of four spring elements.

Show that:

$$C_x = \frac{\alpha}{D} \quad ; \quad C_y = \frac{\beta}{D}$$

Now the plate panel is considered. It is known that a field of constant m_{xy} can exist. In order to reach this situation a set of balanced nodal forces of value $2\,m_{xy}$ has to act on the rectangular element (see Fig. 7.4).

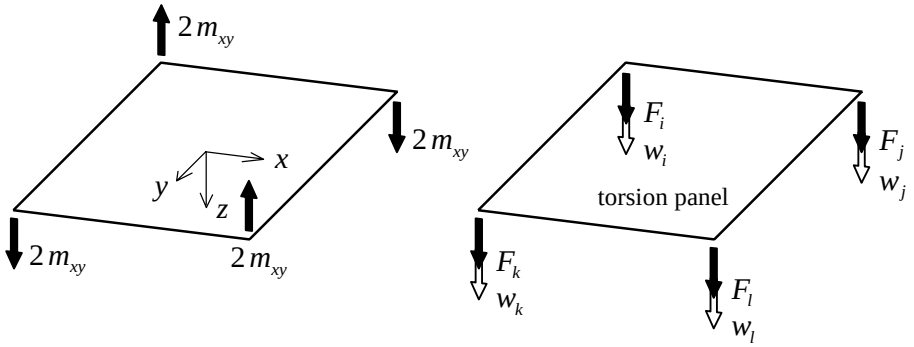

Fig. 7.4: Required loading in order to get a positive torsional moment m_{xy} (left).

The stiffness matrix of the torsion panel is derived as follows:

$$m_{xy} = \frac{1}{2} D \rho_{xy}$$

$$\rho_{xy} = -2\frac{\partial}{\partial y}\left(\frac{\partial w}{\partial x}\right) = -\frac{2}{b}\left(\frac{w_l - w_k}{a} - \frac{w_j - w_i}{a}\right)$$

Hence:

$$m_{xy} = \frac{D}{a\,b}\left(-w_i + w_j + w_k - w_l\right)$$

So, the forces are found to be:

$$F_i = -2\,m_{xy} = \frac{D}{a\,b}\left(\ 2w_i - 2w_j - 2w_k + 2w_l\right)$$

$$F_j = \ 2\,m_{xy} = \frac{D}{a\,b}\left(-2w_i + 2w_j + 2w_k - 2w_l\right)$$

$$F_k = \ 2\,m_{xy} = \frac{D}{a\,b}\left(-2w_i + 2w_j + 2w_k - 2w_l\right)$$

$$F_l = -2\,m_{xy} = \frac{D}{a\,b}\left(\ 2w_i - 2w_j - 2w_k + 2w_l\right)$$

In matrix notation this reads:

$$\begin{Bmatrix} F_i \\ F_j \\ F_k \\ F_l \end{Bmatrix} = \frac{D}{a\,b}\begin{bmatrix} 2 & -2 & -2 & 2 \\ -2 & 2 & 2 & -2 \\ -2 & 2 & 2 & -2 \\ 2 & -2 & -2 & 2 \end{bmatrix}\begin{Bmatrix} w_i \\ w_j \\ w_k \\ w_l \end{Bmatrix}$$

Any plate that may be considered a composition of rectangular plate elements can now be modelled. In order to do this, spring elements (both field and edge elements) and torsion elements (panels) are necessary.
A simply supported plate with two lines of symmetry is considered to elucidate how the global stiffness matrix is filled with values that are not equal to zero (see Fig. 7.5). The rows and columns that correspond to displacements with a value zero have been removed.

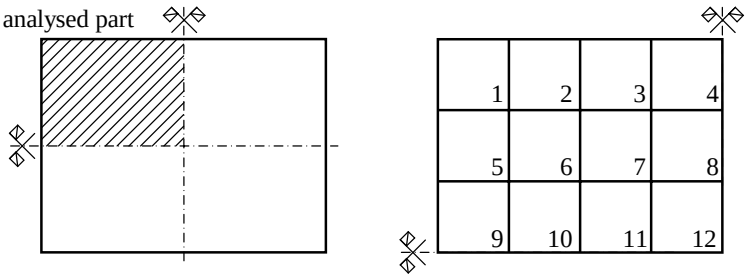

	1	2	3	4	5	6	7	8	9	10	11	12
1	*	*	*		*	*			*			
2	*	*	*	*	*	*	*			*		
3	*	*	*	*		*	*	*			*	
4		*	*	*			*	*				*
5	*	*			*	*	*		*	*		
6	*	*	*		*	*	*	*	*	*	*	
7		*	*	*	*	*	*	*		*	*	*
8			*	*		*	*	*			*	*
9	*				*	*			*	*	*	
10		*			*	*	*		*	*	*	*
11			*			*	*	*	*	*	*	*
12				*			*	*		*	*	*

Fig. 7.5: Assembly of the global stiffness matrix for a slab (approximation 1).

Exercise
Show that row 8 of the global stiffness matrix contains the following values in the case of a square mesh with size a:

Position	3	4	6	7	8	11	12
Value (times D/a^3)	2	-4	1	-8	$10\frac{1}{2}$	2	-4

In the given example, rows that are not affected by boundary conditions are not present. This occurs only a when a finer mesh is applied. A complete field “molecule” for a particular node i is influenced by 6 spring elements and 4 shear elements as depicted in Fig. 7.6.
In the case of a square mesh with size a, the “molecule” of particular node i, apart from the multiplication factor D/a^3, becomes as shown in Fig. 7.7.

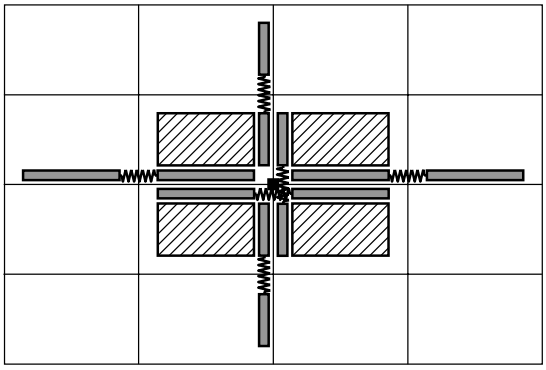

Fig. 7.6: Required configuration of spring elements and torsion panels in order to generate a complete field "molecule".

Exercise
Derive the molecule shown in Fig. 7.7 yourself.

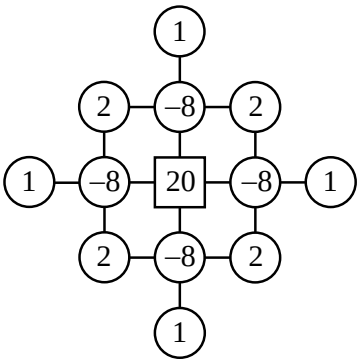

Fig. 7.7: Molecule for a complete field element of square mesh size.

Remark
The same scheme (molecule) is found when the classical finite difference method is applied to the governing differential equation:

$$D\left(\frac{\partial^4 w}{\partial x^4}+2\frac{\partial^4 w}{\partial x^2\partial y^2}+\frac{\partial^4 w}{\partial y^4}\right)=p$$

A reference to chapter 6 is made for the approximation of the fourth derivative, in which case the scheme 1, –4, 6, –4, 1 was found. This can be applied to both $\partial^4 w/\partial x^4$ and $\partial^4 w/\partial y^4$. The term $\partial^4 w/\partial x^2\partial y^2$ can be replaced by:

$$\frac{\partial^4 w}{\partial x^2\partial y^2}=\frac{\partial^2 H}{\partial x\partial y} \quad \text{with} \quad H=\frac{\partial^2 w}{\partial x\partial y} \tag{7.1}$$

In node 5 of Fig. 7.8 it holds that (see section 5.1):

$$\frac{\partial^2 H}{\partial x\partial y}=\frac{H_A-H_B-H_C+H_D}{a^2} \tag{7.2}$$

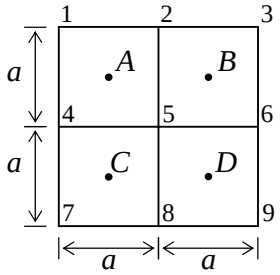

Fig. 7.8: Nomenclature used for the derivation of the fourth derivative.

And it is known that:

$$H_A = \frac{w_1 - w_2 - w_4 + w_5}{a^2} \quad ; \quad H_B = \frac{w_2 - w_3 - w_5 + w_6}{a^2}$$
$$H_C = \frac{w_4 - w_5 - w_7 + w_8}{a^2} \quad ; \quad H_D = \frac{w_5 - w_6 - w_8 + w_9}{a^2} \tag{7.3}$$

Substituting (7.2) and (7.3) in (7.1) and then multiplying the result by 2 delivers the middle scheme shown in Fig. 7.9 (except for a factor $1/a^4$).

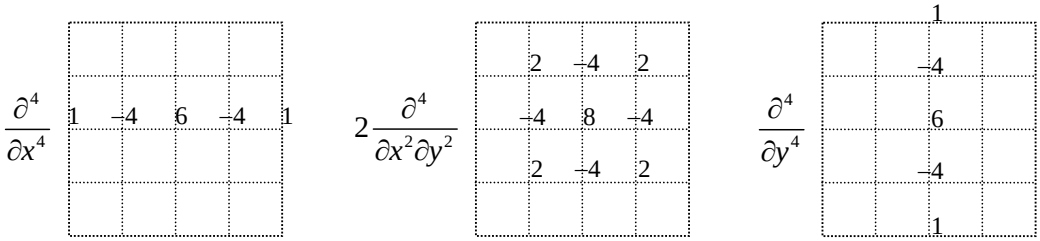

Fig. 7.9: Schemes for the formulation of several fourth derivatives.

Summing up the three found schemes produces the total scheme, which was depicted in Fig. 7.7. As was mentioned before, the method using springs and panels has several important advantages.

Example

A rectangular slab is loaded in bending by a uniformly distributed load p. All edges are simply supported. Due to symmetry, only the top left-hand quarter as shown in Fig. 7.10 will be analysed. The used elements and the results obtained are depicted in Figs. 7.11 and 7.12.

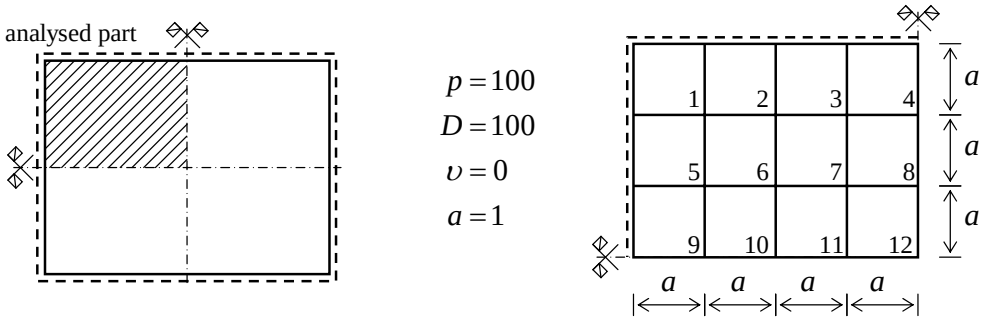

Fig. 7.10: Uniformly loaded simply supported rectangular plate.

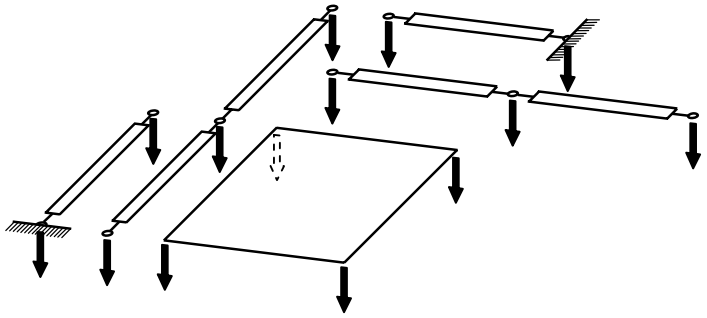

Fig. 7.11: Used types of elements.

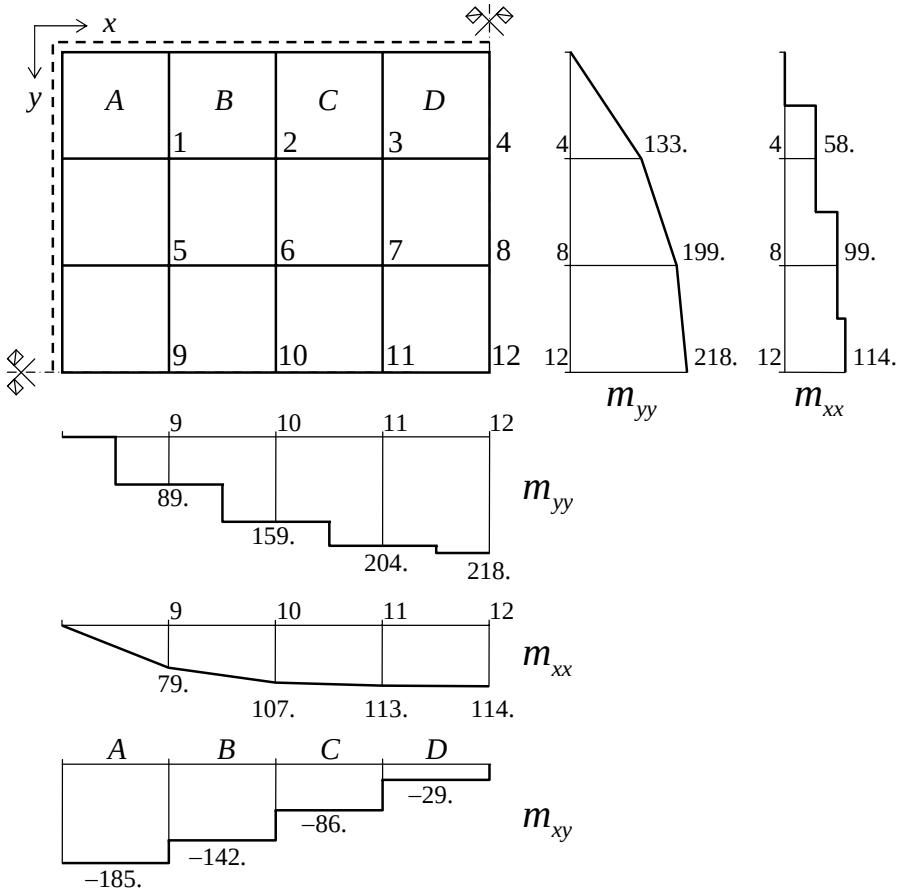

Fig. 7.12: Moment distributions in the slab.

Remark

For the exact solution of the governing differential equation the following maximum values are found:

$m_{xx} = 114$ (114)

$m_{yy} = 223$ (218)

$m_{xy} = 207$ (185)

The data between brackets are the values found in the discrete model of springs and panels. The correspondence is good enough for engineering practice.

7.2 Application of discrete slab model for office building at Amsterdam Airport (Schiphol)

Fig. 7.13 shows a picture of the office building at Amsterdam Airport (Schiphol). A plan view of one of the floors is provided in Fig. 7.14.



Fig. 7.13: Photograph of office building.

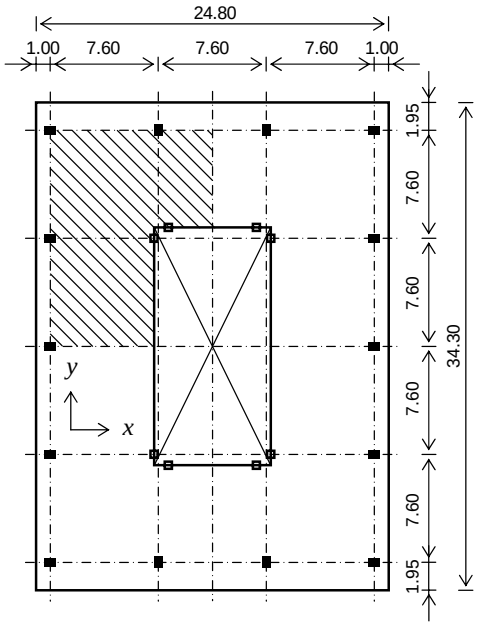

Fig. 7.14: Plan view of lift slab (dimensions in m).

The floor slab was analysed with the assembly of spring elements and torsion panels. The computed moment distributions are displayed in the Figs. 7.15 and 7.16.

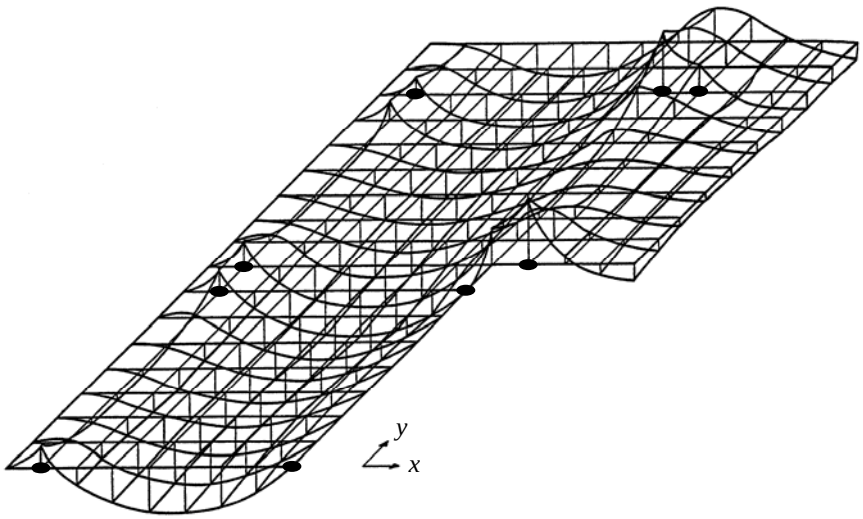

Fig. 7.15: Distribution of moments m_{xx} in a quarter of the slab of Fig. 7.14.

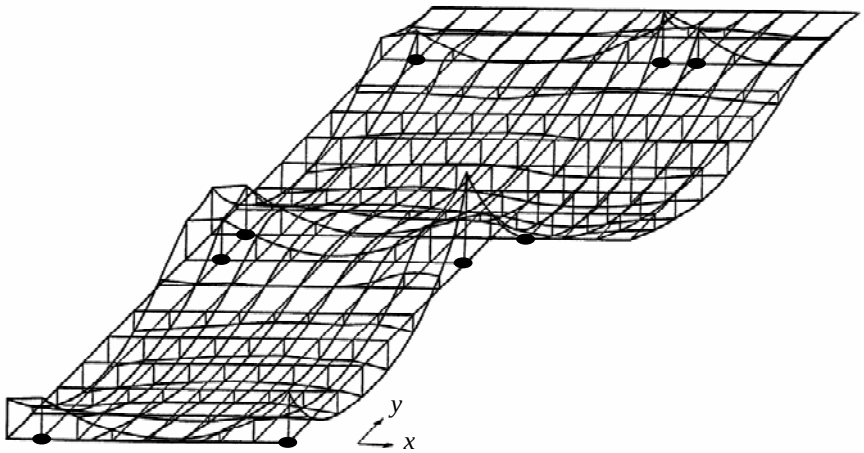

Fig. 7.16: Distribution of moments m_{yy} in a quarter of the slab of Fig. 7.14.

7.3 Comparison with result for double-sine load on Square Plate

7.3.1 Exact solution

In the theory of thin plates an exact solution known for the special case of a square simply supported slab subjected to a double-sine distributed load $p(x, y)$. For graphical results see Fig. 7.17. The analysis is restricted to a Poisson's ratio equal to zero. The deflection *w* and

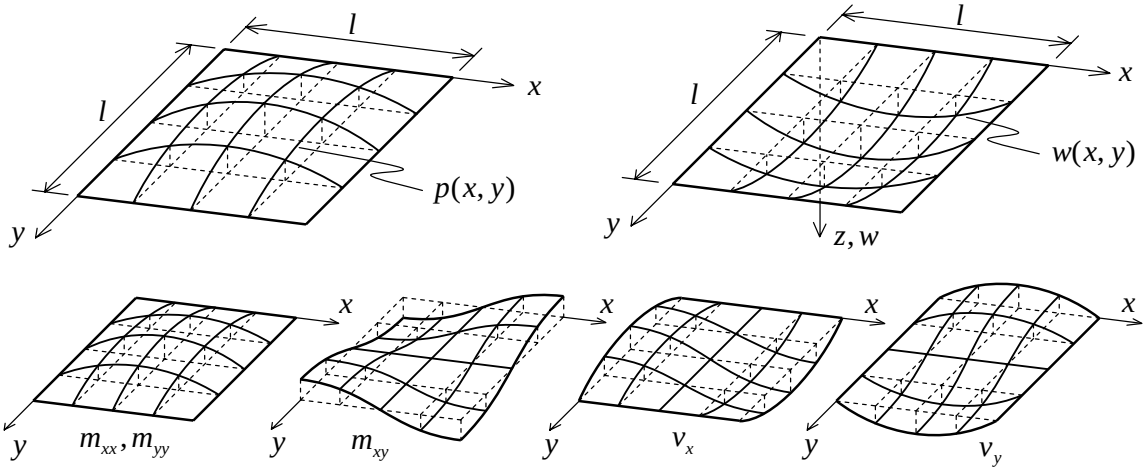

Fig. 7.17: Theoretical results for a square simply supported plate under a double-sine load.

bending moments m_{xx} and m_{yy} have the double-sine distribution. Their maximum in the centre of the plate respectively is:

$$w = \frac{p\,l^4}{4\,\pi^4 D}$$

$$m_{xx} = m_{yy} = \frac{p\,l^2}{4\,\pi^2}$$

in which p is the maximum of the distributed load, l the span of the plate and D the plate bending stiffness. The torsional moment has a double cosine distribution with a value zero in the horizontal and vertical line of symmetry. The maximum value occurs in the four corners and is (apart from the sign):

$$m_{xy} = \frac{p\,l^2}{4\,\pi^2}$$

The shear forces v_x and v_y have distributions that are sine-shaped in the one direction and cosine-shaped in the other direction. Their maximum value appears at the edges and is respectively (apart from the sign):

$$v_x = \frac{1}{2\,\pi}\,p\,l \quad ; \quad v_y = \frac{1}{2\,\pi}\,p\,l$$

The distributed support reactions f_w (positive if directed downward) along the four edges are sine-shaped with a maximum value halfway along the edges:

$$f_w = -\frac{3}{4\,\pi}\,p\,l$$

This support reaction is 50% larger in absolute value than the maximum shear force at the edge. The negative sign means that it concerns a compressive support reaction in the opposite direction to the load p. Finally it was found that four concentrated corner support reactions F occur of the value:

$$F = \frac{p\,l^2}{2\,\pi^2}$$

The positive sign means that the forces are tensile forces, acting on the plate in the direction of the load p.
A check on the equilibrium of the total plate in w-direction can been made. The total applied load $4\,p\,l^2/\pi^2$ is in equilibrium with the shear force along the four edges:

$$2\int_0^l |v_x|\,dy + 2\int_0^l |v_y|\,dx = \frac{4}{\pi^2}\,p\,l^2$$

and with the sum of the distributed and concentrated support reactions:

$$2\int_0^l |f_w|\,dx + 2\int_0^l |f_w|\,dy - 4F = \frac{4}{\pi^2}\,p\,l^2$$

7.3.2 Analysis with a discrete model of Bending Spring Elements and Torsion Panels

Now an analysis for this problem is made with a simple spring-panel model and it will be seen that the findings from the theory are confirmed. A square mesh of three by three plate parts is chosen, see Fig. 7.18.

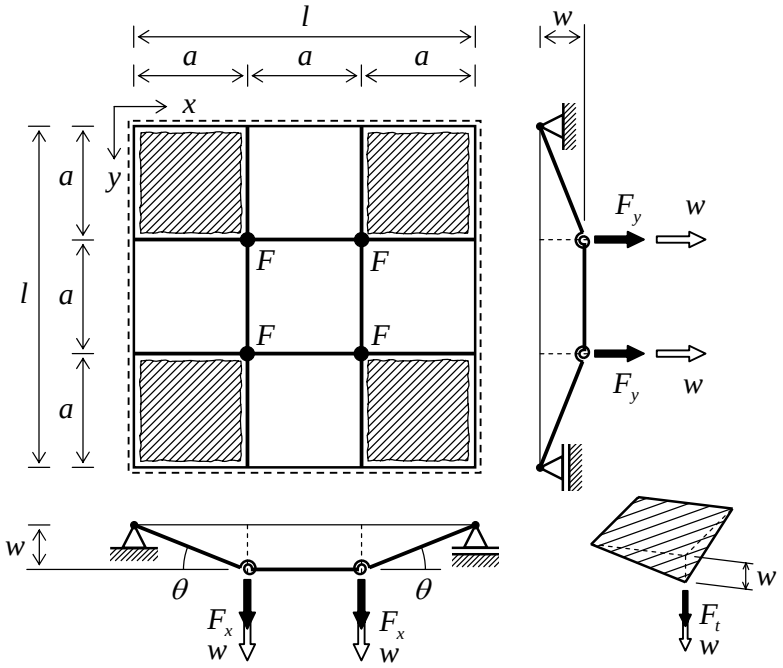

Fig. 7.18: Elementary spring-panel model for a square simply-supported plate.

For convenience we will use a for the size of the plate parts ($3a = l$). Of all 16 nodes only four can undergo a displacement w that is not zero and for reasons of symmetry they are equal, so only one degree of freedom occurs. The load can be only applied in the four free nodes and the same load F is applied in each node. The spring-panel model consists of four beams (two in each direction) and nine torsion panels. Each of the four beams consists of two springs and three rigid elements.
Five of the nine torsion panels are in a position in which no twisting deformation will occur, because the corresponding edges stay parallel. So they can be left out. The resulting model is shown in Fig. 7.18. Only the corner panels will play a role in the model, which confirms that torsion is important in the corners.

The model is so simple that we need not follow the official method in which stiffness matrices of spring elements and panel elements are assembled to a global matrix of the plate. Let us consider a beam in the position $y = a$. The stiffness D_θ of the two rotational springs is equal to the plate stiffness D. The rotation θ is w/a, so a bending moment M occurs in the springs: $M = D\,w/a$. Considering the equilibrium then yields that point loads F_x must be applied of magnitude:

$$F_x = \frac{M}{a} = \frac{D\,w}{a^2}$$

Similarly it holds for the beams in y-direction:

$$F_y = \frac{D\,w}{a^2}$$

A torsion panel is twisted by nodal forces F_t equal to $2\,m_{xy}$. It is easily seen that for the corner panels holds:

$$F_t = 2\,\frac{D\,w}{a^2}$$

Now we account for the fact that each applied load F is carried by a beam in x-direction, a beam in y-direction and a torsion panel, which all have the same displacement w, hence:

$$F_x + F_t + F_y = F \quad ; \quad \frac{D}{a^2}(1+2+1)\,w = F \quad ; \quad w = \frac{F\,a^2}{4D} \qquad \left(= \frac{1}{36}\,\frac{F\,l^2}{D} \right)$$

This very elementary model nicely demonstrates what was seen when solving the biharmonic equation for a double-sine load in Volume 1, Theory. The torsion in the plate carries half the load and the deflection is a quarter of the value that occurs if one beam has to transfer all F. Apparently it holds:

$$F_x = \frac{1}{4}F \quad ; \quad F_y = \frac{1}{4}F \quad ; \quad F_t = \frac{1}{2}F$$

The bending moment M in the rotational springs is $M = F\,a/4$, so the plate moments are:

$$m_{xx} = \frac{M}{a} = \frac{1}{4}F \quad ; \quad m_{yy} = \frac{M}{a} = \frac{1}{4}F$$

The torsional moment in the panel is (apart from the sign):

$$m_{xy} = \frac{1}{2}F_t = \frac{1}{2}\left(\frac{1}{2}F\right) = \frac{1}{4}F$$

Like it was found in the exact solution the maximum torsion moment is equal to the maximum bending moments.

Now we calculate the average shear force v_x in the line $x = \frac{1}{2}a$ over the interval $\frac{1}{2}a < y < \frac{3}{2}a$. We have to take into account the shear force V_x in the rigid beam part which crosses the considered interval and the concentrated edge shear force V_t in the torsion panel:

$$v_x = \frac{V_x + V_t}{a} = \frac{F_x + \frac{1}{2}F_t}{a} = \frac{\frac{1}{4}F + \frac{1}{4}F}{a} = \frac{1}{2}\,\frac{F}{a} \qquad \left(= \frac{3}{2}\,\frac{F}{l} \right)$$

The model ends up with lumped support reaction forces in the corner and edge nodes.

$$R_{corner} = +\frac{1}{2}F \qquad (\textit{tension, downward})$$

$$R_{edge} = -\frac{3}{4}F \qquad (\textit{compression, upward})$$

For vertical equilibrium of the total plate it is required that:

$$4R_{corner} + 8R_{edge} + 4F = \left\{4\left(\frac{1}{2}\right) + 8\left(-\frac{3}{4}\right) + 4\right\}F = 0$$

which is satisfied indeed. The distributed support reaction f_w is:

$$f_w = \frac{R_{edge}}{a} = -\frac{3}{4}\frac{F}{a} \qquad \left(= -\frac{9}{4}\frac{F}{l}\right)$$

which is 50% larger in absolute value than the shear force. All the results that were seen in the solution of the biharmonic equation reappear in this elementary model.

7.3.3 Comparison

The results of the discrete model are compared to the exact solution of the square simply supported plate subjected to a double-sine load. In the table below the maximum occurring values of the displacements w, the moments m, the shear force v and the distributed support reaction f_w are listed. Also the concentrated corner reaction F_c is given. It should be noted that the maximum values in the rough discrete model do not always precisely occur in the same position within the plate as in the exact solution.

	Exact values divided by pl^2/π^2	Values for discrete model divided by $F = pl^2/9$
w	$l^2/(4\pi^2 D)$	$l^2/(4*9D)$
m	$1/4$	$1/4$
v	$\pi/2l$	$3/2l$
f_w	$-3\pi/4$	$-3*3/4$
R_{corner}	$1/2$	$1/2$

The results of the rough discrete model and the exact solution are very close to each other. The simple discrete model nicely shows the main aspects in the force transfer of a simply supported plate:

1. Positive bending moments m_{xx} and m_{yy} in the centre of the plate.
2. Torsional moments in the corners of the plate, which have the same magnitude as the bending moments in the centre.
3. Distributed support reactions, which are 50% larger than the shear forces near the edge.
4. Large corner reactions, which have twice the value of the torsional moments in the corners.

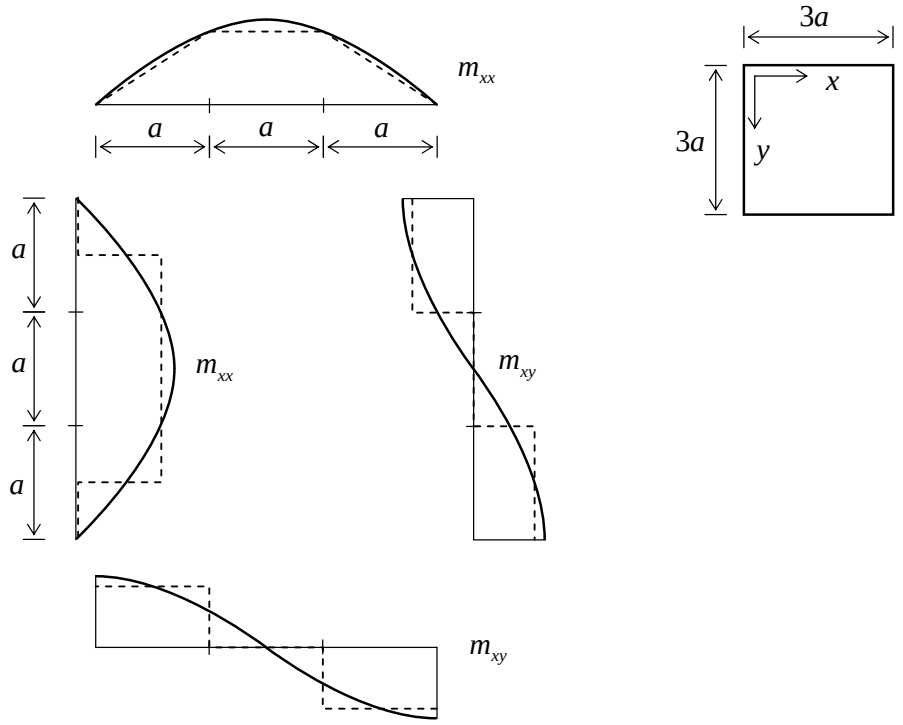

Fig. 7.19: Comparison of moment distribution for elementary discrete model (dashed line) and exact solution (solid line).

In Fig. 7.19 the distributions of the bending moments are shown.

7.4 Assembly of Beam Elements and Torsion Panels. Approximation 2

In approximation 2 the bending stiffness of the plate is lumped in beams situated at the edges of the rectangular element and the torsional stiffness is accounted for by a torsion panel, as was done in “approximation 1”. The stiffness matrix for a beam element is found in every

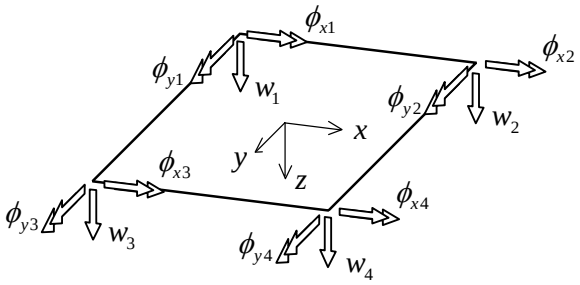

Fig. 7.20: Element consisting of beam elements and torsion panel, approximation 2.

elementary textbook on finite elements. Each node has 3 degrees of freedom, one vertical displacement w and two rotations ϕ_x and ϕ_y as is shown in Fig. 7.20.

Refined approximation 2
In this approximation the beams are distributed over the total element. The panel is still used for torsion.

7.5 Grid Model. Approximation 3

If no proper slab elements are at hand, the solution may be approximated using a program to analyse grids. In this approach Poisson's ratio is set to zero, so $G = E/2$.
A rectangular element is once more replaced by beams along the edges. These beams not only have bending stiffness, but also a torsional stiffness.
A rectangular element of sizes a by b and flexural rigidity $D = E\,t^3/12$ will be considered.
The two beams parallel to the *y*-axis have the following stiffness properties:

$$EI = \frac{1}{2} a\, D \quad \left(= \frac{1}{2} a \frac{1}{12} E\, t^3 \right) \qquad (\textit{bending})$$

$$GI_t = \frac{1}{2} a\, D \quad \left(= \frac{1}{2} a \frac{1}{6} G\, t^3 \right) \qquad (\textit{torsion})$$

Notice that the torsional moment of inertia I_t is $\frac{1}{2}(\frac{1}{6} a\, t^3)$ instead of $\frac{1}{2}(\frac{1}{3} a\, t^3)$, which is what might have been expected for a strip-like cross-section. The reason for the deviation is that only horizontal stresses and no vertical stresses occur.

The stiffnesses for the two beams parallel to the x-axis, are attained similarly but now using $b/2$ instead of $a/2$.

8 Slabs. Finite Element Method

This section discusses the general FEM valid for all values of υ. The explanation keeps to rectangular thin plate elements. Not all derivations will be explained in detail, as was done for plates loaded in their plane. Sufficient insight is assumed now, so only the broad outlines will be expounded. This means that in the explanation only the implicit interpolation method is applied.

8.1 Rectangular Element

The rectangular element to be considered is shown in Fig. 8.1. Four nodes are chosen in the vertices. Per node three degrees of freedom are defined, the displacement w normal to the slab and the rotations ϕ_x and ϕ_y. Note that these rotations differ from the rotations φ_x and φ_y used in Volume1, Theory. Here in Volume 2, the rotations are defined as follows: rotation ϕ_x is the rotation about the x-axis and rotation ϕ_y occurs about the y-axis. In the theory for thin plates it holds:

$$\phi_x = \frac{\partial w}{\partial y} \quad ; \quad \phi_y = -\frac{\partial w}{\partial x}$$

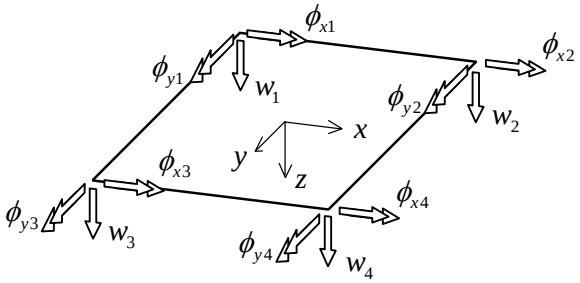

Fig. 8.1: Rectangular slab element for plate bending.

For the displacement field (deflection w) of the rectangular element as shown in Fig. 8.1, the following is chosen:

$$w(x,y) = \begin{bmatrix} 1 & x & y & x^2 & xy & y^2 & x^3 & x^2y & xy^2 & y^3 & x^3y & xy^3 \end{bmatrix} \begin{Bmatrix} \alpha_1 \\ \alpha_2 \\ \cdot \\ \cdot \\ \cdot \\ \cdot \\ \cdot \\ \cdot \\ \cdot \\ \cdot \\ \cdot \\ \alpha_{12} \end{Bmatrix}$$

or in short:

$$w(x,y) = \boldsymbol{N}_{\alpha}(x,y)\,\boldsymbol{\alpha}$$

The element has 12 degrees of freedom, and so 12 generalised coordinates α are necessary. The twelve terms in $\boldsymbol{N}_{\alpha}(x,y)$ represent the combination of the two fields, which are symbolically represented by:

$$\begin{pmatrix}1 & x & x^2 & x^3\end{pmatrix}\begin{pmatrix}1 & y\end{pmatrix}+\begin{pmatrix}1 & y & y^2 & y^3\end{pmatrix}\begin{pmatrix}1 & x\end{pmatrix}$$

It could be said this is a two-fold lattice system. One a system of cubic deflections in the *x*-direction that varies linearly in the *y*-direction, and one of cubic deflections in the *y*-direction that varies linearly in the *x*-direction.

From $w(x,y)$ the angles $\phi_x(x,y)$ and $\phi_y(x,y)$ can be derived. And so we find (remember that $\phi_x = \partial w/\partial y$ and $\phi_y = -\partial w/\partial x$):

$$\begin{Bmatrix} w \\ \phi_x \\ \phi_y \end{Bmatrix} = \left[\begin{array}{ccc|ccc|ccccc|cc} 1 & x & y & x^2 & xy & y^2 & x^3 & x^2y & xy^2 & y^3 & x^3y & xy^3 \\ 0 & 0 & 1 & 0 & x & 2y & 0 & x^2 & 2xy & 3y^2 & x^3 & 3xy^2 \\ 0 & -1 & 0 & -2x & -y & 0 & -3x^2 & -2xy & -y^2 & 0 & -3x^2y & -y^3 \end{array}\right] \begin{Bmatrix} \alpha_1 \\ \alpha_2 \\ \cdot \\ \cdot \\ \cdot \\ \cdot \\ \cdot \\ \cdot \\ \cdot \\ \cdot \\ \cdot \\ \alpha_{12} \end{Bmatrix}$$

Applying this relation to each of the four nodes the matrix $\boldsymbol{A}$ can be determined, which is necessary to transform matrix $\boldsymbol{N}_{\alpha}(x,y)$ into the wanted matrix $\boldsymbol{N}(x,y)$, see section 3.6.

From $w(x,y)$ the curvatures can be derived too:

$$\begin{Bmatrix} \kappa_{xx} \\ \kappa_{yy} \\ \rho_{xy} \end{Bmatrix} = \begin{Bmatrix} -\partial^2 w/\partial x^2 \\ -\partial^2 w/\partial y^2 \\ -2\,\partial^2 w/\partial x \partial y \end{Bmatrix} = \left[\begin{array}{ccc|ccc|cccc|cc} 0 & 0 & 0 & -2 & 0 & 0 & -6x & -2y & 0 & 0 & -6xy & 0 \\ 0 & 0 & 0 & 0 & 0 & -2 & 0 & 0 & -2x & -6y & 0 & -6xy \\ 0 & 0 & 0 & 0 & -2 & 0 & 0 & -4x & -4y & 0 & -6x^2 & -6y^2 \end{array}\right] \begin{Bmatrix} \alpha_1 \\ \alpha_2 \\ \cdot \\ \cdot \\ \cdot \\ \cdot \\ \cdot \\ \cdot \\ \cdot \\ \cdot \\ \cdot \\ \alpha_{12} \end{Bmatrix}$$

In short:

$$\boldsymbol{\kappa} = \boldsymbol{B}_\alpha(x,y)\,\boldsymbol{\alpha}$$

With the use of matrix $\boldsymbol{A}$, matrix $\boldsymbol{B}_\alpha(x,y)$ can be transformed into the sought matrix $\boldsymbol{B}(x,y)$.

Remarks

1) The applied interpolation complies with the two consistency requirements. The first three terms describe 3 rigid body displacements. No curvature is produced, as can be established from the first three columns of $\boldsymbol{B}_\alpha(x,y)$.
   The next three terms produce homogeneous curvatures as may be concluded looking at the corresponding columns of $\boldsymbol{B}_\alpha(x,y)$.
2) The interpolation violates the additional condition on inter-element compatibility, so the element is non-conforming. This may be understood by considering the edge between nodes 1 and 2. Along this edge continuity is only preserved for deflection w and not for ϕ_x. The deflection w has a cubic distribution along the edge (y = constant), and four degrees of freedom are available along the edge, being w_1, ϕ_{y1} in node 1 and w_2, ϕ_{y2} in node 2. This is sufficient to uniquely define w in this edge.
   The angle ϕ_x however has a cubic distribution and only two degrees of freedom, being ϕ_{x1} in node 1 and ϕ_{x2} in node 2. So, no unique interpolation can be reached. The continuity of ϕ_x is only ensured in the nodes. Between the nodes discontinuities will be present, but it will vanish when the mesh is sufficiently refined.
3) The curvature vector $\boldsymbol{\kappa}$ now plays the part that the strain vector $\boldsymbol{\varepsilon}$ plays for plates loaded in-plane. The strains in a plate loaded in bending are:

$$\begin{aligned}\varepsilon_{xx} &= z\,\kappa_{xx}\\ \varepsilon_{yy} &= z\,\kappa_{yy}\\ \gamma_{xy} &= z\,\rho_{xy}\end{aligned}$$

4) The chosen interpolation for $w(x,y)$ complies with the homogeneous biharmonic equation $\nabla^2\nabla^2 w = 0$.

This means that in this special case the equilibrium conditions are satisfied inside the element. The application of prescribed displacements in combination with the virtual work equation normally produces elements in which the equilibrium conditions are violated. Obviously a rectangular plate element in bending is an exception, even though the inter-element stress continuity is not ensured.

Distribution of moments and shear forces
The relation between moments and curvatures is:

$$\begin{aligned}m_{xx} &= D\left(\kappa_{xx} + \upsilon\,\kappa_{yy}\right)\\ m_{yy} &= D\left(\upsilon\,\kappa_{xx} + \kappa_{yy}\right) \qquad ; \qquad D = \frac{1}{12}\frac{E\,t^3}{1-\upsilon^2}\\ m_{xy} &= D\left(1-\upsilon\right)\kappa_{xy}\end{aligned}$$

In matrix notation this yields:

$$\begin{Bmatrix} m_{xx} \\ m_{yy} \\ m_{xy} \end{Bmatrix} = D \begin{bmatrix} 1 & \upsilon & 0 \\ \upsilon & 1 & 0 \\ 0 & 0 & \frac{1-\upsilon}{2} \end{bmatrix} \begin{Bmatrix} \kappa_{xx} \\ \kappa_{yy} \\ \rho_{xy} \end{Bmatrix} \qquad \text{or} \qquad \boldsymbol{m} = \boldsymbol{D}\,\boldsymbol{\kappa}$$

From the known distributions of the curvatures in the element it is deduced that:
- The moments m_{xx} and m_{yy} are linear in the x- and y-direction
- The moment m_{xy} can become parabolic in the x- and y-direction.

In general, 4 different values in the four different nodes of an element are to be expected. The moment distribution may be notated as:

$$\begin{Bmatrix} m_{xx} \\ m_{yy} \\ m_{xy} \end{Bmatrix} = \begin{bmatrix} 1 & x & y & xy & & & & & & & & \\ & & & & 1 & x & y & xy & & & & \\ & & & & & & & & 1 & x & y & x^2 & y^2 \end{bmatrix} \begin{Bmatrix} \beta_1 \\ \beta_2 \\ \cdot \\ \cdot \\ \cdot \\ \cdot \\ \cdot \\ \cdot \\ \cdot \\ \cdot \\ \cdot \\ \cdot \\ \beta_{13} \end{Bmatrix}$$

The generalised coordinates β are functions of α, D and υ.

The distribution of the shear forces q_x and q_y can now be determined from

$$q_x = \frac{\partial m_{xx}}{\partial x} + \frac{\partial m_{yx}}{\partial y}$$

$$q_y = \frac{\partial m_{yy}}{\partial y} + \frac{\partial m_{xy}}{\partial x}$$

It follows that:

$$\begin{Bmatrix} q_x \\ q_y \end{Bmatrix} = \begin{bmatrix} 1 & y & & \\ & & 1 & x \end{bmatrix} \begin{Bmatrix} \beta_2 + \beta_{11} \\ \beta_4 + 2\beta_{13} \\ \beta_7 + \beta_{10} \\ \beta_8 + 2\beta_{12} \end{Bmatrix}$$

So, shear force q_x is constant in the x-direction and varies linearly in the transverse direction. Similarly q_y is constant in the y-direction and linear in the x-direction. This means that we do not find different values for all four nodal shear forces.

Consistent load vector

In general a plate in bending is loaded by a distributed force p per unit of plate area. Generalised nodal forces can be calculated through:

$$\boldsymbol{f} = \iint_A \boldsymbol{N}(x,y)^T \, p(x,y)\, dA$$

The corresponding vector $\boldsymbol{u}$ contains twelve degrees of freedom; so twelve generalised nodal forces are calculated. Per node a force in the w-direction and moments in the ϕ_x-direction and ϕ_y-direction are found. The moments are quadratic, and the force linear in the size of the element. This means that the finer the mesh the smaller the influence of the moments. In practice the mesh is sufficiently fine to neglect the moments. In that case the bilinear shape function used for plates loaded in their plane can also be applied to calculate the four forces.

8.2 Some other element types

Except the rectangle two other shapes are frequently used, namely triangles and quadrilaterals (see Fig. 8.2). As a rule, no mid-side nodes are used. Each node has three degrees of freedom.

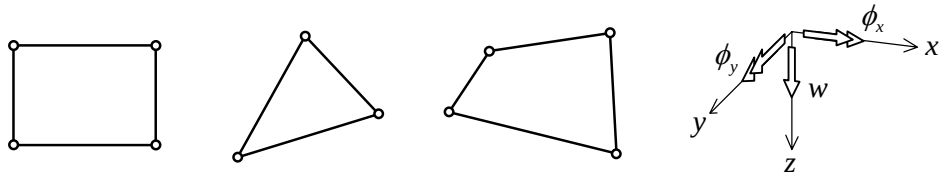

Fig. 8.2: Several element types for plate bending.

Example

The rectangular plate (also see Fig. 8.3) discussed previously in section 7.1 was also analysed with the finite element method based on an assumed displacement field, as is discussed here. The results are shown in Fig. 8.4.

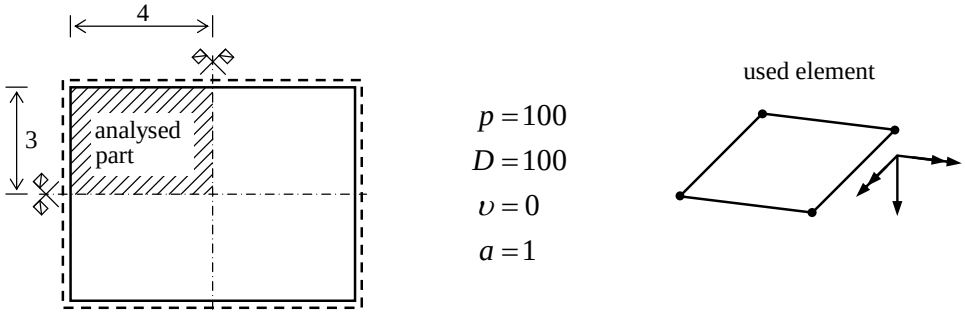

Fig. 8.3: Uniformly loaded simply supported rectangular slab.

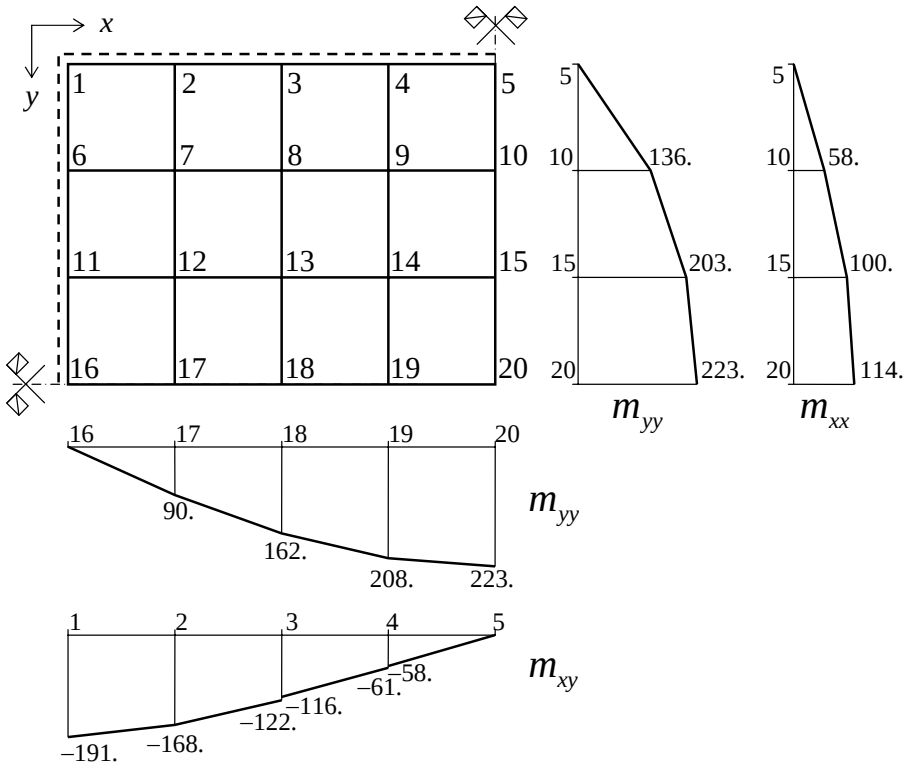

Fig. 8.4: Stress distributions in the slab.

Remark

If the mesh is refined by a factor 4, the same maximum values are found for m_{xx} (114) and m_{yy} (223). The maximum value for m_{xy} increases from 191 to 207. The coarse mesh delivers applicable engineering results.

9 Slabs. FEM for Discrete Elements

An alternative derivation for the stiffness matrix of the discrete bending element and of the discrete torsion element will be presented here applying the approach of generalised stresses and deformations.

9.1 Derivation of Bending Spring Element

The discrete bending element, as shown in Fig. 9.1, has 3 degrees of freedom so $m = 3$. Two independent rigid body motions are possible, a translation in the *w*-direction ($w_i = w_j = w_k$) and a rotation ($w_i = -w_k$; $w_j = 0$), so $l = 2$.

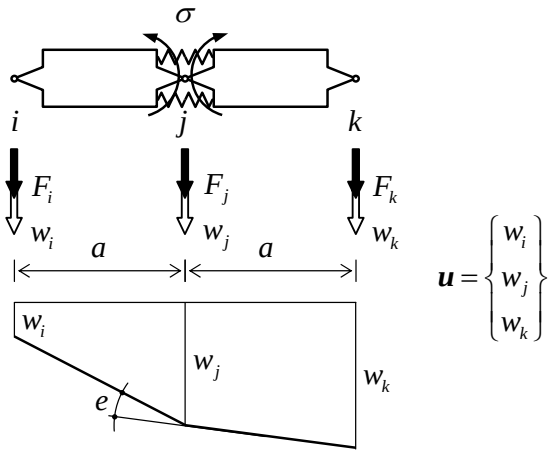

Fig. 9.1: Determination of the generalised deformation e of the discrete bending element.

Consequently, only one generalised deformation exists, so $n = 1$. This deformation is the rotation e of the lumped rotational spring and σ is the moment present in the spring. So, once again the scheme is as shown in Fig. 9.2.

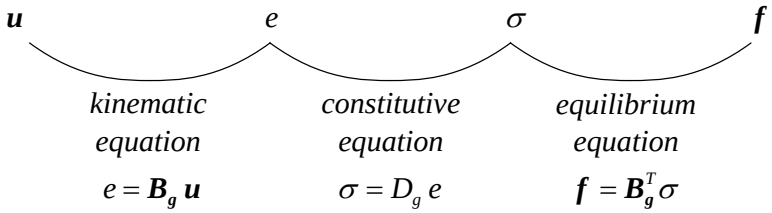

Fig. 9.2: Relation scheme for the discrete bending element.

The rigidity of the spring is:

$$D_g = \frac{EI}{a}$$

The kinematic matrix is:

$$\boldsymbol{B_g} = \left[\frac{-1}{a} \quad \frac{2}{a} \quad \frac{-1}{a} \right]$$

The stiffness matrix can be obtained through:

$$\boldsymbol{K} = \boldsymbol{B_g}^T D_g \boldsymbol{B_g} \quad \rightarrow \quad \boldsymbol{K} = \begin{bmatrix} \frac{-1}{a} \\ \frac{2}{a} \\ \frac{-1}{a} \end{bmatrix} D_g \begin{bmatrix} \frac{-1}{a} & \frac{2}{a} & \frac{-1}{a} \end{bmatrix}$$

and finally becomes:

$$\boldsymbol{K} = \frac{D_g}{a^2} \begin{bmatrix} 1 & -2 & 1 \\ -2 & 4 & -2 \\ 1 & -2 & 1 \end{bmatrix}$$

This is the same result as the one reached in section 6.1.

9.2 Derivation of Torsion Panel

The element (Fig. 9.3) has four degrees of freedom, hence $m = 4$. Three independent rigid

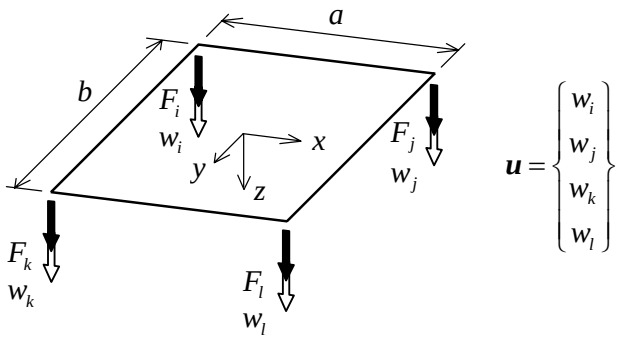

Fig. 9.3: Torsion panel.

body motions can occur: a translation in the w-direction, a rotation around the x-axis and a rotation around the y-axis, so $l = 3$. Consequently, there is one generalised deformation ($n = 1$). This complies with the state of constant moment present in the panel.
Again, the same scheme applies as is shown in Fig. 9.4.

First, a proper generalised stress σ and deformation e must be chosen. The total amount of internal virtual work for a virtual displacement equals:

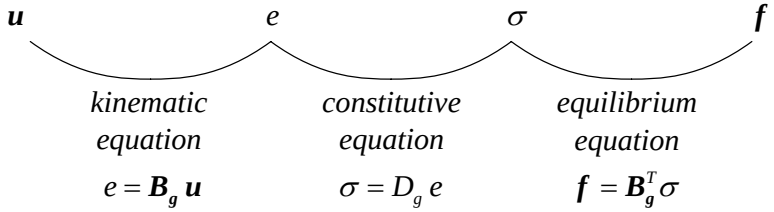

Fig. 9.4: Relation scheme for the torsion panel.

$$\iint_A \delta\rho_{xy}\, m_{xy}\, dA = a\, b\, \delta\rho_{xy}\, m_{xy} = \delta e\, \sigma$$

Hence, it is convenient to choose:

$$\sigma = m_{xy}$$
$$e = \rho_{xy}\, a\, b$$

The relation between m_{xy} and ρ_{xy} is:

$$m_{xy} = \frac{D}{2}\rho_{xy} \quad ; \quad D = \frac{E\, t^3}{12}$$

From this the rigidity D_g is found:

$$D_g = \frac{D}{2\, a\, b}$$

A relation between ρ_{xy} and the displacements was introduced in section 7.2. From this we find:

$$\boldsymbol{B_g} = \begin{bmatrix} -2 & 2 & -2 & 2 \end{bmatrix}$$

Then the stiffness matrix is calculated from:

$$\boldsymbol{K} = \boldsymbol{B_g}^T D_g\, \boldsymbol{B_g} \quad \rightarrow \quad \boldsymbol{K} = \begin{bmatrix} -2 \\ 2 \\ -2 \\ 2 \end{bmatrix} \frac{D}{2\, a\, b} \begin{bmatrix} -2 & 2 & 2 & -2 \end{bmatrix}$$

The final result then is:

$$\boldsymbol{K} = \frac{D}{a\, b} \begin{bmatrix} 2 & -2 & -2 & 2 \\ -2 & 2 & 2 & -2 \\ -2 & 2 & 2 & -2 \\ 2 & -2 & -2 & 2 \end{bmatrix}$$

Once again, the same result was found in section 7.1.

Remark
The chosen σ has the same dimension as the element forces $\boldsymbol{f}$. Similarly, the chosen e has the same dimension as the degrees of freedom $\boldsymbol{u}$. The introduction of a characteristic length l is no longer necessary, as is the case in the constant shear panel.

10 Case study of L-shaped slab with various support conditions

10.1 Problem definition

Fig. 10.1 shows a slab under uniformly distributed load p. The edges are subsequently clamped, simply supported or free. One corner between two free edges is supported to prevent deflection (ball support).

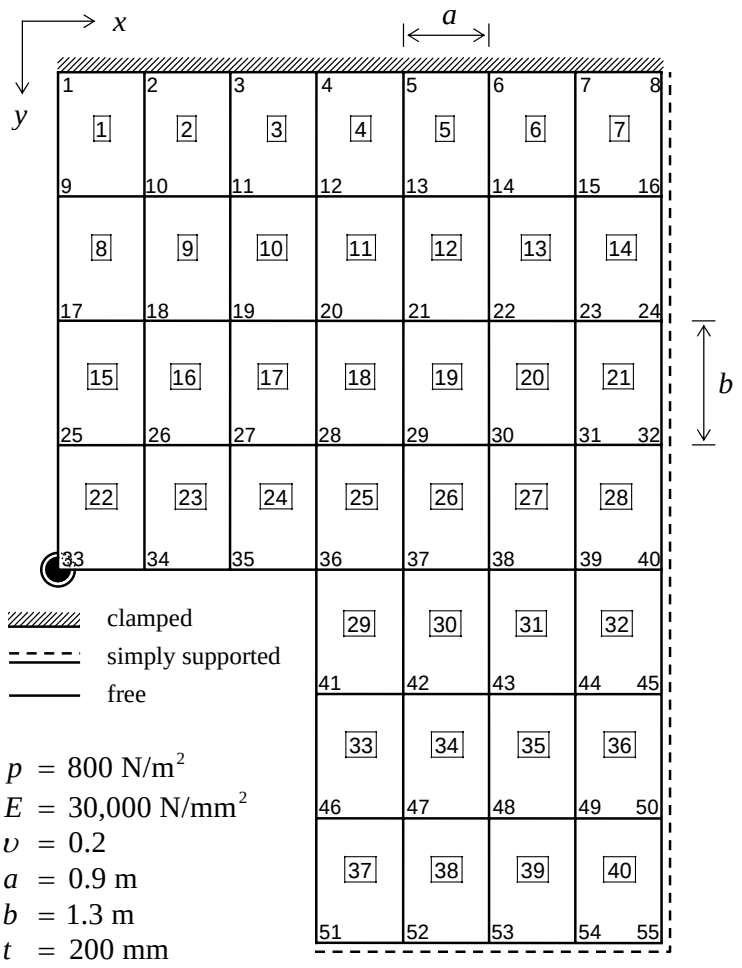

Fig. 10.1: Finite element distribution of a plate subjected to bending by a uniformly distributed load.

Rectangular elements are used with the mesh as shown in Fig. 10.1. The results for the moments, the shear forces and the support reactions are given in the Tables 10.1 and 10.2. Some plotted output is provided in the Figs.10.2 to 10.6.

el-em	node	m_{xx} (N)	m_{yy} (N)	m_{xy} (N)	v_x (N/m)	v_y (N/m)
1	1	278	-2090	77	-2021	910
	2	-896	-3138	2	-2021	2423
	9	-126	-456	-307	443	910
	10	159	-223	-381	443	2423
2	2	-763	-3185	-81	-310	2578
	3	-712	-3556	53	-310	2491
	10	180	-145	-443	-337	2578
	11	49	-391	-309	-337	2491
3	3	-728	-3576	-77	-220	2631
	4	-811	-3734	85	-220	2758
	11	143	-355	-205	-20	2631
	12	188	-418	-42	-20	2758
4	4	-779	-3734	-87	218	2681
	5	-777	-3514	114	218	2760
	12	131	-422	79	234	2681
	13	306	-332	279	234	2760
5	5	-709	-3486	-78	642	2419
	6	-677	-2855	138	642	2534
	13	76	-393	409	560	2419
	14	450	-132	626	560	2534
6	6	-585	-2790	-54	1294	1887
	7	-356	-1661	134	1294	1793
	14	29	-263	728	719	1887
	15	529	53	916	719	1793
7	7	-375	-1587	-9	2042	996
	8	45	162	83	2042	-45
	15	111	-108	853	-291	996
	16	73	-348	945	-291	-45
8	9	-39	-112	-325	68	949
	10	137	-245	-383	68	1255
	17	-76	1460	-651	353	949
	18	579	1216	-710	353	1255
9	10	7	-349	-437	150	1338
	11	183	-381	-250	150	1450
	18	519	1282	-656	175	1338
	19	938	1070	-468	175	1450
10	11	127	-433	-277	-3	1451
	12	173	-495	48	-3	1604
	19	880	1099	-409	153	1451
	20	1153	1005	-84	153	1604

el-em	node	m_{xx} (N)	m_{yy} (N)	m_{xy} (N)	v_x (N/m)	v_y (N/m)
11	12	264	-480	-1	-115	1416
	13	131	-489	369	-115	1631
	20	1036	985	-42	110	1416
	21	1220	937	329	110	1631
12	13	426	-398	342	-320	1156
	14	47	-395	694	-320	1522
	21	1015	863	338	64	1156
	22	1170	808	690	64	1522
13	14	604	-209	695	-669	671
	15	-101	-271	957	-669	1237
	22	832	666	679	-39	671
	23	923	578	941	-39	1237
14	15	538	-34	855	-272	146
	16	-197	361	962	-272	-19
	23	573	399	865	-1042	146
	24	111	-218	973	-1042	-19
15	17	42	1465	-706	238	32
	18	468	1254	-630	238	460
	25	-122	1761	-1248	627	32
	26	981	1377	-1172	627	460
16	18	555	1203	-718	255	415
	19	896	1120	-407	255	481
	26	1019	1452	-1067	196	415
	27	1566	1135	-755	196	481
17	19	832	1064	-493	260	814
	20	1196	1016	-98	260	324
	27	1884	1242	-568	-308	814
	28	1580	1177	-173	-308	324
18	20	1012	936	-122	86	1090
	21	1221	870	272	86	444
	28	2234	1350	-126	-635	1090
	29	1536	1312	268	-635	444
19	21	1167	882	340	-337	719
	22	999	696	607	-337	530
	29	1826	1347	135	-597	719
	30	1436	1083	402	-597	530
20	22	1114	755	683	-826	403
	23	615	359	853	-826	441
	30	1447	1049	330	-773	403
	31	994	669	501	-773	441

Table 10.1a: Output for the elements 1 to 20 of the finite element programme.

el-em	no-de	m_{xx} (N)	m_{yy} (N)	m_{xy} (N)	v_x (N/m)	v_y (N/m)
21	23	793	446	850	-1097	149
	24	-38	96	905	-1097	-21
	31	930	604	443	-1468	149
	32	16	-62	498	-1468	-21
22	25	-22	1851	-1434	535	-1000
	26	916	1458	-1005	535	-447
	33	65	215	-2123	1254	-1000
	34	1691	-25	-1694	1254	-447
23	26	873	1388	-1235	860	-397
	27	1757	1426	-611	860	-408
	34	1645	28	-1485	773	-397
	35	2578	-63	-861	773	-408
24	27	1687	1301	-769	-209	-195
	28	1749	975	177	-209	1506
	35	2428	18	-443	2617	-195
	36	4081	1229	503	2617	1506
25	28	1999	1432	113	-470	-806
	29	1759	1171	118	-470	146
	36	1594	325	583	1387	-806
	37	2009	1402	588	1387	146
26	29	1735	1178	298	-352	24
	30	1484	1040	278	-352	113
	37	1651	1318	146	-277	24
	38	1547	1133	126	-277	113
27	30	1496	1038	415	-931	35
	31	928	594	423	-931	106
	38	1474	1123	-1	-855	35
	39	1011	669	8	-855	106
28	31	981	611	466	-1455	15
	32	-16	32	473	-1455	2
	39	980	657	-48	-1523	15
	40	9	-12	-41	-1523	2
29	36	2657	1611	1262	-1370	-2017
	37	1202	1399	298	-1370	279
	41	-617	2013	790	1090	-2017
	42	1239	1522	174	1090	279
30	37	1814	1378	343	-536	-524
	38	1402	1164	4	-536	-90
	42	883	1594	-53	-184	-524
	43	1194	1130	-392	-184	-90

el-em	no-de	m_{xx} (N)	m_{yy} (N)	m_{xy} (N)	v_x (N/m)	v_y (N/m)
31	38	1529	1142	88	-940	-257
	39	961	678	-60	-940	-95
	43	1137	1166	-411	-798	-257
	44	831	627	-560	-798	-95
32	39	1006	656	-17	-1554	-113
	40	-17	-9	-61	-1554	40
	44	835	658	-577	-1363	-113
	45	9	22	-621	-1363	40
33	41	-438	2117	32	762	60
	42	1079	1508	37	762	-798
	46	156	1448	-681	-7	60
	47	306	1206	-677	-7	-798
34	42	876	1518	-166	-31	-397
	43	1197	1180	-405	-31	-623
	47	552	1205	-619	-294	-397
	48	565	858	-858	-294	-623
35	43	1091	1134	-404	-586	-348
	44	888	711	-613	-586	-485
	48	763	922	-878	-775	-348
	49	397	444	-1086	-775	-485
36	44	806	637	-570	-1394	-147
	45	15	-75	-652	-1394	54
	49	612	545	-1072	-993	-147
	50	-50	132	-1154	-993	54
37	46	-130	1494	-682	362	-685
	47	603	1217	-635	362	-1310
	51	189	-28	-880	-170	-685
	52	-98	10	-833	-170	-1310
38	47	399	1232	-652	20	-984
	48	741	943	-854	20	-1170
	52	27	-21	-859	-24	-984
	53	-31	-20	-1061	-24	-1170
39	48	571	906	-863	-234	-904
	49	620	615	-1109	-234	-883
	53	22	-7	-1088	-88	-904
	54	-6	-85	-1334	-88	-883
40	49	505	542	-1040	-1149	-626
	50	-8	-190	-1174	-1149	173
	54	-60	-47	-1284	325	-626
	55	50	199	-1418	325	173

Table 10.1b: Output for the elements 21 to 40 of the finite element programme.

node	direction	support reaction (N)
1	*z*	217
1	*x*	-898
2	*z*	-3154
2	*x*	-2856
3	*z*	-2904
3	*x*	-3230
4	*z*	-3161
4	*x*	-3390
5	*z*	-3063
5	*x*	-3181
6	*z*	-2764
6	*x*	-2567
7	*z*	-1760
7	*x*	-1397

node	direction	support reaction (N)
8	*z*	1262
8	*x*	86
16	*z*	-69
24	*z*	-2142
32	*z*	-2807
40	*z*	-2979
45	*z*	-2815
50	*z*	-2087
55	*z*	2413
54	*z*	-1221
53	*z*	-1566
52	*z*	-1582
51	*z*	-2257
33	*z*	-5004

Table 10.2: Support reactions in the boundary nodes.

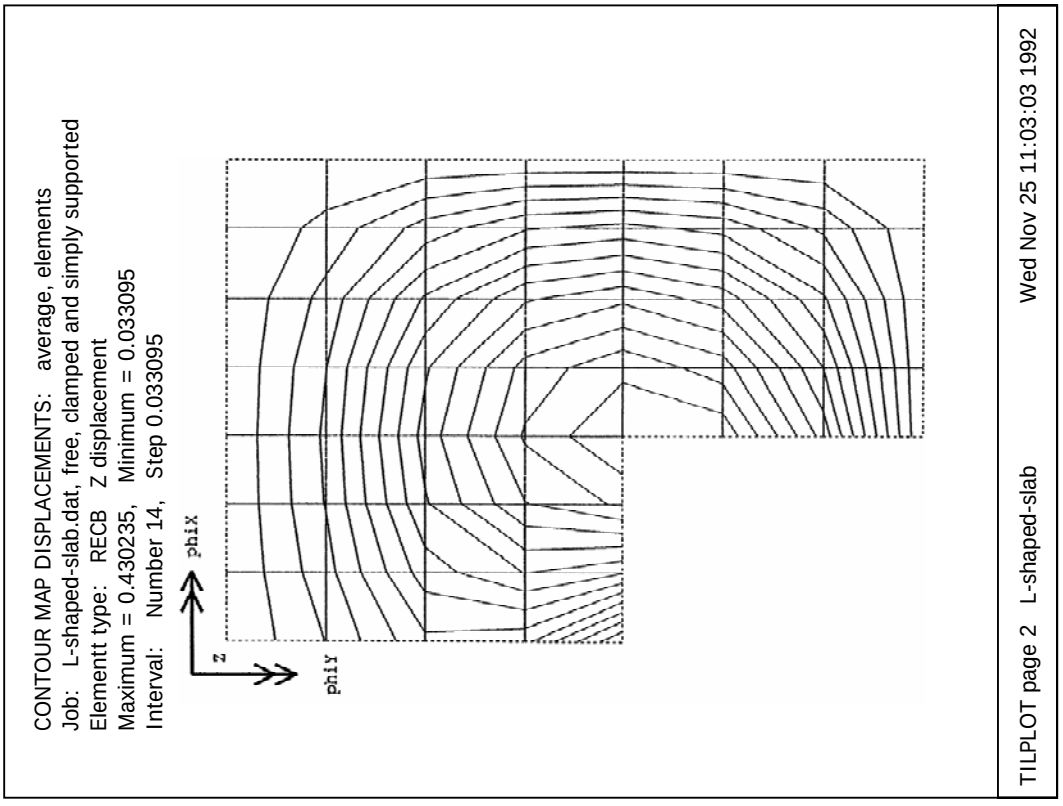

Fig. 10.2: Contour plot of displacements.

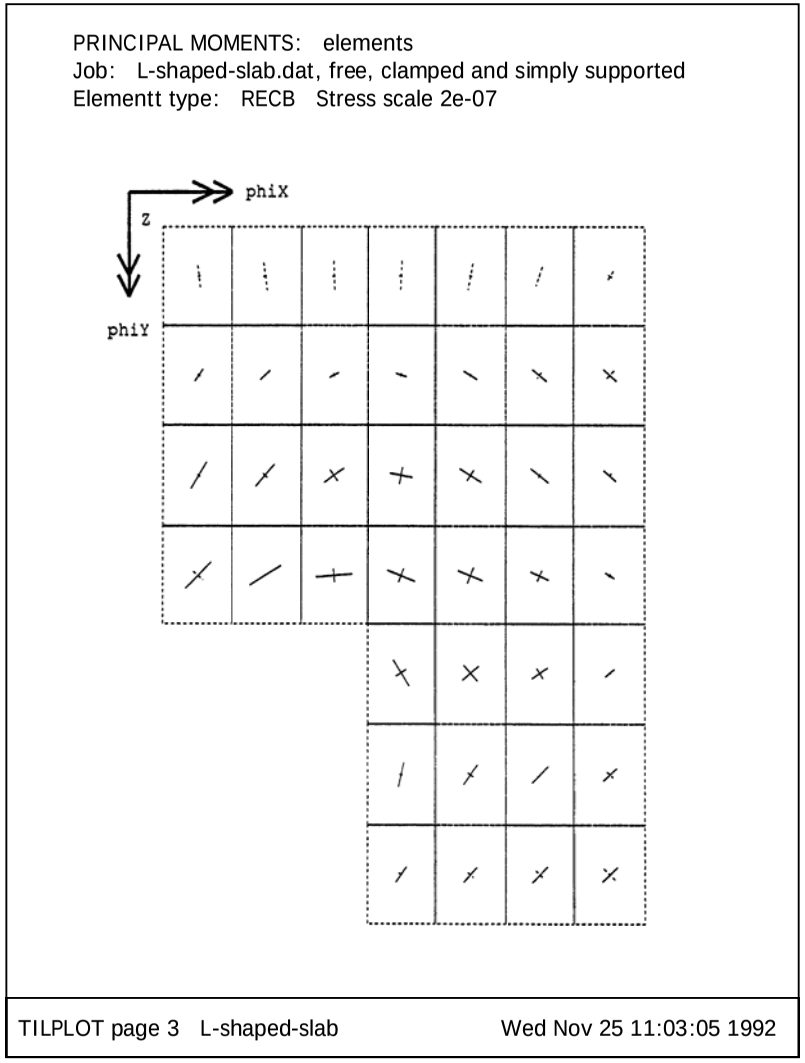

Fig. 10.3: Principal moments.

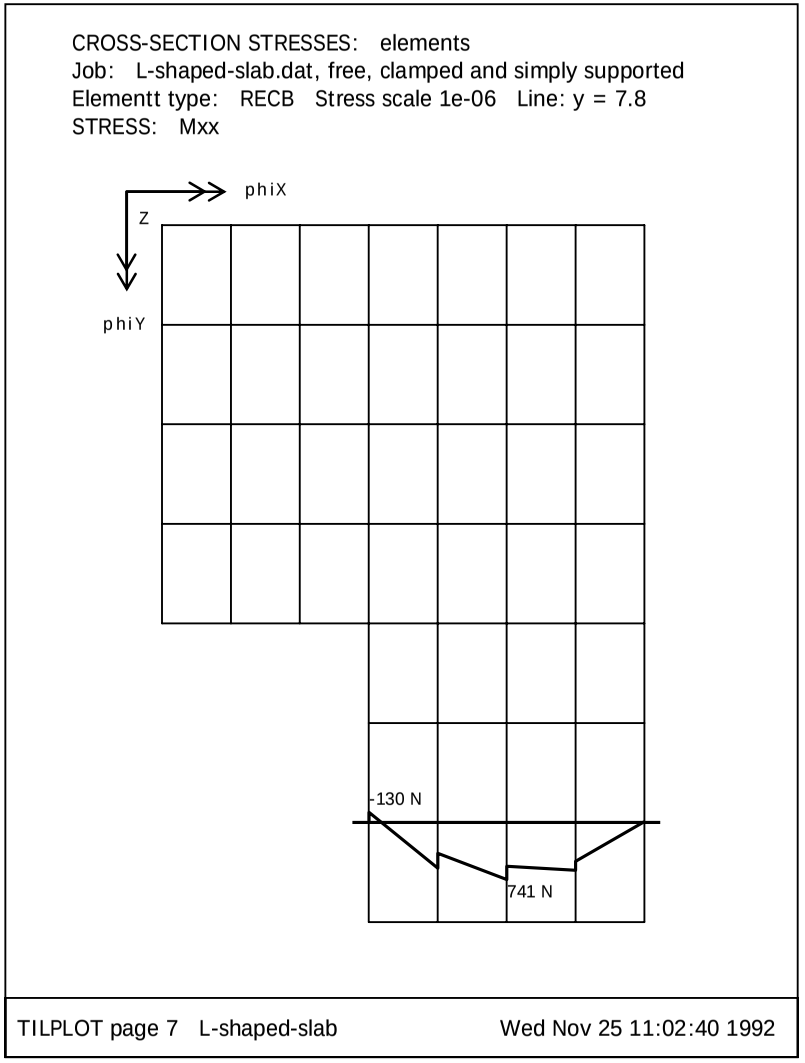

Fig. 10.4: Stresses m_{xx} in cross-section at $y = 7.8$ m.

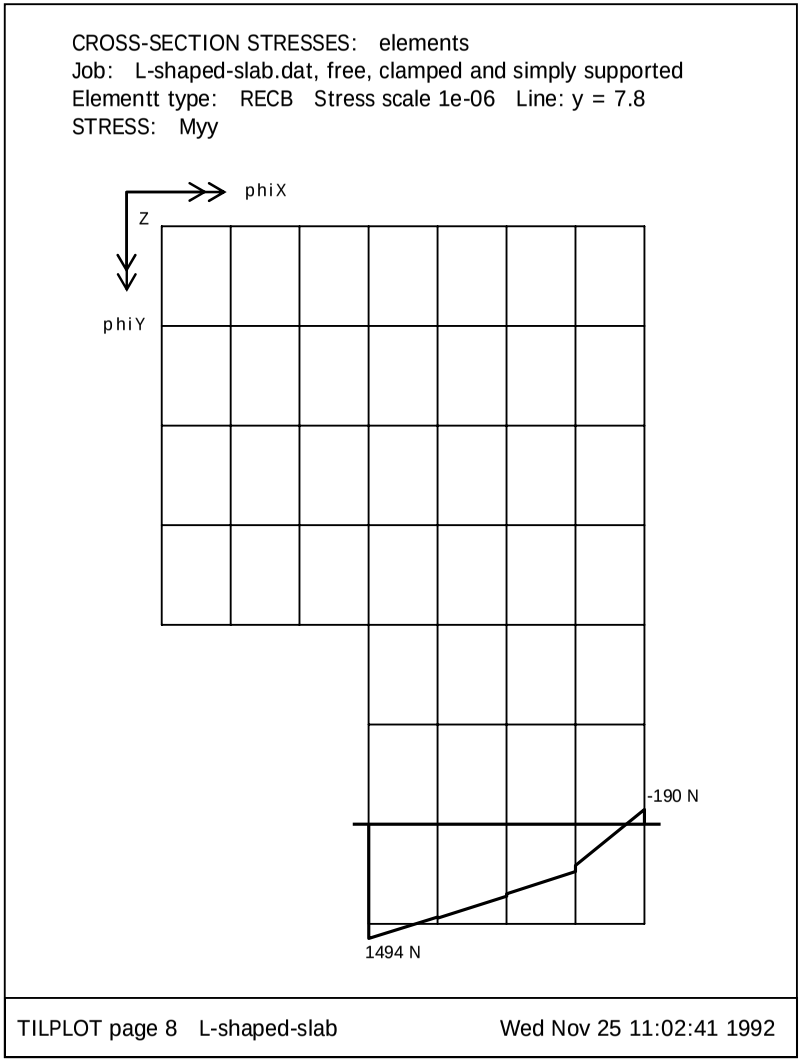

Fig. 10.5: Stresses m_{yy} in cross-section at y = 7.8 m.

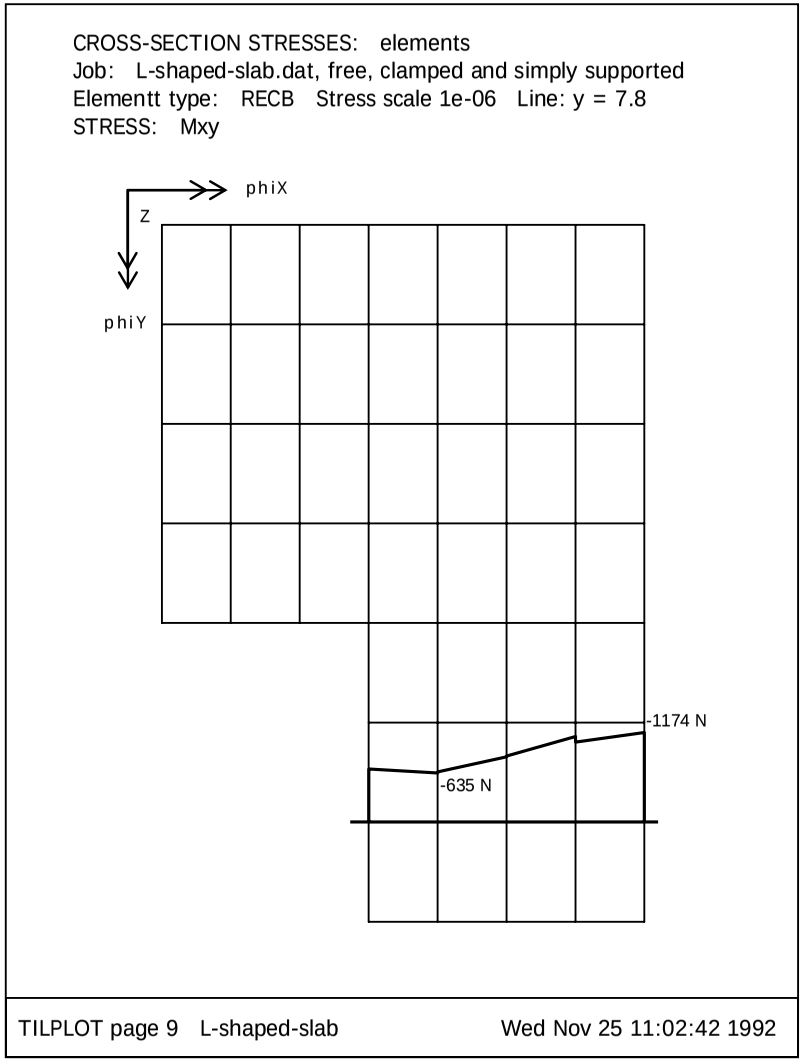

Fig. 10.6: Stresses m_{xy} in cross-section at y = 7.8 m.

10.2 Bending moments and equilibrium

Assignment 1

A. Plot the moment distribution m_{yy} in line I as shown in Fig. 10.7. Show the discontinuities in every node (do not average).

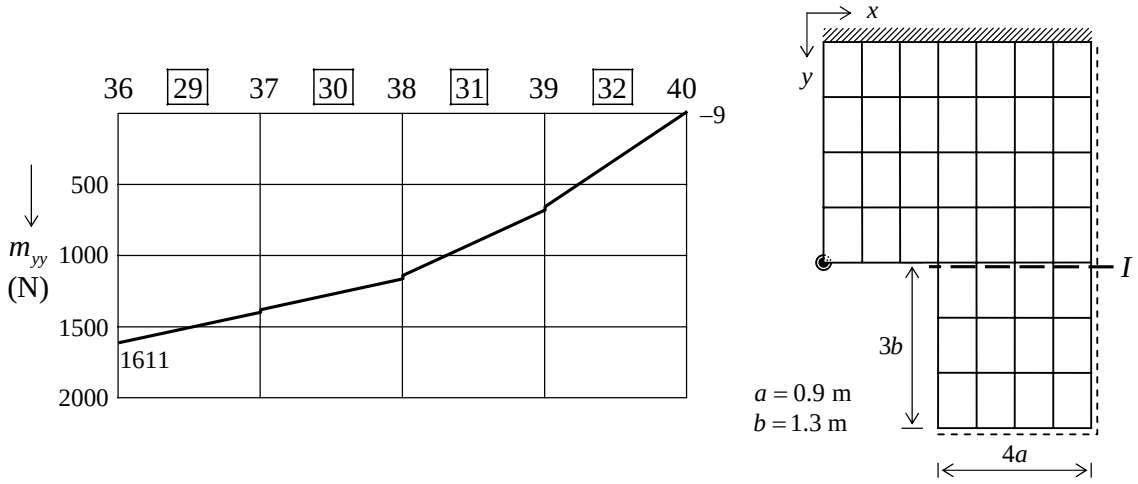

Fig. 10.7: Plot of the distribution of m_{yy} on line I.

B. Calculate the sum of moments for m_{yy} in line I.

$$m_{average} = \frac{1}{8}\left[\overbrace{m_{36}+m_{37}}^{29} + \overbrace{m_{37}+m_{38}}^{30} + \overbrace{m_{38}+m_{39}}^{31} + \overbrace{m_{39}+m_{40}}^{32}\right] = 1002.4$$

The length of the line is $4a$	=	3.6
The sum of the moments $\sum m_{yy}$	=	3609 Nm ×

C. Verify this sum of moments by also determining it from the external load that acts on the plate part under line I. This load consists of the distributed load q and the support reactions R in the nodes 45, 50, 51, 52, 53, 54 and 55.

$4a * 3b * q * 1\frac{1}{2}b$	=	−21902
$R_{45} * b$	=	3659
$R_{50} * 2b$	=	5427
$(R_{51}+R_{52}+R_{53}+R_{54}+R_{55}) * 3b$	=	16425
Total external moment	=	3611 Nm + (very close to 3609 Nm)

Assignment 2

Plot the moment distributions in Fig. 10.8 (do <u>not</u> average per node) for the moments:

- m_{xx} in line II;
- m_{xy} in line II;
- m_{xx} in line III;
- m_{yy} in line IV;
- m_{xy} in line IV.

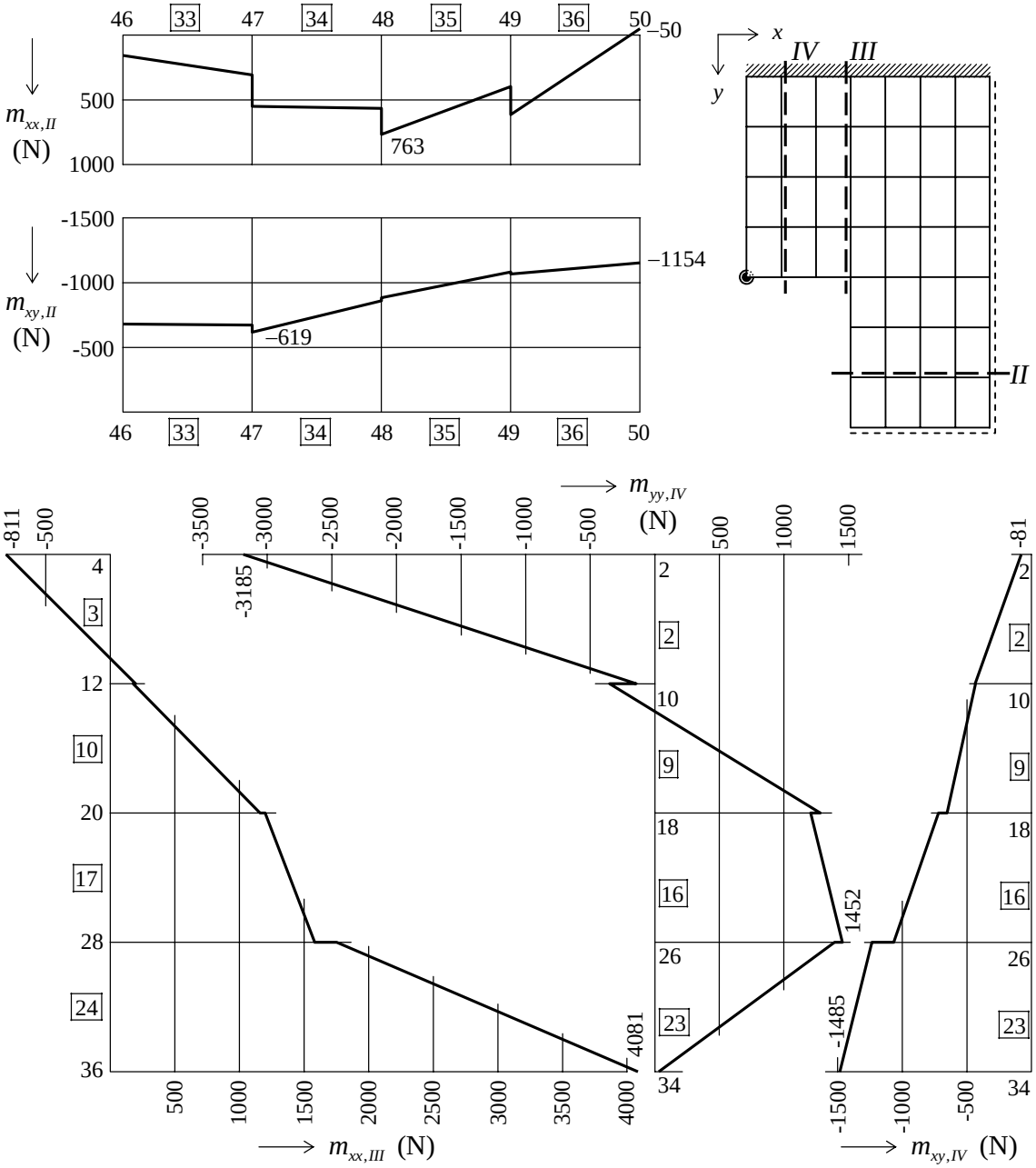

Fig. 10.8: Plot of the distributions of several moments.

10.3 Shear forces, support reactions and equilibrium

The same plate as the one considered in section 10.1 (Fig. 10.1) is chosen as a starting point. For the computer output, it is referred to the Tables 10.1 and 10.2.

Assignment 3

Plot in Fig. 10.9 the shear force distribution (scale: 1 cm = 1000 N/m) for:

- v_y in line *V* ;
- v_x in line *VI* ;

and the distribution of the support reactions (scale: 1 cm = 1000 N) for:

– R_z in line V^a (node 1, 2, 3 and 4 have already been drawn);
– R_z in line VI^a.

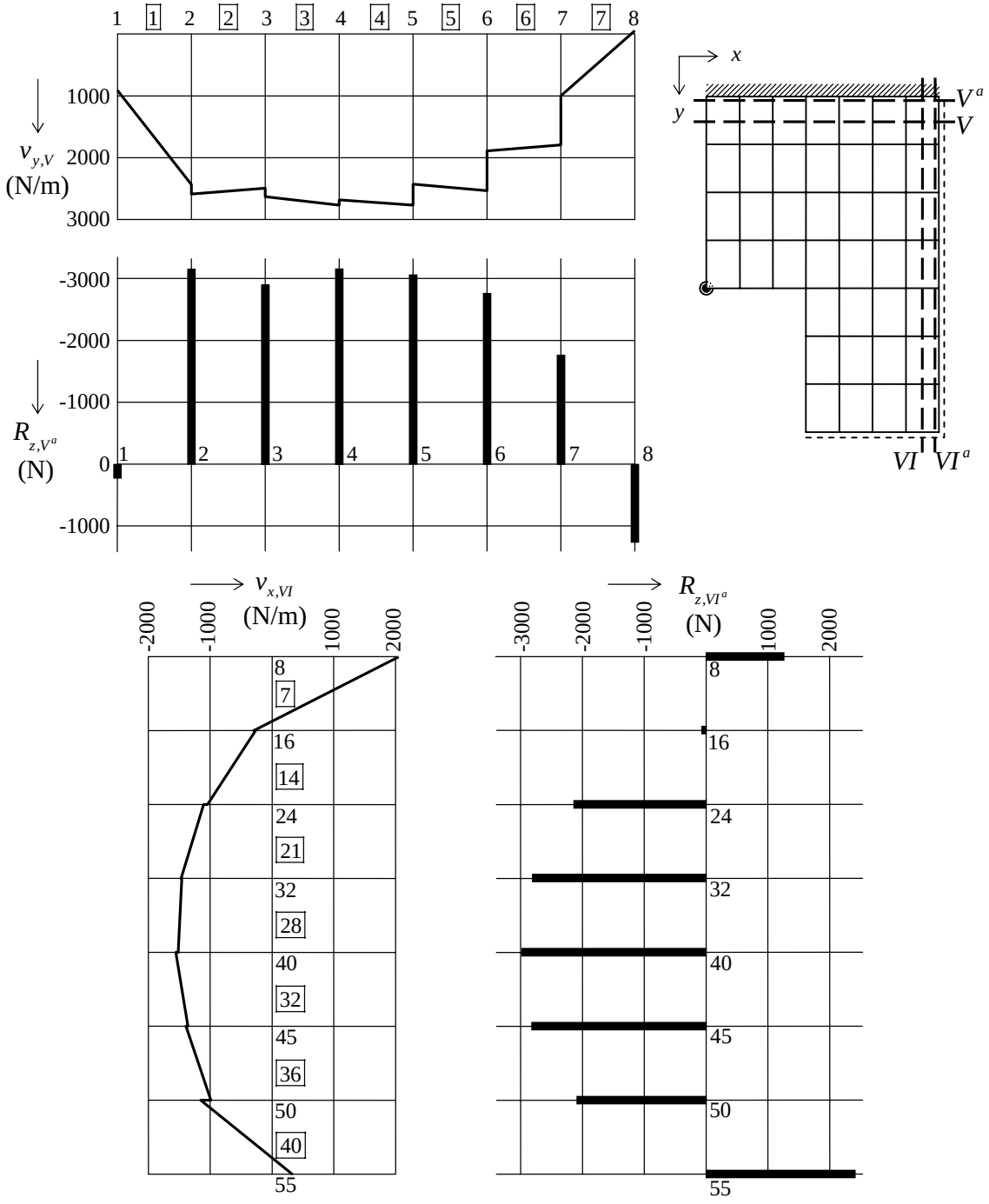

Fig. 10.9: Plot for the distribution of shear forces and support reactions.

Assignment 4

In a number of nodes, it has to be checked whether the magnitude of the support reaction can be calculated from the shear forces. To start with, the calculation will be elucidated for node 4 along the clamped edge (see Fig. 10.10). Because the shear forces are accurate about halfway the elements, a plate part is cut out around node 4 through the middle of the elements. Externally this plate part is subjected to:

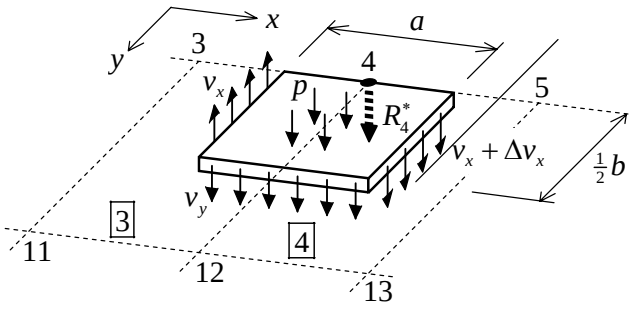

Fig. 10.10: Calculation of R_4^* from the shear forces.

- the support reaction R_4^*
- the distributed load p

and internally in the three cuts:

- The average shear force v_x, and $v_x + \Delta v_x$
- The average transverse force v_y

The equation for the vertical equilibrium of the plate part is:

$$R_4^* + \frac{1}{2} a\, b\, p + \frac{1}{2} b\, \Delta v_x + a\, v_y = 0$$

From this the formula for the support reaction follows:

$$R_4^* = -\frac{1}{2} a\, b\, p - \frac{1}{2} b\, \Delta v_x - a\, v_y$$

Then considering the input and output the following can be calculated:

$$\left.\begin{aligned} v_x &= \frac{1}{4}\left(3 * -220 - 20\right) = -170 \\ v_x + \Delta v_x &= \frac{1}{4}\left(3 * 218 + 234\right) = 222 \end{aligned}\right\} \quad \rightarrow \quad \Delta v_x = 222 + 170 = 392 \text{ N/m}$$

$$v_y = \frac{1}{2}\left\{\frac{1}{4}\left(3 * 2758 + 2631\right) + \frac{1}{4}\left(3 * 2681 + 2760\right)\right\} = 2713.5 \text{ N/m}$$

$$\begin{aligned} -\tfrac{1}{2} a\, b\, p &= -468 \text{ kN} \\ -\tfrac{1}{2} b\, \Delta v_x &= -255 \text{ kN} \\ -a\, v_y &= -2442 \text{ kN} \\ \hline R_4^* &= -3165 \text{ kN} \end{aligned} +$$

The computer output delivers a practically equal value:

$$R_4 = -3161\,\text{kN}$$

Above verification is subsequently carried out for the nodes 40, 55 and 33. The results are displayed in the Figs.10.11, 10.12 and 10.13. What can be pointed out in these nodes?

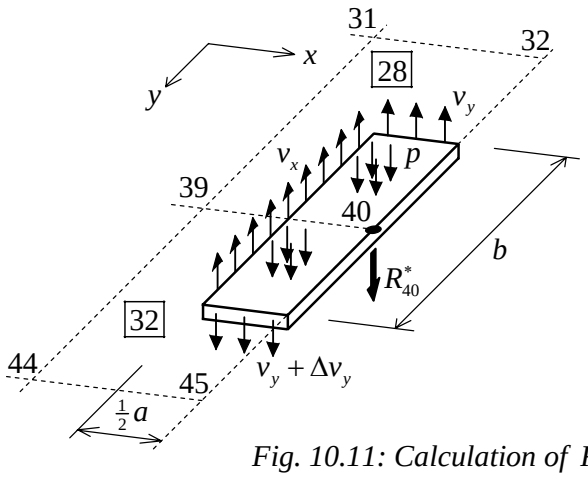

$$R^*_{40} + \tfrac{1}{2}a\,b\,p - b\,v_x + \tfrac{1}{2}a\,\Delta v_y = 0$$

$-\tfrac{1}{2}a\,b\,p$	=	–468 N
$+b\,v_x$	=	–1958 N
$-\tfrac{1}{2}a\,\Delta v_y$	=	+2 N
R^*_{40}	=	–2424 N
output R_{40}	=	–2979 N

Fig. 10.11: Calculation of R^*_{40} from the shear forces.

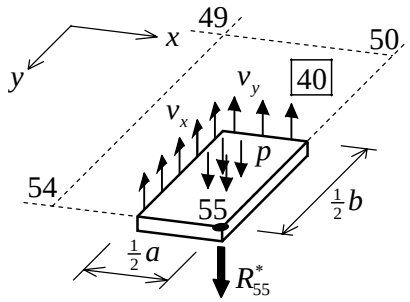

$$R^*_{55} + \tfrac{1}{4}a\,b\,p - \tfrac{1}{2}b\,v_x - \tfrac{1}{2}a\,v_y = 0$$

$-\tfrac{1}{4}a\,b\,p$	=	–234 N
$+\tfrac{1}{2}b\,v_x$	=	–28 N
$+\tfrac{1}{2}a\,v_y$	=	–12 N
R^*_{55}	=	–274 N
output R_{55}	=	+2413 N

Fig. 10.12: Calculation of R^*_{55} from the shear forces.

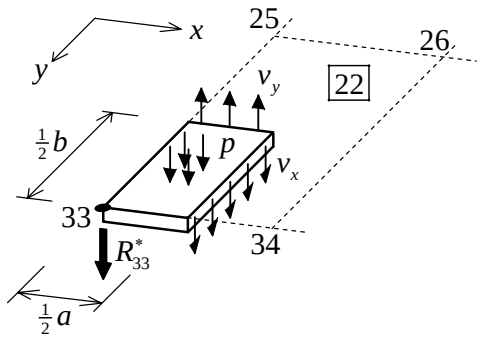

$$R^*_{33} + \tfrac{1}{4}a\,b\,p + \tfrac{1}{2}b\,v_x - \tfrac{1}{2}a\,v_y = 0$$

$-\tfrac{1}{4}a\,b\,p$	=	–234 N
$-\tfrac{1}{2}b\,v_x$	=	–698 N
$+\tfrac{1}{2}a\,v_y$	=	–388 N
R^*_{33}	=	–1320 N
output R_{33}	=	–5004 N

Fig. 10.13: Calculation of R^*_{33} from the shear forces.

The mismatch between R^* and R in nodes 40, 55 and 33 occurs because the torsional moment m_{xy} is not zero. The above calculated support reactions must be corrected by the concentrated edge shear forces due to the torsional moment. The results of this exercise are shown in the Figs. 10.14, 10.15 and 10.16. The concentrated edge shear forces are drawn as they act in case of a positive m_{xy}. After correction, no mismatch occurs anymore.

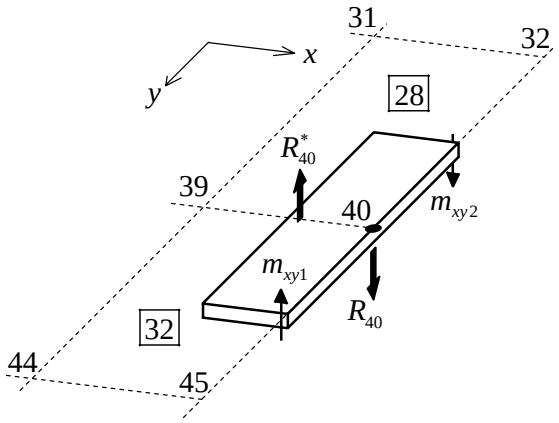

The quantity R^*_{40} is the sum of the upward directed forces v_x, v_y and q.

$$R_{40} - R^*_{40} - m_{xy1} + m_{xy2} = 0$$

$+ R^*_{40}$	=	–2424 kN
$+ m_{xy1}$	=	–341 kN
$- m_{xy2}$	=	–216 kN
R_{40}	=	–2981 kN +
output R_{40}	=	–2979 kN

Fig. 10.14: Correction of support reaction R_{40} along the simply supported edge.

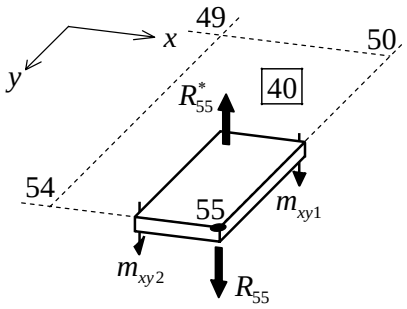

$$R_{55} - R^*_{55} + m_{xy1} + m_{xy2} = 0$$

$+ R^*_{55}$	=	–274 kN
$- m_{xy1}$	=	+1296 kN
$- m_{xy2}$	=	+1351 kN
R_{55}	=	+2373 kN +
output R_{55}	=	+2413 kN

Fig. 10.15: Correction of support reaction R_{55} in the simply supported corner.

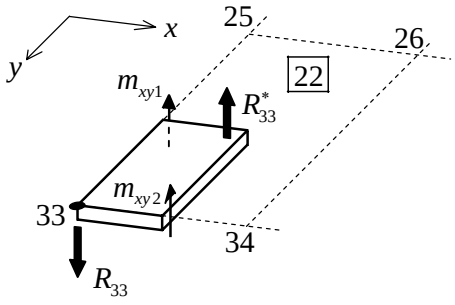

$$R_{33} - R^*_{55} - m_{xy1} - m_{xy2} = 0$$

$+ R^*_{33}$	=	–1320 kN
$+ m_{xy1}$	=	–1778.5 kN
$+ m_{xy2}$	=	–1908.5 kN +
R_{33}	=	–5007 kN
output R_{33}	=	–5004 kN

Fig. 10.16: Correction of support reaction R_{33} in the ball supported corner.

11 Non-linear applications of plates, slabs and shells

11.1 Masonry mechanics

Fig. 11.1 shows an example of masonry mechanics. A brick wall with a window is subjected to a horizontal shear load. The experimental failure pattern is compared with the numerical one. Further the deformed mesh at a horizontal displacement of 25 mm and the load displacement diagrams are shown.

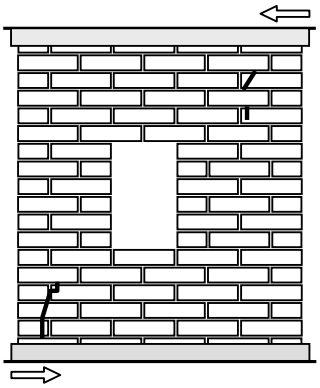

a) Experimental failure pattern

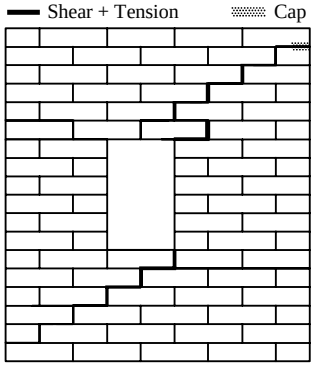

b) Numerical damage at d = 2.5 mm

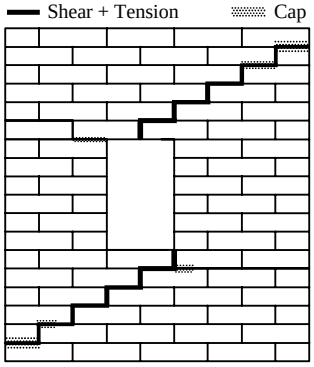

c) Numerical damage at d = 25.0 mm

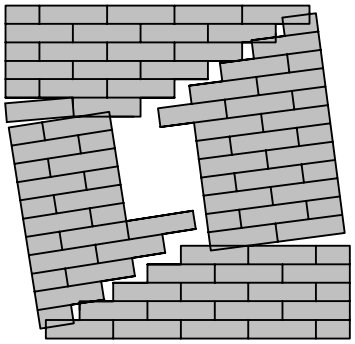

d) Deformed mesh at d = 25.0 mm

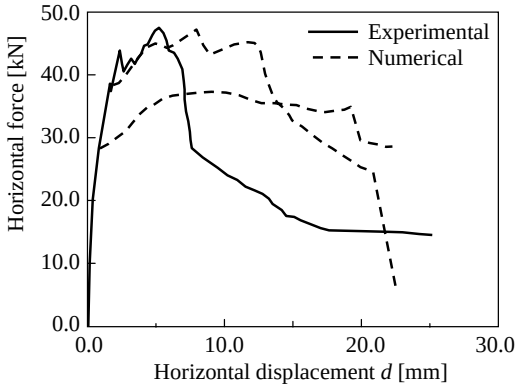

e) Load-displacement diagrams

Fig. 11.1: Brick wall with window subjected to a horizontal shear load.

11.2 Slab of Mc Neice

Fig. 11.2 shows the slab of Mc. Neice, which is square slab that is simply supported at the four corners and loaded in its centre. An experimental and a numerical solution of the load displacement diagram of node number 7 on the edge of the slab halfway between the supports are provided as well (Fig. 11.3).

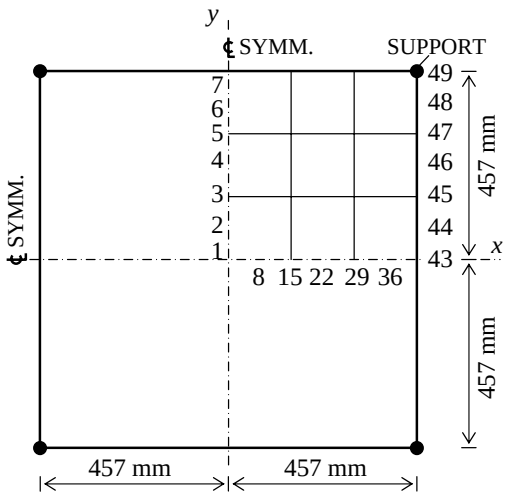

Fig. 11.2: Slab of McNeice.

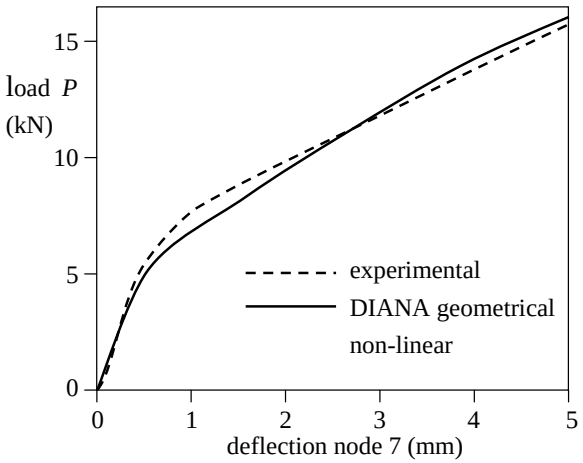

Fig. 11.3: Experimental and computed load-displacement curves.

11.3 Shell A2 tested by Bouma

Fig. 11.4 shows the geometry and reinforcement structure of the shell. The finite element mesh of the shell is displayed in Fig. 11.5. For reasons of symmetry, only half the shell needs to be modelled. In Fig. 11.6 the numerical and experimental comparison of the load displacement diagram can be found.

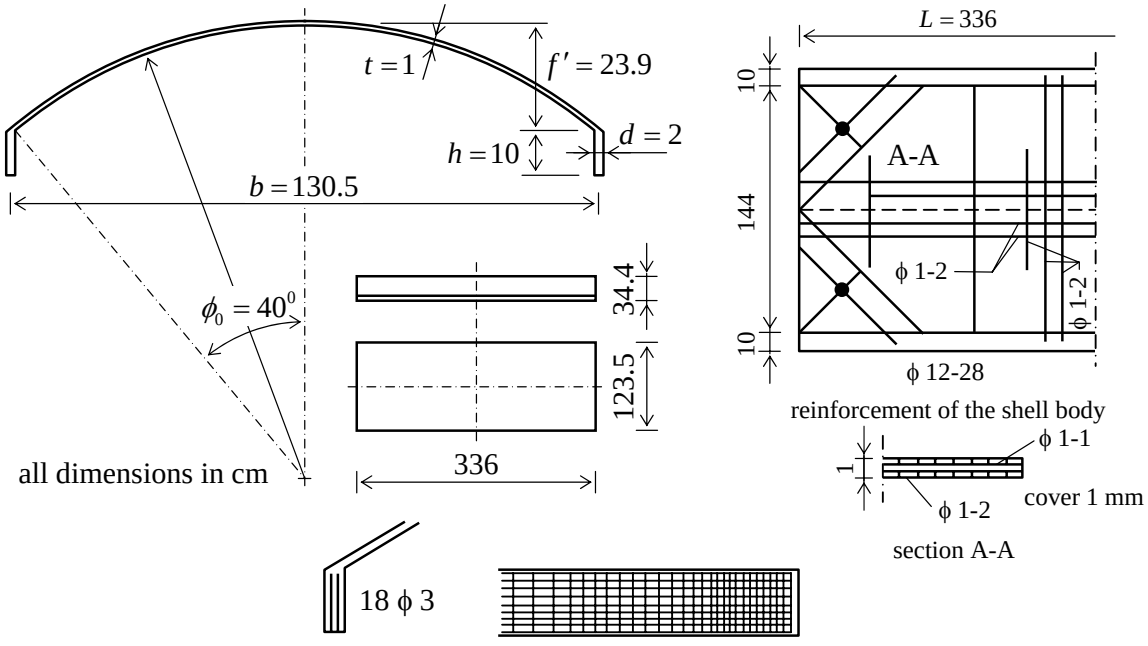

Fig. 11.4: Shell geometry and reinforcement.

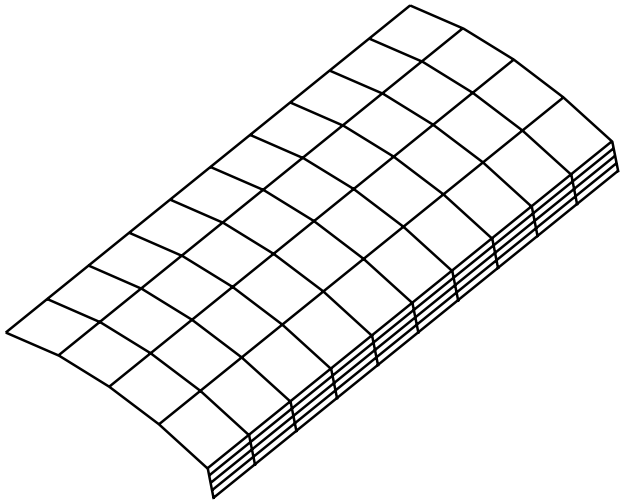

Fig. 11.5: Finite element model of shell.

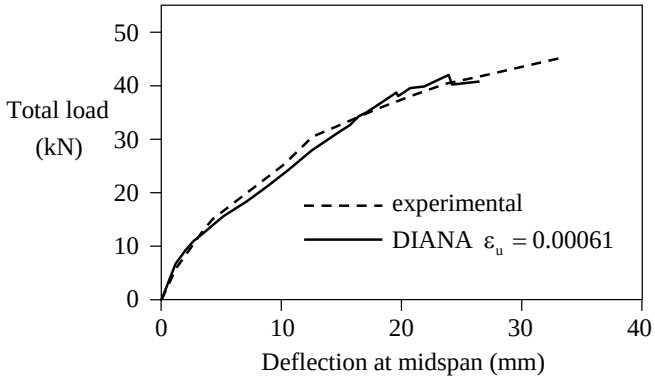

Fig. 11.6: Experimental and computed load-displacement curves.

Books on the Finite Element Method

1. Bathe K.J., Wilson E.L.: "*Numerical Methods in Finite Element Analysis*", Prentice-Hall International, Inc., Englewood Cliffs, New Jersey.

2. Blaauwendraad J.: "*Elementenmethode voor staafconstructies*", Academic Service, Schoonhoven.

3. Blaauwendraad J., Kok A.W.M.: "*Elementenmethode voor constructeurs*", Agon Elsevier, Amsterdam (antiquarian).

4. Hughes T.J.R.: "*The Finite Element Method*", Prentice-Hall International, Inc., Englewood Cliffs, New Jersey (very formal).

5. Zienkiewicz O.C.: "*The Finite Element Method*", McGraw-Hill, London.

6. Zienkiewicz O.C., Morgan K.: "*Finite Elements and Approximation*", John Wiley & Sons, New York.